NASA TECHNICAL MEMORANDUM

NASA TM X-1759

NASA TM X-1759

WIND-TUNNEL FORCE AND PRESSURE TESTS OF ROCKET-ENGINE NOZZLE EXTENSIONS ON THE 0.0667-SCALE X-15-2 MODEL AT SUPERSONIC AND HYPERSONIC SPEEDS

by Earl J. Montoya and Jack Nugent

Flight Research Center

Edwards, Calif.

NATIONAL AERONAUTICS AND SPACE ADMINISTRATION • WASHINGTON, D. C. • MARCH 1969

NASA TM X-1759

WIND-TUNNEL FORCE AND PRESSURE TESTS OF ROCKET-ENGINE NOZZLE EXTENSIONS ON THE 0.0667-SCALE X-15-2 MODEL AT SUPERSONIC AND HYPERSONIC SPEEDS

By Earl J. Montoya and Jack Nugent

Flight Research Center
Edwards, Calif.

NATIONAL AERONAUTICS AND SPACE ADMINISTRATION

For sale by the Clearinghouse for Federal Scientific and Technical Information
Springfield, Virginia 22151 – CFSTI price $3.00

WIND-TUNNEL FORCE AND PRESSURE TESTS OF ROCKET-ENGINE NOZZLE EXTENSIONS ON THE 0.0667-SCALE X-15-2 MODEL AT SUPERSONIC AND HYPERSONIC SPEEDS

By Earl J. Montoya and Jack Nugent
Flight Research Center

SUMMARY

Wind-tunnel force and pressure test results of nozzle extensions on the 0.0667-scale X-15-2 model over the free-stream Mach number range from 2.3 to 8.0 at angles of attack from -5° to 18° and Reynolds numbers of 2.0×10^6 per foot (6.56×10^6 per meter) and 3.4×10^6 per foot (1.12×10^7 per meter) are presented. The effects of the presence of an aft-mounted ramjet shape and control-surface deflections are shown.

Force data indicate that the addition of the nozzle extensions did not appreciably affect the overall drag or static margin of the model. On the basis of these results as well as other considerations, a nozzle with an internal expansion ratio of 22.1 was deemed most suitable. The presence of this nozzle extension slightly increased the model base pressure. Fuselage afterbody flows impinged on the nozzle extension and formed a shock wave at the impingement point. Large longitudinal and circumferential pressure variations existed on the nozzle extension. Deflecting the speed brakes and horizontal tails significantly affected the nozzle pressures; whereas, the addition of the model ramjet did not have an effect.

INTRODUCTION

During the later phases of the X-15 program, the U.S. Air Force and the NASA Flight Research Center sought inexpensive and simple methods of increasing the performance of the airplane. One such method that had been used successfully on the D-558-II research airplane involved the use of nozzle extensions fitted to rocket engines (ref. 1). These extensions were small, radiation-cooled members that permitted the rocket exhaust gases to attain higher exit velocities by expanding within the nozzle to ambient pressures for the higher altitude flights. Because of their small size, the extensions presented no serious aerodynamic interference or structural design problems.

It appeared that a lightweight, radiation-cooled nozzle extension added to the YLR99 engine of the X-15-2 (refs. 2 and 3) could provide a desirable performance improvement. Designing the nozzle extension for the YLR99 engine presented a more difficult problem than the D-558-II design because of the more severe operating environment and larger size of the extension. Because of the large size of the extension relative to the airplane base configuration, there was a possibility of adverse aerodynamic interference occurring with the airplane's afterbody external flow. Accordingly, wind-tunnel force and pressure tests were conducted to investigate the effects of several nozzle-extension configurations on the aerodynamics of the X-15-2 airplane.

This report presents the results of the wind-tunnel tests with the candidate nozzle extensions planned for the YLR99 engine on the X-15-2. The speed-brake and horizontal-tail positions were varied during the tests, and variations in the ventral-fin configuration were tested. Test configurations also included two ramjet shapes, since the X-15-2 had been proposed as a test vehicle for the hypersonic research engine (ref. 4). Tests were conducted over the free-stream Mach number range from approximately 2.3 to 8.0 utilizing the Unitary Plan Tunnel at the NASA Langley Research Center (LaRC) and the von Kármán Gas Dynamics Facility Tunnel B at the Arnold Engineering Development Center (AEDC). The test Reynolds numbers were 2.0×10^6 per foot (6.56×10^6 per meter) and 3.4×10^6 per foot (1.12×10^7 per meter).

SYMBOLS

The units used for the physical quantities in this paper are given in U.S. Customary Units and parenthetically in the International System of Units (SI). Factors relating the two systems are presented in reference 5.

C_{D_o} — zero-lift drag coefficient, total configuration, $\frac{\text{Drag}}{q_\infty S}$

C_L — lift coefficient, $\frac{\text{Lift}}{q_\infty S}$

C_m — pitching-moment coefficient (moment taken about $0.20\bar{c}$), $\frac{\text{Pitching moment}}{q_\infty S\bar{c}}$

C_p — pressure coefficient, $\frac{p_l - p_\infty}{q_\infty}$

$C_{p,b}$ — model base pressure coefficient

$\bar{c}$ — mean geometric chord based on S, 8.22 inches (20.88 centimeters), inches (centimeters)

l — length of nozzle extension, inches (centimeters)

M — Mach number

N_{Re} — Reynolds number

p — static pressure, pounds per square inch absolute (kilonewtons per square meter)

q	dynamic pressure, pounds per square inch absolute (kilonewtons per square meter); also pounds per square foot (kilonewtons per square meter)
S	model wing area, 127.73 square inches (824.06 square centimeters)
x	distance aft from model base, inches (centimeters)
α	angle of attack, degrees
Δ	error
δ_h	horizontal-tail setting, degrees
δ_{sb}	speed-brake setting, degrees
ϵ	nozzle internal expansion ratio, $\frac{\text{Exit area}}{\text{Throat area}}$
θ	radial location from vertical centerline (see fig. 4), degrees
σ	standard-deviation error

Subscripts:

1,2,3 ...	orifice 1, orifice 2, orifice 3 ...
a	ahead of shock wave on nozzle extension
b	behind shock wave on nozzle extension
l	local
r	rise across shock wave on nozzle extension
∞	free stream

MODELS

Airplane

The 1/15-scale (0.0667) force model of the X-15-2 airplane with the extended fuselage (29 inches (73.66 centimeters) full scale) was used for the nozzle-extension wind-tunnel investigations. Because of the temperature environment at the high Mach number tests, the model was modified to withstand a temperature of 1360° R (755° K) for up to 30 minutes. These modifications consisted mainly of replacing the aluminum alloy model components with steel components and removing all electrical components from the model. Overall dimensions of the model with the 22.1 internal-expansion-ratio nozzle extension are shown in figure 1. The ventral-fin configuration can be varied from no fin, to a short fin, to a full fin on this model. References 6 and 7 provide additional information on the model.

Nozzle Extensions

Nozzle extensions of various exit diameters and lengths representing expansion ratios of 22.1 to 33.6 were tested. Extensions with external shrouds to reduce aerodynamic effects were also tested, although these types of full-scale nozzles were not planned. Figures 2(a) to 2(d) show details of the model nozzle extensions used and their installation for the force and pressure tests. The unshrouded nozzle extensions (figs. 2(a) and 2(d)) were designed primarily to simulate the external shape of the full-scale nozzle extensions. The full-scale nozzle extensions were to have an extremely thin wall, so there would be only a small difference between the external and internal exit diameters. This wall thickness was not simulated in the models tested.

The external bell shape of the unshrouded full-scale nozzle extension was approximated with the 15° conical angle shown. The exit diameter for each model nozzle extension (fig. 2(a)) was obtained by dividing the full-scale nozzle exit diameter by 15. The model nozzle-extension throat diameter could not be scaled to the full-scale engine because of the method of sting attachment used and the inability to simulate nozzle-extension wall thickness.

Nine candidate nozzle extensions were used for the LaRC force investigation. The unshrouded nozzle extensions (fig. 2(a)) varied in their axial lengths and the presence or absence of the external turbine exhaust manifolds. Stiffener ribs were simulated on these nozzle extensions (see fig. 2(c)). The unshrouded nozzles were machined out of stainless steel. The shrouded nozzle extensions (fig. 2(b)) varied in shroud shape and the presence or absence of perforations in the $\epsilon = 33.6$ nozzle extension. These nozzles were machined out of aluminum. All the nozzle extensions had the same internal contours.

Figure 2(c) shows how the nozzles were mounted to the model. Figure 2(d) shows the two $\epsilon = 22.1$ nozzle extensions used for the LaRC pressure investigation and the AEDC force and pressure tests. One nozzle had a smooth external wall and the other a ribbed wall. Most of the results presented in this report were obtained with the ribbed $\epsilon = 22.1$ nozzle.

Ramjet

The two ramjet models shown in figure 3 were installed in place of the lower portion of the ventral fin on the airplane model. For the LaRC drag investigation, the model ramjet shown in figure 3(a) was used. Figure 3(b) shows the model ramjet used for the pressure investigation at LaRC and the force and pressure tests conducted at AEDC. This model (fig. 3(b)) was a shortened version of the previous model and provided improved simulation of the hypersonic research engine.

Pressure Instrumentation

The nozzle extensions used in the wind-tunnel pressure investigations (see fig. 2(d)) were instrumented with 17 pressure orifices, as shown in figure 4(a). Because of model symmetry, only one-half of the nozzle was instrumented. There were three rows of circumferential orifices, 5 orifices in each row, on the nozzle surface for a total of 15 nozzle surface orifices. Orifices 16 ($\theta = 177°$) and 17 ($\theta = 45°$) were on the aircraft flame shield. Because the nozzles were split along the vertical centerline, for ease of attachment, the upper and lower orifices were displaced 3° from this centerline.

Seven base pressure orifices were located on the model airplane base as shown in figure 4(b). Orifices 18 to 24 are on the bases of the fuselage, side fairings, upper vertical tail, and ventral fin.

WIND TUNNELS

The following table summarizes pertinent characteristics of the wind-tunnel facilities used in these nozzle-extension investigations. More detailed information on the tunnels is presented in reference 8 (AEDC) and reference 9 (LaRC).

	AEDC von Kármán Gas Dynamics Facility Tunnel B	Langley 4- by 4-foot Unitary Plan Tunnel, test section 2
Type	Continuous flow, closed circuit, variable density, interchangeable nozzles	Continuous flow, closed circuit, variable density, asymmetric sliding block nozzle
Test-section shape	Circular	Square
Test-section dimension	50 in. (127 cm) diameter	48 in. (122 cm)
Mach number range	6 and 8	2.29 to 4.65

TESTS

The nozzle-extension wind-tunnel investigations were conducted at LaRC ($M = 2.30$, 2.96, 3.95, and 4.63) and at AEDC ($M = 6.04$ and 8.01). Since it was desired to simulate only the portion of the X-15 flight after engine shutdown, there was no requirement for gas flow through the nozzles for these tests. Figure 5 shows the model installed in the AEDC von Kármán Gas Dynamics Facility Tunnel B. The average tunnel test conditions were as follows:

M_∞	Stagnation pressure, psia (kN/m^2)	Stagnation temperature, °R (°K)	N_{Re} per foot (per meter)	p_∞, psia (kN/m^2)	q_∞, psia (kN/m^2)
2.30	10.7 (73.8)	610 (339)	2.0×10^6 (6.56×10^6)	0.852 (5.874)	3.16 (21.79)
2.96	15.1 (104.1)	610 (339)	2.0×10^6 (6.56×10^6)	.435 (2.999)	2.67 (18.41)
3.95	26.9 (185.5)	635 (352)	2.0×10^6 (6.56×10^6)	.189 (1.303)	2.06 (14.20)
4.63	36.6 (252.3)	635 (352)	2.0×10^6 (6.56×10^6)	.108 (0.745)	1.62 (11.17)
6.04	190 (1310)	850 (472)	3.4×10^6 (1.12×10^7)	.114 (.786)	2.92 (20.13)
8.01	755 (5206)	1335 (741)	3.4×10^6 (1.12×10^7)	.079 (.545)	3.55 (24.48)

Force and moment tests were conducted at LaRC with the X-15-2 model alone and with the components shown in figures 2(a), 2(b), and 3(a). Force and moment tests at AEDC were conducted using the X-15-2 model and the components shown in figures 2(d) and 3(b). The X-15-2 alone was not tested at AEDC. Pressure tests at LaRC and AEDC were conducted using the model components shown in figures 2(d) and 3(b). The angle of attack ranged from -5° to 18° and sideslip angle was zero for all tests.

Figure 6 and the following table give details of the configurations used for the pressure tests. Reference 10 presents additional details on the AEDC tests.

Configuration number	Nozzle	δ_h, deg	δ_{sb}, deg	Ventral		Ramjet
				Stub	Lower	
1	Ribbed	0	0	On	On	Off
2	Ribbed	-35	0	On	On	Off
3	Ribbed	0	0	On	Off	Off
4	Ribbed	0	35	On	On	Off
5	Ribbed	-35	35	On	On	Off
6	Ribbed	0	0	On	Off	On
7	Smooth	0	0	On	On	Off
8*	Ribbed	-35	0	Off	Off	Off
9**	Ribbed	0	35	On	Off	On
10**	Ribbed	-35	35	On	Off	On
11**	Ribbed	-35	0	On	Off	On

*Tested at $M_\infty = 6.04$ only.

**Tested at $M_\infty = 6.04$ and 8.01 only.

Photographic coverage of the tests at both AEDC and LaRC included schlieren and oil-flow pictures.

DATA REDUCTION

Drag Coefficient

By using a single pressure measured in the sting cavity region, a base axial-force adjustment was made for the entire model base area, 21.82 in.^{2} (140.8 cm^2). This adjustment to the LaRC and AEDC drag data provided the overall drag coefficient C_{D_o} value with free-stream static pressure acting on the base of the model.

Pressures

Pressure measurements are presented in two forms: (1) as a pressure ratio $\left(\frac{p_l}{p_\infty}, \frac{p_{16}}{p_5}, \frac{p_{17}}{p_2}, \text{and } \frac{p_b}{p_a} = p_r\right)$ and (2) in terms of a pressure coefficient, $C_p = \frac{p_l - p_\infty}{q_\infty}$.

The pressure rise p_r across a shock wave existing on the nozzle extension was determined by using surface-pressure-orifice values at a given radial location θ. At the radial location of concern, the pressures ahead of and behind the shock were determined and used to calculate the pressure rise. For example, at $\theta = 45°$, pressures p_2, p_7, and p_{12} were considered.

ACCURACY

Tunnel operating experience indicates that the Mach number error is within ±0.01 for the AEDC tests and within ±0.01 for $M_\infty = 2.3$ and 2.96 and ±0.015 for $M_\infty = 3.95$ and 4.63 for the LaRC tests.

Based upon repeatibility during the tests and balance precision, the force and moment coefficient errors were no greater than the following:

C_{D_o}	±0.0010
C_m	±0.0017
C_L	±0.0006

Pressures were measured with the standard pressure systems of the AEDC and LaRC tunnels; these systems are described in references 8 and 11, respectively. The AEDC Tunnel B pressure data are accurate to ±0.003 psia (±0.0207 kN/m^2) or ±1.0 percent, whichever is greater. The error in the LaRC pressure data (ref. 11) is no greater than 2 percent for individual measurements.

The standard-deviation error in the pressure ratio $\frac{p_l}{p_\infty}$ was determined by taking the square root of the sum of the squares of the standard-deviation errors of the measured quantities (eq. 50 of ref. 12) as follows:

$$\sigma\left(\frac{p_l}{p_\infty}\right) = \left[(\sigma p_l)^2 + (\sigma p_\infty)^2\right]^{\frac{1}{2}} \tag{1}$$

The standard-deviation errors were taken as the errors cited.

Equation 37 of reference 12 was used to determine the standard-deviation error in the pressure coefficient C_p as follows:

$$\sigma(C_p) = \left[\left(\frac{\partial C_p}{\partial p_l}\right)^2 (\Delta p_l)^2 + \left(\frac{\partial C_p}{\partial p_\infty}\right)^2 (\Delta p_\infty)^2 + \left(\frac{\partial C_p}{\partial M_\infty}\right)^2 (\Delta M_\infty)^2\right]^{\frac{1}{2}} \tag{2}$$

The partial derivatives were obtained from the expression

$$C_p = \frac{(p_l - p_\infty)}{0.7 M_\infty{}^2 p_\infty}$$

Substituting the resulting values into equation (2) gives

$$\sigma(C_p) = \left\{\left[\frac{1}{0.7M_\infty{}^2 p_\infty}\right]^2 (\Delta p_l)^2 + \left[\frac{-p_l}{0.7M_\infty{}^2 p_\infty{}^2}\right]^2 (\Delta p_\infty)^2 + \left[\frac{-(p_l - p_\infty)}{0.35M_\infty{}^3 p_\infty}\right]^2 (\Delta M_\infty)^2\right\}^{\frac{1}{2}} \tag{3}$$

The standard deviations in pressure coefficients (using eq. (3)) and pressure ratios (using eq. (1)) were calculated for three different Mach numbers at two values of C_p, which cover the range of test values. The values of the various quantities were as follows:

M_∞	ΔM_∞	p_∞, psia (kN/m^2)	Δp_∞, psia (kN/m^2)	$C_p = 0$		$C_p = 0.3$	
				p_l, psia (kN/m^2)	Δp_l, psia (kN/m^2)	p_l, psia (kN/m^2)	Δp_l, psia (kN/m^2)
2.3	0.01	0.852 (5.874)	±0.0170 (0.117)	0.852 (5.874)	±0.0170 (0.117)	1.798 (12.397)	±0.0360 (0.248)
4.63	.015	.108 (.745)	±.0022 (.015)	.108 (.745)	±.0022 (.015)	.594 (4.095)	±.0199 (.137)
8.01	.01	.079 (.545)	±.0030 (.021)	.079 (.545)	±.0030 (.021)	1.143 (7.881)	±.0114 (.079)

Substituting the above values into equations (1) and (3) gives the following standard deviations:

σ	M_∞		
	2.3	4.63	8.01
$C_p = 0$			
$\frac{p_l}{p_\infty}$	±0.024	±0.0031	±0.0042
C_p	±.008	±.002	±.001
$C_p = 0.3$			
$\frac{p_l}{p_\infty}$	±.04	±.01	±.01
C_p	±.016	±.011	±.013

RESULTS AND DISCUSSION

Force-Test Results

The main objective of the initial LaRC force tests was to determine the drag of the various nozzle extensions and, thus, to be able to evaluate these extensions from a thrust-minus-drag, or airplane performance, standpoint. A secondary objective of these tests was the determination of the static-margin characteristics of the X-15-2 airplane equipped with the nozzle extensions.

Effect of nozzle shape.– Figures 7(a) and 7(b) present, as a function of Mach number, the zero-lift drag coefficient C_{D_o} for the X-15-2 model alone and with several of the nozzle-extension configurations tested. The zero-lift drag-coefficient increment due to adding the dummy ramjet to the X-15-2 model was approximately constant (increment approximately 0.0070) for the Mach 2.3 to 4.63 range. The drag coefficient of the X-15-2 with the ramjet is not shown since it did not appear to affect the drag increments due to the nozzle extensions. The effect of adding shrouded nozzle extensions (see fig. 2(b)) to the basic X-15-2 model is shown in figure 7(a) for the test Mach number range from 2.3 to 4.63. Figure 7(b) shows the effect on the overall drag of adding unshrouded nozzle extensions (see fig. 2(a)). For the unshrouded nozzle extensions, the test Mach numbers ranged from 2.3 to 4.63, except for the $\epsilon = 22.1$ extension with no manifold. For this nozzle extension, the data ranged from $M_\infty = 2.3$ to 8.

The largest differences in the measured drag coefficients occurred at the lowest Mach numbers tested. Adding nozzle extensions to the basic airplane generally caused an increase in drag coefficient. However, the differences in drag approached the measurement uncertainty of $C_{D_o} = \pm 0.0010$, so that only a slight drag penalty can be attributed to the nozzle extensions.

A representative plot of pitching-moment coefficient C_m as a function of lift coefficient C_L for several configurations is presented in figure 8 for a free-stream Mach number of 4.63. No significant differences in C_m versus C_L resulted when $\epsilon = 22.1$ and $\epsilon = 33.6$ nozzles were added to the model at $\delta_h = 0°$ and $\delta_h = -20°$, which indicates no change in static margin. Test results using a smaller model (ref. 13) for the same horizontal-tail setting and no nozzle extensions are compared with the present data in figure 8. This comparison shows good agreement. Similar results for $\delta_h = 0°$ were obtained at the other test Mach numbers. These results indicate that the static margin of the airplane would not be affected significantly by the addition of nozzle extensions.

Effect of nozzle expansion ratio.– To investigate the effects of nozzle expansion ratio on X-15-2 performance, several performance calculations were made on the X-15 six-degree-of-freedom flight simulator. Overall X-15-2 performance in terms of increased burnout velocity for the various nozzle expansion ratios is shown in figure 9. These performance figures are based on the following X-15-2 conditions:

Launch weight, lb (kg)	54,217 (24,592)
Burnout weight, lb (kg)	19,073 (8,651)
Total burn time, sec	150.3
Drag for nozzle extension	None
Drag for ablatives	None
Launch conditions –	
Altitude, ft (m)	43,500 (13,259)
Airspeed, ft/sec (m/sec)	770 (235)
Vacuum thrust (lb (kg)) for expansion ratios of –	
9.8 (basic YLR99 engine)	58,500 (26,535)
22.1	62,200 (28,213)
28.8	63,000 (28,576)
33.6	63,400 (28,758)

Full-power ascents were performed at various climb angles to achieve burnout altitudes of 85,000 feet (26,000 meters), 103,000 feet (31,400 meters), and 123,000 feet (37,500 meters).

The data of figure 9 indicate that increasing the expansion ratio from 9.8 to 22.1 increased the burnout velocity by about 400 feet per second (122 meters per second), depending on the burnout altitude. A further increase of approximately 70 feet per second (21.3 meters per second) is realized in going from $\epsilon = 22.1$ to $\epsilon = 28.8$, which appears to be an optimum expansion ratio.

Effect of afterbody flows. – The results of reference 14 indicate that afterbody flows can cause strong shock waves to impinge on the unshrouded nozzle extension. Since the nozzle extension would be used in conjunction with a ramjet attached to the stub ventral (ref. 4), the possibility of ramjet exhaust-gas impingement on the extension was considered. The study of reference 15 indicated that ramjet exhaust-plume impingement occurred near the nozzle exit plane during simulated ramjet operation for exit-to-ambient static-pressure ratios of about 10. This nozzle extension was approximately equivalent to the $\epsilon = 33.6$ nozzle.

Center-of-gravity considerations. – Additions to the X-15-2 airplane which cause aft center-of-gravity shifts must be carefully considered because of possible stability problems. Since the weight of the ramjet and its associated hardware would cause the aft center-of-gravity limit to be approached on the X-15-2, the additional weight of the nozzle extension becomes critical. Accordingly, the lightest nozzle extension is desired.

Final selection of nozzle extension. – Considering the effects of nozzle-extension shape, expansion ratio, afterbody flow impingement, and weight discussed in the preceding sections, it was decided to conduct the pressure tests with the $\epsilon = 22.1$ nozzle extension only.

Pressure-Test Results

Results from the nozzle-extension wind-tunnel pressure investigations at the LaRC and AEDC facilities are presented in table I. Pressure coefficients C_p are listed by test configuration for the 24 pressure orifices at the various Mach numbers and angles of attack tested with each configuration. For each of the 11 configurations, the maximum and minimum pressure coefficients are noted for each Mach number.

Base pressures. – Base pressure coefficients are shown in figures 10(a) and 10(b) for an angle of attack approximately equal to zero. The data for configuration 1 are presented in figure 10(a). These results are typical of those configurations characterized by undeflected stabilizers and speed brakes. The ramjet configuration (see configuration 6, fig. 6) is included in this category. The data agree with the empirical relationship $C_{p,b} = -\frac{1}{M_\infty^2}$ (ref. 16) at the higher Mach numbers. Less favorable agreement with $C_{p,b} = -\frac{1}{M_\infty^2}$ is noted for the lower Mach numbers, especially for orifices 16 and 17.

The results for configuration 2 are presented in figure 10(b). Although configuration 2 has the speed brakes closed, these results are representative of those configurations having either or both speed brakes and horizontal tails deflected. The data of figure 10(b) for $M_\infty > 4$ have the same level and trend as the corresponding data of figure 10(a). For $M_\infty < 4$, the data agree with the empirical relationship $C_{p,b} = -\frac{1}{M_\infty^2}$ except along the upper vertical tail and on the flame shield. A large variation in $C_{p,b}$ is noted on the upper vertical tail at $M_\infty = 2.3$.

Figure 11 shows angle-of-attack effects on the base pressure coefficients for configuration 1. These results are typical of those from the other configurations tested. The results indicate that base pressures along the upper half (orifices 19 and 21) of the X-15-2 base remained constant over the angle-of-attack range at a given Mach number. Similar results were found for the side-fairing base pressure coefficients. Along the bottom of the base (orifices 16 and 23), the pressure coefficients at a given Mach number remained relatively constant for $\alpha = -5°$ to $4°$ but increased markedly ($C_{p,b}$ in positive direction) as angle of attack increased from 4° to 18°. The pressure coefficient for orifice 18 showed the same trend as for orifices 16 and 23, as indicated in table I.

A comparison of the base pressures on X-15 models with and without nozzle extensions is shown in figure 12. Data for 1/15-scale and 1/50-scale X-15 models without nozzle extensions were obtained from references 7, 17, and 18. Over the Mach number range of 2.3 to approximately 4.7, where comparisons can be made, the results indicate that the nozzle extension slightly increased the base pressure ($C_{p,b}$ more positive) on the model. This result indicates that the expected increase in overall drag due to the addition of the nozzle extension was offset by the increased base pressure (decreased base drag). This increase in base pressure is believed to be the reason that the overall drag was only slightly increased when the nozzle extensions were added to the X-15-2.

Reference 19 compares model and flight base-pressure-coefficient data for the X-15 without nozzle extensions for free-stream Mach numbers up to 6.

Nozzle-extension surface pressures. – Nozzle-extension surface-pressure ratios $\frac{p_l}{p_\infty}$ are plotted in terms of longitudinal station $\frac{x}{l}$ for test configurations 1, 2, 4, and 5 in figures 13(a) to 13(d), respectively. Three Mach numbers ($M_\infty = 2.30$, 4.63, and 8.01) are considered at an angle of attack of approximately zero. The data were faired along lines where the radial location was constant at 3°, 45°, 90°, 135°, and 177°. For fairing purposes, pressure p_{18} was considered to be located at $\theta = 177°$ instead of at 180°.

Configurations having $\delta_h = 0°$ and $\delta_{sb} = 0°$, as typified by configuration 1, showed the following common trends (see fig. 13(a)). Steep pressure-ratio variations occurred at $\theta = 45°$ and 135° as $\frac{x}{l}$ increased from about 0.5 to 1.0. At these angular locations, peak pressure ratios occurred at $\frac{x}{l}$ near 1.0, the end of the nozzle extension. These steep rises are similar to pressure rises across trailing-shock waves (ref. 14). At $M_\infty = 2.3$, the peak value of $\frac{p_l}{p_\infty}$ for $\theta = 45°$ was high, diminished at $M_\infty = 4.63$, and increased at $M_\infty = 8.01$. However, at $\theta = 135°$, the peak value of $\frac{p_l}{p_\infty}$ increased steadily with increasing Mach number. In general, $\frac{p_l}{p_\infty}$ for $\theta = 3°$, 90°, and 177° remained low and unchanged at all Mach numbers, indicating a masking effect due to the upper vertical tail, the left side fairing, and the lower vertical tail, respectively. For $\frac{x}{l} = 0.167$ (flame-shield location) and $\theta = 177°$, a large value of $\frac{p_l}{p_\infty}$ is noted at $M_\infty = 4.63$. The trends discussed for configuration 1 also apply to configuration 6 (ramjet on).

Configuration 2 results (fig. 13(b)) indicate that deflecting the horizontal tail, leading edge down 35° ($\delta_h = -35°$), markedly changed the pressure distributions on the nozzle extension from those obtained with the undeflected tail (configuration 1, fig. 13(a)). Peak pressure ratios at $\theta = 45°$ and $\frac{x}{l} = 0.633$ are noted for all Mach numbers. This increase in maximum pressure at $\theta = 45°$ appears to be 2 to 4 times larger than the $\theta = 45°$ pressures for the undeflected ($\delta_h = 0°$) tail for the Mach numbers shown. This result indicates that the trailing-shock wave increased in strength and moved forward on the nozzle extension at $\theta = 45°$ for this configuration. The pressures at $\theta = 135°$ did not appear to be affected by the trailing-shock wave. The pressures at $\theta = 3°$, 90°, and 177° remained relatively unchanged through the Mach number range.

Opening the speed brakes ($\delta_{sb} = 35°$, fig. 13(c)) also caused changes in the nozzle surface pressures $\frac{p_l}{p_\infty}$ from the undeflected speed-brake position (fig. 13(a)). The peak pressure along $\theta = 45°$ was approximately halved at $M_\infty = 2.3$, remained relatively unchanged at $M_\infty = 4.63$, and increased at $M_\infty = 8.01$.

The combined effects on nozzle-extension pressures of deflecting the horizontal tail ($\delta_h = -35°$) and opening the speed brakes ($\delta_{sb} = 35°$) are presented in figure 13(d) (configuration 5). The largest pressure ratios occurred along $\theta = 45°$ and increased with increasing Mach number. Pressures at $\theta = 3°$, $90°$, $135°$, and $177°$ were on the order of $\frac{p_l}{p_\infty} = 0.2$ to 0.4 for $M_\infty = 2.30$ and 4.63, then doubled in magnitude at $M_\infty = 8.01$. Results for the other test configurations are presented in table I.

Angle-of-attack effects on the nozzle-extension pressure ratios for configuration 1 are shown in figure 14 for angles of attack of approximately 0°, 8°, and 17° for $M_\infty = 2.30$ (fig. 14(a)), $M_\infty = 4.63$ (fig. 14(b)), and $M_\infty = 8.01$ (fig. 14(c)). The results indicate that $\frac{p_l}{p_\infty}$ for $\theta = 3°$ decreased slightly with increasing Mach number and changed little with angle of attack. However, for $\theta = 45°$, the value of $\frac{p_l}{p_\infty}$ generally decreased (except at $M_\infty = 8.01$ and $\alpha = 15.92°$) with increasing angles of attack at a given Mach number.

At $\theta = 90°$ the pressures showed mixed effects with increasing angles of attack at a given Mach number. The maximum values of $\frac{p_l}{p_\infty}$ occurred at $\alpha = 8.83°$ for $M_\infty = 2.30$, $\alpha = 17.05°$ for $M_\infty = 4.63$, and $\alpha = 15.92°$ for $M_\infty = 8.01$. These maximum values of $\frac{p_l}{p_\infty}$ remained the same in magnitude for $M_\infty = 2.3$ to 4.63 but increased sharply in magnitude at $M_\infty = 8.01$, suggesting that the trailing-shock wave had become stronger.

An opposite trend in pressures for $\theta = 135°$, when compared with $\theta = 45°$ results, occurred with increasing angle of attack and Mach number. Along $\theta = 177°$ the pressures increase with increasing angle of attack . For the high angles of attack the maximum pressures increased with increasing Mach number. Results for the other configurations are shown in table I.

Figures 13 and 14 showed that there were large variations in the circumferential pressures on the nozzle extension as a function of the test variables and configurations. The pressure-coefficient distributions around the nozzle at $\frac{x}{l} = 0.367$, 0.633, and 0.900 are presented in figure 15 as a function of the circumferential location and angle of attack for configurations 8 (fig. 15(a)), 9 (fig. 15(b)), and 10 (fig. 15(c)) at a Mach number of 6.04. These results indicate that at $\frac{x}{l} = 0.367$ the pressure coefficients remained unaffected by the angle-of-attack and configuration changes. For $\frac{x}{l} > 0.367$, the effect of increased angle of attack was to increase the pressure in the bottom region of the nozzle extension. This effect increases with increasing downstream distance on the nozzle extension.

The limited test results obtained with the smooth-wall nozzle extension (configuration 7) were compared with the ribbed-wall nozzle-extension results (configuration 1). Small pressure differences were noted for corresponding orifices, but these effects were mixed and varied both with angle of attack and Mach number, although the trends were similar to those of the ribbed-nozzle extension.

Flame-shield pressures. – The measured flame-shield peak pressure ratios $\frac{p_{16}}{p_\infty}$ and $\frac{p_{17}}{p_\infty}$ shown in figures 13 and 14 are believed to have resulted from the pressurizing effect due to recirculating flow. An analysis of LaRC schlieren photographs and AEDC oil-flow photographs suggests that the shock-wave system at $\theta = 135°$ and surface flows, at both $\theta = 45°$ and 135°, on the extension are as shown in the following sketches:

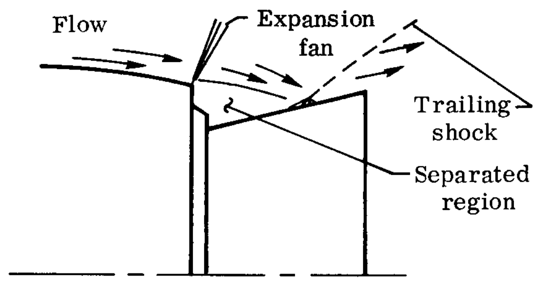

Shock-wave system

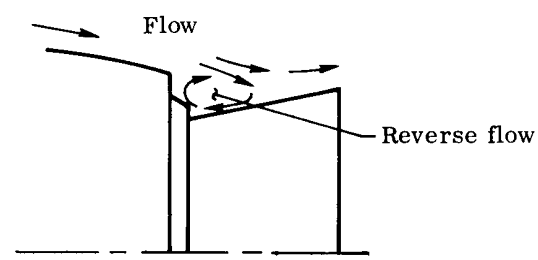

Surface oil flows

These results and the trends in pressure variation (fig. 13) agree qualitatively with the flow model of reference 14, as shown in the sketch below:

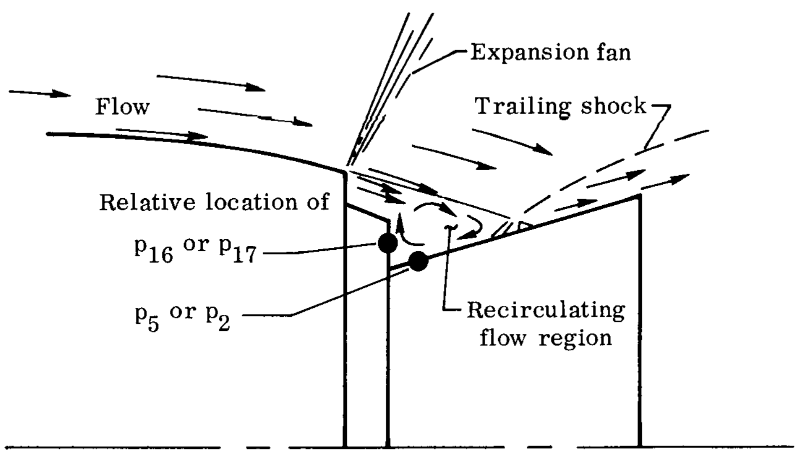

Figure 16 presents the pressure ratios $\frac{p_{16}}{p_5}$ ($\theta = 177°$) and $\frac{p_{17}}{p_2}$ ($\theta = 45°$) for configuration 1 at three angles of attack for $M_\infty = 2.3$ to 8. It is believed that these pressure ratios indicate the amount of recirculation on the nozzle extension and flame shield. The results show that increasing recirculation occurred with increasing Mach number up to $M_\infty = 4.63$, with little recirculation at $M_\infty = 6$ and 8 for $\theta = 177°$. At $\theta = 45°$, the amount of recirculation was significantly less than at $\theta = 177°$ for $M_\infty = 2.3$ to 4.63 and slightly less at $M_\infty = 6$ and 8. The difference in the amount of recirculation between $\theta = 45°$ and 177° for $M_\infty < 4.7$ is attributed to the masking effect of the lower vertical tail. In general, increased angle of attack did not appreciably affect the amount of recirculation.

Trailing-shock strength. – To assess the strength of the trailing-shock wave on the nozzle extension, the pressures ahead of the shock wave p_a and behind the shock wave p_b were considered. The ratio $\frac{p_b}{p_a} = p_r$ indicates the strength of the shock wave. This pressure rise p_r is plotted against Mach number in figure 17 for configuration 1 at three angles of attack. Since the largest pressures occurred at $\theta = 45°$ and 135°, only results in these regions are shown.

A Mach number increase from 2.3 to 6 caused the pressure rise (shock strength) at $\theta = 135°$ to increase markedly. Above $M_\infty = 6$, p_r remained relatively unchanged for given angles of attack. Along $\theta = 45°$, there were mixed effects for $\alpha = 0°$ and 8° with increasing Mach number. However, for $\alpha \approx 17°$ ($\theta = 45°$), p_r decreased with increasing Mach number above 2.96. Above $M_\infty = 4$, the shock strength along $\theta = 135°$ was stronger than along $\theta = 45°$ at all angles of attack.

For $\alpha = 0°$, the peak value of p_r ($\theta = 135°$) was 4.7 at $M_\infty = 6$. Along $\theta = 45°$ a maximum pressure rise of 4 occurred at $\alpha = 0°$ and $M_\infty = 6$. Increasing angle of attack caused p_r to decrease for $\theta = 45°$. Strong angle-of-attack effects on p_r along $\theta = 135°$ are shown, with p_r increasing with increased angle of attack except for $\alpha \approx 17°$ above $M_\infty = 5$. A maximum p_r of 9.3 occurred at $\alpha \approx 17°$ and $M_\infty = 4.63$.

CONCLUSIONS

Wind-tunnel force and pressure tests of rocket-engine nozzle extensions on the 0.0667-scale X-15-2 model were made over the free-stream Mach number range from about 2.3 to 8. These tests, which included the effects of an aft-mounted ramjet shape and control-surface deflections, led to the following conclusions:

1. The addition of any of the nozzle extensions did not appreciably affect the overall airplane drag or static margin. The nozzle extension having a 22.1 expansion ratio was found to be the most suitable. Increasing the rocket-engine expansion ratio from 9.8 to 22.1 increased the calculated airplane burnout velocity by about 400 feet per second (122 meters per second).

2. The design of a nozzle extension should consider the measured large variations in both the circumferential and longitudinal pressure distributions and the

shock-impingement effects on the nozzle. Deflecting the speed brakes and horizontal tail significantly affected the nozzle pressures, whereas the addition of the model ramjet did not have an effect.

3. The nozzle extension increased the base pressure of the X-15-2 model over that for X-15 models having no nozzle extensions. For free-stream Mach numbers greater than 4, the base pressure coefficients agreed with the empirical expression $C_{p,b} = -\frac{1}{{M_\infty}^2}$, in which the base pressure coefficient is equal to the negative reciprocal of the free-stream Mach number squared.

Flight Research Center,
National Aeronautics and Space Administration,
Edwards, Calif., November 15, 1968,
729-00-00-01-24.

REFERENCES

1. Bellman, Donald R.; and Kleinkneckt, Kenneth S.: Operational Experience With Rocket Propelled Airplanes. Presented at the IAS Eleventh Annual Flight Propulsion Meeting, Cleveland, Ohio, March 9, 1956. (Available from ASTIA as AD-83 378.)

2. Davies, Harold: The Design and Development of the Thiokol XLR99 Rocket Engine for the X-15 Aircraft. J. Roy. Aeron. Soc., vol. 67, no. 626, Feb. 1963, pp. 79-91.

3. Maher, James F.; Ottinger, C. Wayne; and Capasso, Vincent N., Jr.: YLR99-RM-1 Rocket Engine Operating Experience in the X-15 Aircraft. NASA TN D-2391, 1964.

4. Rubert, Kennedy F.: Hypersonic Air-Breathing Propulsion-System Testing on the X-15. Progress of the X-15 Research Airplane Program, NASA SP-90, 1965, pp. 127-132.

5. Mechtly, E. A.: The International System of Units - Physical Constants and Conversion Factors. NASA SP-7012, 1964.

6. Patterson, James C., Jr.: Aerodynamic Characteristics of a 0.0667-Scale Model of the X-15A-2 Research Airplane at Transonic Speeds. NASA TM X-1198, 1966.

7. Franklin, Arthur E.; and Lust, Robert M.: Investigation of the Aerodynamic Characteristics of a 0.067-Scale Model of the X-15 Airplane (Configuration 3) at Mach Numbers of 2.29, 2.98, and 4.65. NASA TM X-38, 1959.

8. Anon.: Test Facilities Handbook. Sixth ed., vol. 4, Arnold Eng. Dev. Center, Nov. 1966.

9. Schaefer, William T., Jr.: Characteristics of Major Active Wind Tunnels at the Langley Research Center. NASA TM X-1130, 1965.

10. Burchfield, C. G.: Pressure, Static Stability, and Drag Tests of a 0.0667-Scale Model of the X-15-2 Research Airplane. AEDC-TR-67-34, Arnold Eng. Dev. Center, Mar. 1967.

11. Anon.: Manual for Users of the Unitary Plan Wind Tunnel Facilities of the National Advisory Committee for Aeronautics. NACA, 1956.

12. Beers, Yardley: Introduction to the Theory of Error. Second ed., Addison-Wesley Publishing Co., Inc., 1962.

13. Weaver, Robert W.: Tests of the X-15 Model for NASA Flight Research Center in the JPL 20-Inch Supersonic and 21-Inch Hypersonic Wind Tunnels. WT 20-561, Jet Propulsion Lab., Calif. Inst. of Tech., June 15, 1964.

14. Beheim, Milton A.: Flow in the Base Region of Axisymmetric and Two-Dimensional Configurations. NASA TR R-77, 1961.

15. Andrews, Earl H., Jr.; and Rogers, R. Clayton: Study of Underexpanded Exhaust Jets of an X-15 Airplane Model and Attached Ramjet Engine Simulator at Mach 6.86. NASA TM X-1571, 1968.

16. Stallings, Robert L., Jr.: Experimentally Determined Local Flow Properties and Drag Coefficients for a Family of Blunt Bodies at Mach Numbers From 2.49 to 4.63. NASA TR R-274, 1967.

17. Franklin, Arthur E.; and Silvers, H. Norman: Investigation of the Aerodynamic Characteristics of a 0.067-Scale Model of the X-15 Airplane (Configuration 2) at Mach Numbers of 2.29, 2.98, 3.96, and 4.65. NASA Memo 4-27-59L, 1959.

18. Leupold, Mathias J.; and Freeman, Elizabeth M.: A Second Series of Supersonic Force Tests on the Full-Span Model X-15 for North American Aviation Incorporated. WTR 200, Mass. Inst. of Tech. (Naval Supersonic Laboratory), Sept. 1958.

19. Saltzman, Edwin J.: Base Pressure Coefficients Obtained From the X-15 Airplane for Mach Numbers Up to 6. NASA TN D-2420, 1964.

TABLE I.– TEST RESULTS

(a) Configuration 1 ($\delta_h = 0°$, $\delta_{sb} = 0°$, ventral on).

Orifice number	$M_\infty = 2.30$					$M_\infty = 2.96$					$M_\infty = 3.95$				
	C_p for α =					C_p for α =					C_p for α =				
	-4.94°	-0.41°	4.21°	8.83°	18.26°	-4.86°	-0.51°	3.90°	8.32°	17.27°	-4.40°	-0.20°	4.05°	8.31°	16.97°
1	-0.164	-0.164	-0.152	-0.143	-0.154	-0.109	-0.111	-0.105	-0.106	-0.113	-0.062	-0.060	-0.059	-0.061	-0.062
2	-.155	-.159	-.154	-.146	-.163	-.116	-.107	-.106	-.113	-.110	-.062	-.060	-.060	-.063	-.065
3	-.154	-.150	-.146	-.145	-.155	-.103	-.098	-.099	-.094	-.105	-.059	-.056	-.054	-.057	-.064
4	-.150	-.143	-.147	-.140	-.156	-.099	-.099	-.096	-.099	-.086	-.064	-.060	-.059	-.061	-.046
5	-.147	-.142	-.144	-.136	-.068	-.099	-.099	-.096	-.085	-.032	-.064	-.060	-.060	-.057	-.019
6	-.150	-.152	-.145	-.145	-.154	-.103	-.103	-.104	-.105	-.113	-.060	-.060	-.059	-.062	-.064
7	.002	-.033	-.089	-.127	-.157	-.015	-.048	-.052	-.083	-.075	-.031	-.048	-.028	-.051	-.065
8	-.165	-.156	-.145	-.134	-.172	-.109	-.099	-.094	-.089	-.119	-.062	-.056	-.054	-.059	-.064
9	-.142	-.141	-.135	-.117	.091	-.092	-.080	-.075	-.023	.133	-.055	-.051	-.030	.054	.262*
10	-.139	-.136	-.131	-.104	.026	-.095	-.091	-.085	-.062	.026	-.062	-.059	-.056	-.046	.012
11	-.117	-.122	-.130	-.139	-.149	-.088	-.091	-.094	-.099	-.103	-.056	-.057	-.056	-.060	-.061
12	.080	.065	.011	-.040	-.093	.068	.037	.012	-.025	-.054	.047	-.001	-.007	-.034	-.061
13	-.112	-.101	-.098	-.082	-.175	-.092	-.077	-.060	-.068	-.122	-.056	-.049	-.046	-.054	-.038
14	-.058	-.069	-.044	.020	.157*	-.033	-.013	.013	.058	.161*	-.004	.002	.024	.013	.130
15	-.117	-.110	-.091	-.045	.075	-.081	-.073	-.057	-.017	.083	-.057	-.052	-.044	-.014	.075
16	-.131	-.125	-.120	-.120	-.037	-.082	-.082	-.073	-.051	.005	-.043	-.041	-.039	-.031	.028
17	-.152	-.155	-.148	-.141	-.156	-.104	-.104	-.102	-.106	-.114	-.058	-.059	-.058	-.061	-.062
18	-.145	-.141	-.148	-.141	-.084	-.110	-.096	-.098	-.092	-.044	-.062	-.060	-.058	-.053	-.020
19	-.161	-.160	-.151	-.145	-.152	-.107	-.105	-.104	-.107	-.103	-.062	-.060	-.059	-.059	-.061
20	-.163	-.159	-.152	-.142	-.156	-.103	-.105	-.098	-.095	-.120	-.061	-.059	-.056	-.060	-.067
21	-.168	-.178	-.171	-.166	-.185	-.113	-.115	-.114	-.111	-.113	-.064	-.066	-.068	-.067	-.066
22	-.173	-.164	-.165	-.163	-.190*	-.116	-.110	-.113	-.121	-.109	-.066	-.066	-.067	-.066	-.065
23	-.176	-.175	-.171	-.159	-.103	-.126*	-.123	-.115	-.102	-.060	-.072*	-.071	-.067	-.060	-.037
24	-.161	-.162	-.155	-.143	-.158	-.104	-.102	-.099	-.097	-.114	-.061	-.058	-.057	-.059	-.067

*Maximum or minimum value.

TABLE I.– TEST RESULTS - Continued

(a) Configuration 1 ($\delta_h = 0°$, $\delta_{sb} = 0°$, ventral on) - Concluded.

Orifice number	$M_\infty = 4.63$					$M_\infty = 6.04$					$M_\infty = 8.01$				
	C_p for α =					C_p for α =					C_p for α =				
	-3.89°	0.23°	4.42°	8.59°	17.05°	-4.01°	-0.01°	4.01°	8.01°	16.03°	-4.00°	0.00°	4.01°	8.01°	15.92°
1	-0.043	-0.040	-0.041	-0.041	-0.042	-0.030	-0.029	-0.029	-0.029	-0.027	-0.015	-0.016	-0.015	-0.015	-0.015
2	-.044	-.042	-.041	-.043	-.043	-.024	-.029	-.029	-.029	-.028	-.011	-.014	-.015	-.016	-.014
3	-.042	-.040	-.039	-.040	-.039	-.028	-.027	-.026	-.029	-.031*	-.015	-.015	-.015	-.016	-.015
4	-.044	-.044	-.043	-.043	-.029	-.029	-.028	-.027	-.023	.002	-.014	-.014	-.014	-.011	.012
5	-.046	-.044	-.043	-.040	-.015	-.029	-.028	-.026	-.017	.008	-.016	-.015	-.013	-.006	.014
6	-.042	-.040	-.041	-.041	-.042	-.029	-.029	-.029	-.029	-.028	-.014	-.015	-.015	-.015	-.016
7	-.033	-.037	-.037	-.041	-.043	.001	-.010	-.023	-.028	-.029	.001	.000	-.014	-.016	-.007
8	-.044	-.040	-.040	-.046	-.039	-.031	-.027	-.027	-.029	.000	-.016	-.015	-.015	-.017	.003
9	-.037	-.032	-.018	.074	.284*	-.023	-.020	.006	.097	.280*	-.012	-.008	.006	.070	.229*
10	-.046	-.043	-.041	-.032	.006	-.029	-.027	-.022	-.008	.026	-.016	-.014	-.010	-.001	.027
11	-.039	-.039	-.040	-.041	-.040	-.027	-.028	-.028	-.029	-.028	-.014	-.015	-.015	-.015	-.016
12	.014	-.015	-.019	-.030	-.042	.031	.002	-.006	-.020	-.030	.013	.002	-.007	-.014	-.016
13	-.039	-.036	-.036	-.041	-.019	-.024	-.022	-.023	-.018	-.002	-.015	-.012	-.016	-.007	.009
14	-.005	.007	.021	.021	.137	-.007	.015	.011	.041	.148	-.007	.014	.021	.044	.163
15	-.042	-.039	-.032	-.008	.063	-.026	-.023	-.016	.005	.070	-.015	-.012	-.008	.004	.065
16	-.016	-.016	-.021	-.009	.023	-.029	-.027	-.024	-.014	.020	-.015	-.015	-.012	-.005	.023
17	-.033	-.036	-.037	-.040	-.040	-.029	-.027	-.028	-.028	-.028	-.015	-.015	-.015	-.015	-.014
18	-.043	-.042	-.041	-.035	-.007	-.029	-.028	-.025	-.017	.014	-.016	-.015	-.013	-.006	.015
19	-.044	-.042	-.041	-.040	-.042	-.030	-.029	-.026	-.027	-.027	-.016	-.016	-.015	-.014	-.015
20	-.044	-.042	-.040	-.044	-.044	-.029	-.026	-.026	-.028	-.027	-.016	-.014	-.015	-.015	-.016
21	-.044	-.044	-.046	-.046	-.042	------	------	------	------	------	-.013	-.016	-.016	-.015	-.015
22	-.044	-.046	-.046	-.046	-.040	------	------	------	------	------	-.014	-.016	-.017*	-.017	-.014
23	-.049*	-.049	-.046	-.041	-.023	------	------	------	------	------	------	------	------	------	------
24	-.043	-.040	-.041	-.044	-.044	-.028	-.025	-.026	-.029	-.031	-.015	-.013	-.015	-.016	-.016

*Maximum or minimum value.

TABLE I. – TEST RESULTS - Continued

(b) Configuration 2 (δ_h = -35°, δ_{sb} = 0°, ventral on).

Orifice number	M_∞ = 2.30					M_∞ = 2.96					M_∞ = 3.95				
	C_p for α =					C_p for α =					C_p for α =				
	-5.04°	-0.53°	4.11°	8.70°	18.10°	-4.91°	-0.61°	3.83°	8.22°	17.15°	-4.43°	0.25°	4.01°	8.23°	16.90°
1	-0.142	-0.162	-0.162	-0.169	-0.167	-0.093	-0.103	-0.110	-0.111	-0.109	-0.051	-0.054	-0.061	-0.064	-0.066
2	.032	-.002	.003	-.124	-.166	.104	.011	-.006	-.090	-.110	.083	.011	-.033	-.055	-.067
3	-.179	-.175	-.178	-.170	-.162	-.114	-.118	-.112	-.106	-.107	-.066	-.065	-.071*	-.059	-.061
4	-.165	-.172	-.167	-.153	-.163	-.108	-.114	-.110	-.106	-.101	-.064	-.064	-.063	-.062	-.052
5	-.167	-.171	-.164	-.155	-.100	-.109	-.115	-.110	-.104	-.064	-.064	-.064	-.064	-.062	-.038
6	-.111	-.128	-.137	-.144	-.161	-.068	-.082	-.092	-.100	-.109	-.032	-.034	-.046	-.060	-.066
7	.282	.328*	.264	.133	-.063	.203	.221*	.140	.079	-.082	.205*	.162	.185	.010	-.056
8	-.190	-.194	-.201*	-.183	-.155	-.119	-.122	-.115	-.106	-.109	-.068	-.068	-.062	-.057	-.066
9	-.152	-.160	-.155	-.149	-.102	-.104	-.102	-.093	-.092	-.011	-.062	-.057	-.055	-.056	.022
10	-.154	-.165	-.153	-.147	-.067	-.104	-.110	-.106	-.100	-.043	-.063	-.062	-.062	-.059	-.022
11	-.077	-.107	-.091	-.110	-.145	-.043	-.054	-.067	-.084	-.106	-.013	-.016	-.033	-.054	-.065
12	.012	-.018	-.037	.014	-.069	.052	.046	.033	-.002	-.065	.068	.094	.049	-.004	-.035
13	-.105	-.133	-.175	-.159	-.145	-.063	-.074	-.097	-.089	-.103	-.032	-.044	-.053	-.053	-.061
14	-.121	-.105	-.078	-.106	-.009	-.080	-.056	-.042	.005	.081	-.040	-.040	-.027	.017	.129
15	-.139	-.150	-.137	-.128	-.020	-.095	-.102	-.087	-.083	-.019	-.061	-.060	-.052	-.043	.034
16	-.151	-.159	-.148	-.145	-.083	-.093	-.103	-.094	-.092	-.052	-.045	-.044	-.043	-.042	-.019
17	-.168	-.176	-.173	-.171	-.166	-.093	-.100	-.101	-.110	-.109	-.047	-.040	-.059	-.062	-.065
18	-.163	-.170	-.166	-.163	-.115	-.110	-.115	-.111	-.106	-.071	-.063	-.064	-.062	-.060	-.037
19	-.192	-.187	-.177	-.175	-.167	-.116	-.117	-.112	-.111	-.109	-.063	-.063	-.064	-.063	-.066
20	-.177	-.180	-.175	-.168	-.156	-.110	-.114	-.111	-.107	-.106	-.063	-.064	-.062	-.061	-.065
21	-.110	-.144	-.132	-.134	-.181	-.097	-.100	-.104	-.102	-.122	-.053	-.052	-.059	-.057	-.070
22	-.110	-.110	-.123	-.129	-.195	-.095	-.098	-.104	-.101	-.119	-.050	-.050	-.056	-.057	-.068
23	-.169	-.176	-.178	-.188	-.159	-.119	-.124*	-.119	-.111	-.083	-.070	-.070	-.066	-.064	-.043
24	-.177	-.175	-.173	-.171	-.161	-.110	-.113	-.110	-.106	-.108	-.063	-.064	-.062	-.060	-.066

* Maximum or minimum value.

TABLE I. – TEST RESULTS - Continued

(b) Configuration 2 (δ_h = -35°, δ_{sb} = 0°, ventral on) - Concluded.

Orifice number	M_∞ = 4.63					M_∞ = 6.04					M_∞ = 8.01				
	C_p for α =					C_p for α =					C_p for α =				
	-3.92°	0.19°	4.40°	8.54°	16.99°	-4.00°	0.00°	3.98°	8.00°	16.00°	-4.00°	0.01°	3.99°	8.01°	15.99°
1	-0.035	-0.038	-0.041	-0.043	-0.046	-0.020	-0.026	-0.028	-0.030*	-0.029	-0.013	-0.014	-0.014	-0.016	-0.016
2	.049	-.007	-.030	-.043	-.046	.006	-.024	-.027	-.028	-.027	.001	-.010	-.014	-.015	-.016
3	-.046	-.046	-.042	-.042	-.043	-.026	-.026	-.026	-.028	-.030	-.014	-.013	-.014	-.015	-.016
4	-.043	-.045	-.043	-.043	-.035	-.026	-.026	-.024	-.021	.000	-.014	-.012	-.010	-.005	.018
5	-.043	-.045	-.043	-.042	-.023	-.027	-.026	-.026	-.019	.000	-.015	-.011	-.011	-.006	.017
6	-.019	-.023	-.035	-.045	-.046	-.008	-.020	-.027	-.030	-.029	-.010	-.011	-.013	-.015	-.016
7	.182*	.141	.074	-.037	-.045	.133	.030	-.008	-.020	-.028	.039	.045	-.009	-.014	-.014
8	-.049	-.048	-.043	-.042	-.049	-.028	.025	-.024	-.027	-.020	-.015	-.013	-.012	-.016	-.015
9	-.042	-.041	-.039	-.034	.107	-.025	-.024	-.002	.048	.198*	-.015	-.011	-.002	.023	.156*
10	-.043	-.043	-.042	-.038	-.012	-.027	-.026	-.024	-.013	.007	-.015	-.011	-.009	-.003	.021
11	-.008	-.012	-.030	-.042	-.043	-.004	-.020	-.025	-.030	-.029	-.008	-.008	-.011	-.016	-.016
12	.073	.082	.025	-.011	-.033	.053	.015	.017	-.014	-.024	.026	.029	.012	-.008	-.010
13	-.022	-.031	-.037	-.037	-.042	-.009	-.011	-.021	-.027	-.016	-.005	------	-.011	-.015	-.005
14	-.028	-.033	-.012	.041	.090	-.015	.000	.026	.033	.085	-.010	.006	.034	.047	.103
15	-.042	-.041	-.035	-.020	.057	-.026	-.023	-.017	-.004	.042	-.014	-.006	-.001	.014	.036
16	-.018	-.018	-.016	-.016	.004	-.027	-.026	-.026	-.018	.005	-.015	-.011	-.012	-.005	.021
17	-.031	-.030	-.037	-.037	-.042	-.020	-.025	-.027	-.029	-.027	-.012	-.010	-.014	-.015	-.016
18	-.042	-.042	-.042	-.039	-.018	-.028	-.026	-.026	-.020	.002	-.015	-.012	-.012	-.005	.019
19	-.043	-.045	-.045	-.045	-.045	-.026	-.027	-.028	-.028	-.027	-.016	-.015	-.015	-.014	-.017
20	-.045	-.045	-.043	-.043	-.048	-.025	-.026	-.026	-.028	-.029	-.014	-.014	-.013	-.013	-.018
21	-.035	-.039	-.039	-.042	-.049	------	------	------	------	------	-.012	-.013	-.015	-.016	-.015
22	-.034	-.038	-.039	-.043	-.050*	------	------	------	------	------	-.012	-.014	-.014	-.016	-.015
23	-.048	-.048	-.046	-.042	-.028	------	------	------	------	------	------	------	------	------	------
24	-.043	-.045	-.043	-.043	-.048	-.026	-.026	-.026	-.028	-.029	-.013	-.012	-.014	-.015	-.018*

*Maximum or minimum value.

TABLE I.– TEST RESULTS - Continued

(c) Configuration 3 ($\delta_h = 0°$, $\delta_{sb} = 0°$, ventral off).

Orifice number	$M_\infty = 2.30$					$M_\infty = 2.96$					$M_\infty = 3.95$				
	C_p for α =					C_p for α =					C_p for α =				
	-4.95°	-0.41°	4.22°	8.80°	18.22°	-4.88°	-0.53°	3.88°	8.28°	17.23°	-4.45°	-0.24°	4.02°	8.25°	16.92°
1	-0.162	-0.162	-0.156	-0.141	-0.155	-0.113	-0.114	-0.112	-0.109	-0.117	-0.070	-0.069	-0.067	-0.067	-0.065
2	-.157	-.160	-.157	-.143	-.166	-.108	-.112	-.112	-.111	-.113	-.070	-.068	-.068	-.069	-.066
3	-.156	-.152	-.151	-.141	-.157	-.107	-.106	-.105	-.099	-.107	-.068	-.065	-.062	-.064	-.065
4	-.147	-.141	-.143	-.143	-.150	-.104	-.102	-.103	-.104	-.080	-.069	-.065	-.065	-.064	-.045
5	-.144	-.141	-.143	-.132	-.059	-.103	-.102	-.102	-.086	-.020	-.069	-.066	-.065	-.055	-.011
6	-.149	-.149	-.148	-.143	-.155	-.106	-.108	-.109	-.109	-.117	-.068	-.067	-.066	-.067	-.065
7	-.010	-.043	-.093	-.128	-.145	-.017	-.051	-.057	-.089	-.080	-.038	-.055	-.032	-.059	-.065
8	-.168	-.161	-.156	-.136	-.167	-.116	-.110	-.104	-.096	-.121	-.073	-.066	-.063	-.065	-.074
9	-.140	-.141	-.143	-.122	.025	-.102	-.101	-.094	-.049	.058	-.065	-.065	-.051	-.013	.145
10	-.139	-.136	-.123	-.076	.085	-.100	-.098	-.081	-.043	.067	-.068	-.065	-.060	-.043	.031
11	-.119	-.127	-.135	-.139	-.150	-.096	-.096	-.099	-.103	-.107	-.064	-.064	-.064	-.065	-.062
12	.072	.057	.009	-.045	-.103	.062	.034	.007	-.031	-.062	.042	-.005	-.011	-.042	-.061
13	-.123	-.125	-.115	-.101	-.161	-.102	-.091	-.076	-.076	-.110	-.065	-.061	-.057	-.059	-.043
14	-.072	-.080	-.057	.014	.172*	-.045	-.041	.004	.054	.171*	-.017	-.015	.024	.033	.146*
15	-.117	-.101	-.061	.010	.156	-.088	-.077	-.040	.008	.126	-.063	-.054	-.041	-.013	.087
16	-.130	-.126	-.130	-.119	-.017	-.086	-.085	-.088	-.071	-.011	-.050	-.048	-.044	-.030	.015
17	-.153	-.154	-.151	-.140	-.158	-.109	-.110	-.107	-.109	-.110	-.068	-.068	-.066	-.069	-.066
18	-.144	-.149	-.148	-.143	-.083	-.103	-.103	-.105	-.095	-.044	-.067	-.065	-.064	-.056	-.022
19	-.161	-.159	-.155	-.142	-.155	-.112	-.112	-.111	-.109	-.111	-.070	-.069	-.066	-.066	-.064
20	-.160	-.157	-.153	-.139	-.161	-.110	-.108	-.102	-.099	-.114	-.069	-.067	-.063	-.065	-.073
21	-.169	-.183	-.174	-.166	-.186	-.117	-.121	-.121	-.114	-.118	-.071	-.074	-.075*	-.071	-.065
22	-.175	-.169	-.166	-.162	-.193*	-.122*	-.116	-.116	-.111	-.112	-.073	-.074	-.074	-.070	-.063
23	-.146	-.158	-.164	-.159	-.105	-.113	-.117	-.118	-.110	-.065	-.074	-.074	-.074	-.069	-.042
24	-.160	-.162	-.158	-.140	-.159	-.111	-.110	-.104	-.103	-.120	-.069	-.067	-.064	-.066	.071

*Maximum or minimum value.

TABLE I.– TEST RESULTS - Continued

(c) Configuration 3 ($\delta_h = 0°$, $\delta_{sb} = 0°$, ventral off) - Concluded.

Orifice number	$M_\infty = 4.63$					$M_\infty = 6.04$					$M_\infty = 8.01$				
	C_p for α =					C_p for α =					C_p for α =				
	-3.97°	0.19°	4.38°	8.53°	17.02°	-4.00°	-0.02°	4.00°	8.01°	16.22°	-4.00°	0.00°	4.00°	7.99°	16.00°
1	-0.052	-0.051	-0.049	-0.051	-0.048	-0.029	-0.029	-0.028	-0.028	-0.027	-0.015	-0.016	-0.015	-0.015	-0.014
2	-.053	-.052	-.051	-.052	-.051	-.023	-.028	-.029	-.028	-.029	-.012	-.014	-.015	-.015	-.014
3	-.051	-.049	-.047	-.048	-.047	-.028	-.027	-.026	-.029	-.030	-.015	-.015	-.015	-.016	-.015
4	-.052	-.051	-.049	-.048	-.029	-.027	-.026	-.025	-.021	.005	-.015	-.015	-.014	-.008	.016
5	-.052	-.051	-.049	-.041	-.005	-.028	-.027	-.022	-.012	.033	-.015	-.015	-.013	-.003	.039
6	-.051	-.051	-.049	-.051	-.049	-.028	-.029	-.028	-.028	-.027	-.014	-.015	-.015	-.015	-.014
7	-.041	-.047	-.044	-.051	-.049	-.002	-.007	-.024	-.028	-.026	.000	-.001	-.014	-.016	-.015
8	-.053	-.051	-.048	-.052	-.056*	-.031	-.026	-.026	-.030	-.030	-.016	-.015	-.015	-.017*	-.014
9	-.048	-.048	-.036	-.009	.126	-.025	-.025	-.013	.017	.177*	-.012	-.012	.001	.027	.157
10	-.051	-.051	-.044	-.034	.027	-.028	-.026	-.014	-.004	.066	-.015	-.014	-.010	.001	.058
11	-.048	-.047	-.048	-.049	-.047	-.027	-.028	-.027	-.028	-.026	-.014	-.015	-.015	-.015	-.014
12	.010	-.022	-.026	-.040	-.048	-.029	.000	-.009	-.024	-.027	.013	.002	-.007	-.014	-.014
13	-.048	-.047	-.045	-.049	-.021	-.023	-.023	-.023	-.021	.007	-.015	-.014	-.013	-.005	.219*
14	-.017	-.002	.020	.038	.136*	-.014	.007	.019	.033	.152	-.007	.010	.023	.054	.146
15	-.047	-.042	-.032	-.016	.066	-.025	-.021	-.003	.017	.127	-.014	-.012	-.004	.006	.094
16	-.024	-.025	-.022	-.016	.029	-.027	-.027	-.022	-.009	.041	-.015	-.015	-.013	-.003	.048
17	-.044	-.047	-.047	-.048	-.049	-.029	-.027	-.028	-.028	-.028	-.016	-.015	-.015	-.015	-.014
18	-.048	-.048	-.047	-.040	-.012	-.028	-.027	-.024	-.015	.023	-.016	-.015	-.013	-.005	.031
19	-.053	-.052	-.049	-.051	-.048	-.030	-.028	-.027	-.026	-.028	-.017	-.016	-.015	-.014	-.013
20	-.053	-.051	-.049	-.051	-.053	-.028	-.026	-.025	-.029	-.029	-.017	-.014	-.014	-.015	-.012
21	-.053	-.055	-.055	-.055	-.047	------	------	------	------	------	-.014	-.016	-.016	-.015	-.013
22	-.053	-.055	-.055	-.053	-.047	------	------	------	------	------	-.015	-.016	-.017	-.016	-.014
23	-.056	-.056	-.056	-.053	-.030	------	------	------	------	------	------	------	------	------	------
24	-.052	-.051	-.049	-.052	-.055	-.028	-.026	-.026	-.029	-.032*	-.016	-.014	-.015	-.016	-.015

*Maximum or minimum value.

TABLE I. – TEST RESULTS - Continued

(d) Configuration 4 ($\delta_h = 0°$, $\delta_{sb} = 35°$, ventral on).

Orifice number	$M_\infty = 2.30$					$M_\infty = 2.96$					$M_\infty = 3.95$				
	C_p for α =					C_p for α =					C_p for α =				
	-5.22°	-0.58°	3.98°	8.52°	17.93°	-5.13°	-0.76°	3.62°	8.03°	17.00°	-4.67°	-0.49°	3.17°	8.00°	16.67°
1	-0.180	-0.180	-0.181	-0.177	-0.173	-0.118	-0.118	-0.122	-0.125	-0.115	-0.068	-0.069	-0.073	-0.072	-0.073
2	-.180	-.178	-.176	-.173	-.174	-.119	-.120	-.121	-.121	-.116	-.070	-.072	-.073	-.072	-.073
3	-.180	-.180	-.178	-.171	-.182	-.117	-.116	-.118	-.119	-.117	-.060	-.062	-.072	-.070	-.067
4	-.177	-.173	-.173	-.178	-.178	-.114	-.111	-.112	-.118	-.106	-.063	-.064	-.065	-.067	-.054
5	-.175	-.172	-.160	-.121	-.019	-.112	-.110	-.098	-.073	.007	-.064	-.065	-.063	-.047	.017
6	-.179	-.182	-.180	-.175	-.174	-.115	-.118	-.121	-.125	-.116	-.068	-.069	-.073	-.072	-.073
7	-.163	-.175	-.175	-.174	-.176	-.120	-.124	-.125	-.121	-.116	-.072	-.073	-.073	-.073	-.073
8	-.168	-.173	-.173	-.171	-.182	-.070	-.074	-.092	-.117	-.121	-.043	-.034	-.072	-.056	-.072
9	-.174	-.169	-.171	-.178	-.158	-.111	-.107	-.107	-.108	-.079	-.063	-.065	-.063	-.063	-.035
10	-.148	-.143	-.118	-.047	.256*	-.095	-.094	-.069	-.023	.150	-.057	-.058	-.048	-.011	.085
11	-.148	-.155	-.153	-.146	-.168	-.089	-.098	-.112	-.115	-.112	-.061	-.067	-.067	-.067	-.072
12	-.137	-.148	-.151	-.153	-.151	-.076	-.088	-.107	-.110	-.107	-.025	-.031	-.050	-.068	-.060
13	-.098	-.089	-.091	-.149	-.164	-.019	.014	-.005	-.089	-.111	-.048	-.046	-.055	.056	-.056
14	-.157	-.153	-.154	-.150	-.135	-.097	-.093	-.094	-.070	-.035	-.059	-.059	-.053	-.029	.036
15	-.123	-.102	-.073	.037	.213	-.076	-.069	-.049	.027	.313*	-.043	-.045	-.034	-.004	.154*
16	-.165	-.157	-.158	-.138	.001	-.103	-.098	-.097	-.078	-.005	-.046	-.047	-.046	-.041	.006
17	-.177	-.175	-.174	-.173	-.173	-.117	-.118	-.121	-.121	-.114	-.068	-.070	-.073	-.072	-.073
18	-.186	-.180	-.189	-.194	-.188	-.119	-.115	-.121	-.124	-.111	-.064	-.065	-.067	-.070	-.055
19	-.180	-.175	-.175	-.173	-.176	-.116	-.118	-.121	-.121	-.116	-.068	-.069	-.073	-.073	-.074
20	-.180	-.176	-.171	-.165	-.168	-.121	-.116	-.114	-.116	-.112	-.072	-.072	-.073	-.065	-.066
21	-.209*	-.204	-.199	-.188	-.194	-.123	-.129	-.130	-.127	-.120	-.073	-.074	-.076	-.072	-.070
22	-.202	-.198	-.200	-.198	-.202	-.129	-.130	-.134*	-.130	-.116	-.075	-.076	-.077*	-.073	-.069
23	------	------	------	------	------	------	------	------	------	------	------	------	------	------	------
24	-.179	-.173	-.172	-.168	-.171	-.124	-.128	-.120	-.118	-.117	-.072	-.073	-.070	-.070	-.069

*Maximum or minimum value.

TABLE I. – TEST RESULTS - Continued

(d) Configuration 4 ($\delta_h = 0°$, $\delta_{sb} = 35°$, ventral on) - Concluded.

Orifice number	$M_\infty = 4.63$					$M_\infty = 6.04$					$M_\infty = 8.01$				
	C_p for α =					C_p for α =					C_p for α =				
	-4.19°	-0.05°	4.14°	8.28°	16.76°	-4.01°	-0.01°	4.00°	8.00°	16.00°	-4.00°	0.00°	3.99°	8.00°	16.22°
1	-0.052	-0.052	-0.052	-0.052	-0.053	-0.025	-0.027	-0.027	-0.027	-0.027	-0.012	-0.013	-0.013	-0.013	-0.015
2	-.052	-.053	-.053	-.053	-.054	-.026	-.028	-.027	-.027	-.027	-.014	-.014	-.013	-.014	-.014
3	-.048	-.046	-.050	-.050	-.049	-.025	-.025	-.022	-.026	-.029	-.014	-.010	-.013	-.014	-.017*
4	-.046	-.048	-.048	-.049	-.036	-.022	-.023	-.024	-.021	-.008	-.012	-.010	-.012	-.008	.013
5	-.046	-.048	-.049	-.048	-.013	-.022	-.022	-.022	-.014	.020	-.012	-.009	-.008	-.003	.019
6	-.052	-.052	-.053	-.053	-.054	-.025	-.027	-.027	-.027	-.027	-.012	-.012	-.012	-.013	-.015
7	-.053	-.054	-.054	-.053	-.054	-.025	-.024	-.027	-.027	-.025	-.009	-.004	-.013	-.013	-.013
8	-.042	-.036	-.030	-.045	-.053	-.020	-.023	.002	-.020	-.030*	-.014	-.008	-.011	-.013	-.017
9	-.046	-.048	-.048	-.048	-.027	-.023	-.020	-.023	-.019	.007	-.012	-.008	-.008	-.002	.021
10	-.041	-.044	-.026	.000	.063	-.020	-.020	-.006	.016	.083	-.012	-.006	-.001	.022	.070
11	-.045	-.049	-.050	-.050	-.052	-.021	-.025	-.027	-.027	-.026	-.010	-.010	-.012	-.014	-.015
12	.008	-.021	-.042	-.050	-.052	.049	.019	-.020	-.022	-.025	.029	.020	-.012	-.011	-.015
13	-.037	-.033	.010	.002	-.041	-.013	-.015	.028	-.012	-.023	-.006	-.004	.005	-.011	-.007
14	-.042	-.040	-.037	-.011	.075	-.023	-.008	.003	.026	.105*	-.007	.014	.030	.034	.103*
15	-.034	-.036	-.015	.006	.094*	-.017	-.013	.002	.032	.104	-.010	-.002	.005	.024	.076
16	-.021	-.022	-.022	-.021	.009	-.022	-.022	-.022	-.014	.013	-.012	-.008	-.009	-.003	.021
17	-.044	-.048	-.048	-.048	-.052	-.025	-.027	-.027	-.026	-.027	-.011	-.013	-.013	-.013	-.014
18	-.045	-.046	-.049	-.048	-.033	-.022	-.023	-.025	-.021	-.030	-.013	-.009	-.012	-.007	.010
19	-.050	-.052	-.053	-.053	-.054	-.025	-.027	-.027	-.027	-.028	-.014	-.014	-.013	-.014	-.015
20	-.052	-.053	-.049	-.050	-.050	-.025	-.025	-.027	-.026	-.024	-.014	-.011	-.013	-.012	-.010
21	-.054	-.054	-.054	-.052	-.053	------	------	------	------	------	------	------	------	------	------
22	-.054	-.056*	-.056	-.052	-.053	------	------	------	------	------	------	------	------	------	------
23	------	------	------	------	------	------	------	------	------	------	------	------	------	------	------
24	-.052	-.052	-.052	-.052	-.050	-.026	-.025	-.025	-.026	-.025	-.014	-.010	-.013	-.013	-.015

*Maximum or minimum value.

TABLE I. – TEST RESULTS - Continued

(e) Configuration 5 (δ_h = -35°, δ_{sb} = 35°, ventral on).

Orifice number	M_∞ = 2.30					M_∞ = 2.96					M_∞ = 3.95				
	C_p for α =					C_p for α =					C_p for α =				
	-5.17°	-0.75°	3.76°	8.24°	17.41°	-5.18°	-0.84°	3.56°	7.95°	16.88°	-4.74°	-0.52°	3.74°	7.97°	12.26°
1	-0.164	-0.172	-0.175	-0.177	-0.190	-0.110	-0.118	-0.118	-0.119	-0.122	-0.063	-0.067	-0.073	-0.070	-0.074
2	-.185	-.187	-.186	-.178	-.180	-.117	-.122	-.121	-.118	-.121	-.067	-.063	-.064	-.070	-.074
3	-.187	-.189	-.187	-.179	-.180	-.122	-.125	-.122	-.117	-.126	-.072	-.072	-.072	-.072	-.075
4	-.184	-.182	-.182	-.179	-.190	-.121	-.120	-.117	-.118	-.128	-.069	-.070	-.070	-.072	-.073
5	-.183	-.180	-.180	-.169	-.079	-.118	-.118	-.117	-.108	-.050	-.068	-.070	-.067	-.060	-.038
6	-.166	-.171	-.174	-.176	-.181	-.108	-.117	-.115	-.119	-.121	-.060	-.064	-.070	-.070	-.074
7	-.173	-.153	-.162	-.167	-.137	-.082	-.077	-.096	-.116	-.121	-.046	-.036	-.050	-.069	-.074
8	-.184	-.189	-.188	-.180	-.178	-.113	-.119	-.122	-.117	-.127	-.070	-.074	-.072	-.072	-.075
9	-.184	-.182	-.184	-.182	-.198	-.123	-.121	-.117	-.122	-.134*	-.069	-.069	-.070	-.074	-.076*
10	-.180	-.176	-.164	-.136	.024*	-.117	-.117	-.106	-.081	.023	-.066	-.067	-.055	-.031	.013
11	-.140	-.144	-.144	-.154	-.173	-.090	-.099	-.097	-.112	-.117	-.050	-.056	-.059	-.069	-.072
12	-.085	-.055	-.069	-.121	-.146	-.050	-.034	-.043	-.109	-.118	.005	.014	-.011	-.068	-.072
13	-.153	-.167	-.179	-.177	-.169	-.097	-.105	-.114	-.117	-.121	-.055	-.067	-.067	-.066	-.067
14	-.179	-.178	-.184	-.177	-.196	-.115	-.113	-.113	-.118	-.118	-.065	-.066	-.067	-.070	-.063
15	-.160	-.151	-.118	-.068	.014	-.102	-.104	-.085	-.029	.082*	-.061	-.060	-.046	-.026	.020*
16	-.171	-.168	-.166	-.145	-.040	-.106	-.105	-.104	-.090	-.014	-.049	-.051	-.051	-.045	-.034
17	-.181	-.184	-.183	-.177	-.182	-.115	-.121	-.119	-.118	-.118	-.062	-.067	-.073	-.072	-.074
18	-.184	-.182	-.188	-.182	-.146	-.119	-.119	-.121	-.120	-.078	-.067	-.068	-.072	-.074	-.073
19	-.188	-.193	-.187	-.178	-.186	-.125	-.128	-.121	-.117	-.121	-.072	-.074	-.073	-.070	-.074
20	-.188	-.189	-.185	-.173	-.171	-.125	-.126	-.120	-.117	-.115	-.074	-.072	-.072	-.072	-.072
21	-.192	-.189	-.195	-.201	-.176	-.117	-.126	-.130	-.125	-.130	-.068	-.072	-.075	-.073	-.074
22	-.186	-.180	-.189	-.202*	-.182	-.127	-.130	-.131	-.127	-.129	-.072	-.073	-.076	-.074	-.073
23	------	------	------	------	------	------	------	------	------	------	------	------	------	------	------
24	-.189	-.187	-.180	-.176	-.162	-.125	-.128	-.121	-.118	-.113	-.073	-.070	-.072	-.072	-.073

*Maximum or minimum value.

TABLE I. – TEST RESULTS - Continued

(e) Configuration 5 (δ_h = -35°, δ_{sb} = 35°, ventral on) - Concluded.

Orifice number	M_∞ = 4.63					M_∞ = 6.04					M_∞ = 8.01				
	C_p for α =					C_p for α =					C_p for α =				
	-4.22°	-0.07°	4.12°	8.27°	16.70°	-4.03°	-0.01°	3.98°	8.00°	16.24°	-4.01°	0.00°	4.00°	7.99°	16.24°
1	-0.045	-0.049	-0.055	-0.053	-0.055	-0.021	-0.022	-0.028	-0.028	-0.030	-0.009	-0.008	-0.014	-0.015	-0.017
2	-.042	-.041	-.051	-.053	-.056	-.017	-.024	-.028	-.022	-.030	-.012	-.008	-.012	-.014	-.017
3	-.052	-.053	-.053	-.053	-.055	-.028	-.026	-.028	-.026	-.031*	-.015	-.011	-.013	-.014	-.018*
4	-.051	-.052	-.052	-.052	-.046	-.025	-.023	-.022	-.019	-.005	-.012	-.010	-.009	-.007	.012
5	-.049	-.052	-.052	-.052	-.025	-.025	-.024	-.025	-.021	.000	-.013	-.010	-.011	-.007	.018
6	-.042	-.048	-.055	-.053	-.055	-.019	-.019	-.028	-.026	-.030	-.008	-.006	-.013	-.013	-.014
7	-.026	-.033	-.045	-.053	-.055	-.006	.012	-.026	-.009	-.028	.021	.007	-.001	-.010	-.017
8	-.053	-.053	-.053	-.055	-.057	-.029	-.028	-.027	-.025	-.031	-.002	-.012	-.012	-.014	-.018
9	-.049	-.051	-.053	-.055	-.048	-.026	-.023	-.026	-.026	-.016	-.014	-.010	-.012	-.010	.002
10	-.047	-.048	-.032	-.006	.066	-.023	-.019	-.005	.010	.069	-.013	-.006	.002	.022	.071
11	-.036	-.042	-.049	-.051	-.053	-.016	-.015	-.028	-.027	-.029	-.005	-.003	-.012	-.013	-.015
12	.017	.014	-.040	-.048	-.052	.017	.018	-.024	-.007	-.028	.026	.032	.004	-.004	-.017
13	-.042	-.051	-.052	-.052	-.053	-.007	-.005	-.021	-.030	-.026	.001	-.004	-.009	-.013	-.018
14	-.047	-.048	-.051	-.051	-.034	-.024	-.021	-.021	-.021	.012	-.013	-.009	-.009	-.001	.029
15	-.044	-.041	-.024	-.001	.077*	-.019	-.014	.006	.017	.091*	-.011	-.001	.008	.032	.080*
16	-.024	-.025	-.026	-.025	-.004	-.024	-.024	-.025	-.021	-.005	-.012	-.010	-.012	-.006	.009
17	-.045	-.048	-.052	-.052	-.053	-.022	-.021	-.028	-.025	-.030	-.010	-.008	-.013	-.014	-.017
18	-.048	-.049	-.052	-.053	-.045	-.026	-.024	-.027	-.027	-.020	-.013	-.011	-.014	-.012	-.005
19	-.052	-.053	-.055	-.053	-.055	-.028	-.026	-.028	-.028	-.031	-.013	-.013	-.015	-.014	-.017
20	-.053	-.053	-.053	-.055	-.055	-.028	-.027	-.026	-.025	-.030	-.015	-.012	-.013	-.014	-.017
21	-.049	-.053	-.056	-.053	-.060*	------	------	------	------	------	------	------	------	------	------
22	-.051	-.053	-.056	-.053	-.060	------	------	------	------	------	------	------	------	------	------
23	------	------	------	------	------	------	------	------	------	------	------	------	------	------	------
24	-.052	-.052	-.055	-.052	-.056	-.027	-.025	-.028	-.026	-.030	-.014	-.012	-.013	-.014	-.017

*Maximum or minimum value.

TABLE I.– TEST RESULTS - Continued

(f) Configuration 6 ($\delta_h = 0°$, $\delta_{sb} = 0°$, ramjet on).

Orifice number	$M_\infty = 2.30$					$M_\infty = 2.96$					$M_\infty = 3.95$				
	C_p for α =					C_p for α =					C_p for α =				
	-4.92°	-0.35°	4.23°	8.84°	18.23°	-4.86°	-0.47°	3.92°	8.33°	17.27°	-4.41°	-0.17°	4.06°	8.31°	16.95°
1	-0.163	-0.162	-0.153	-0.141	-0.156	-0.116	-0.115	-0.113	-0.110	-0.119	-0.070	-0.070	-0.068	-0.069	-0.068
2	-.157	-.162	-.156	-.143	-.167	-.110	-.113	-.112	-.113	-.104	-.069	-.070	-.069	-.070	-.068
3	-.162	-.156	-.150	-.139	-.152	-.110	-.108	-.105	-.100	-.101	-.068	-.068	-.063	-.064	- 065
4	-.152	-.142	-.138	-.139	-.113	-.105	-.100	-.101	-.096	-.068	-.067	-.066	-.063	-.065	-.033
5	-.144	-.144	-.138	-.111	.013	-.103	-.101	-.096	-.062	.015	-.066	-.066	-.063	-.050	.002
6	-.150	-.152	-.148	-.140	-.152	-.109	-.109	-.110	-.109	-.119	-.067	-.069	-.067	-.069	-.068
7	.005	-.038	-.094	-.128	-.088	-.001	-.036	-.038	-.081	-.065	-.033	-.051	-.023	-.062	-.066
8	-.175	-.167	-.157	-.137	-.155	-.122*	-.113	-.104	-.096	-.115	-.074*	-.069	-.064	-.066	-.072
9	-.149	-.141	-.139	-.137	-.057	-.101	-.101	-.095	-.074	-.006	-.061	-.066	-.062	-.029	.024
10	-.138	-.115	-.064	.011	.224	-.100	-.092	-.064	.001	.147	-.066	-.065	-.052	-.027	.084
11	-.121	-.128	-.132	-.132	-.145	-.099	-.098	-.100	-.102	-.107	-.064	-.066	-.065	-.067	-.066
12	.080	.059	.009	-.042	-.065	.068	.044	.024	-.027	-.068	.046	.001	-.006	-.045	-.060
13	-.142	-.137	-.136	-.100	-.154	-.106	-.095	-.084	-.081	-.104	-.060	-.059	-.061	-.061	-.042
14	-.094	-.104	-.082	.018	.144	-.041	-.060	-.032	.020	.159	-.031	-.042	-.002	.055	.149
15	-.105	-.045	.067	.197	.368*	-.084	-.062	.019	.092	.300*	-.062	-.059	-.019	.019	.179*
16	-.133	-.131	-.125	-.103	.006	-.088	-.090	-.087	-.064	.005	-.047	-.047	-.046	-.034	.016
17	-.156	-.155	-.149	-.140	-.158	-.111	-.110	-.110	-.110	-.106	-.067	-.070	-.066	-.069	-.068
18	-.153	-.152	-.152	-.134	-.057	-.101	-.104	-.106	-.087	-.028	-.064	-.064	-.063	-.054	-.016
19	-.163	-.160	-.152	-.142	-.168	-.116	-.113	-.112	-.111	-.119	-.070	-.070	-.067	-.069	-.069
20	-.163	-.158	-.148	-.129	-.157	-.112	-.107	-.100	-.096	-.114	-.069	-.069	-.064	-.065	-.071
21	-.171	-.179	-.170	-.163	-.180*	-.110	-.120	-.119	-.110	-.114	-.065	-.071	-.071	-.070	-.063
22	-.160	-.156	-.154	-.151	-.172	-.105	-.108	-.110	-.106	-.108	-.061	-.067	-.067	-.066	-.059
23	------	------	------	------	------	------	------	------	------	------	------	------	------	------	------
24	-.164	-.156	-.156	-.132	-.149	-.114	-.110	-.100	-.101	-.119	-.069	-.069	-.064	-.065	-.074

*Maximum or minimum value.

TABLE I. – TEST RESULTS - Continued

(f) Configuration 6 ($\delta_h = 0°$, $\delta_{sb} = 0°$, ramjet on) - Concluded.

Orifice number	$M_\infty = 4.63$					$M_\infty = 6.04$					$M_\infty = 8.01$				
	C_p for α =					C_p for α =					C_p for α =				
	-3.91°	0.25°	4.41°	8.57°	17.07°	-4.01°	0.00°	4.00°	8.01°	15.98°	-4.01°	0.00°	4.00°	8.00°	15.98°
1	-0.053	-0.053	-0.050	-0.050	-0.050	-0.029	-0.029	-0.028	-0.028	-0.029	-0.015	-0.015	-0.014	-0.015	-0.015
2	-.053	-.052	-.052	-.052	-.050	-.024	-.029	-.028	-.028	-.029	-.012	-.013	-.014	-.015	-.014
3	-.052	-.052	-.048	-.046	-.048	-.028	-.027	-.026	-.028	-.031	-.016	-.014	-.014	-.016	-.016
4	-.050	-.050	-.048	-.046	-.028	-.027	-.028	-.025	-.020	.006	-.015	-.015	-.013	-.009	.016
5	-.050	-.052	-.048	-.038	.001	-.027	-.026	-.021	-.012	.023	-.015	-.014	-.009	-.002	.024
6	-.052	-.052	-.050	-.052	-.050	-.028	-.029	-.028	-.028	-.028	-.014	-.015	-.014	-.015	-.015
7	-.037	-.045	-.041	-.050	-.050	-.004	-.013	-.025	-.028	-.026	.001	-.001	-.014	-.015	-.012
8	-.055	-.053	-.048	-.050	-.056*	-.030	-.026	-.024	-.027	-.032*	-.016	-.014	-.015	-.016	-.017*
9	-.048	-.050	-.046	-.034	.072	-.023	-.025	-.012	.002	.024	-.012	-.008	.005	.029	.044
10	-.050	-.050	-.040	-.024	.036	-.027	-.025	-.015	-.001	.049	-.015	-.013	-.005	.002	.041
11	-.048	-.048	-.048	-.049	-.049	-.027	-.028	-.027	-.028	-.028	-.014	-.014	-.013	-.015	-.015
12	.020	-.022	-.023	-.042	-.048	.032	-.001	-.005	-.024	-.025	.013	.002	-.008	-.014	-.012
13	-.046	-.048	-.046	-.048	-.029	-.022	-.022	-.024	-.029	-.011	-.016	-.012	-.012	-.016	-.008
14	-.030	-.026	.010	.067	.129*	-.014	-.012	.034	.068	.181*	-.007	.018	.035	.058	.148*
15	-.048	-.045	-.021	.012	.109	-.026	-.019	.002	.024	.116	-.014	-.011	.000	.009	.085
16	-.024	-.025	-.022	-.015	.020	-.027	-.027	-.022	-.012	.030	-.014	-.014	-.009	.000	.032
17	-.044	-.048	-.048	-.050	-.050	-.029	-.029	-.028	-.027	-.029	-.016	-.015	-.014	-.015	-.015
18	-.046	-.048	-.045	-.038	-.006	-.028	-.027	-.023	-.015	.014	-.015	-.014	-.010	-.004	.019
19	-.053	-.053	-.050	-.050	-.052	-.030	-.029	-.028	-.027	-.028	-.017	-.015	-.014	-.014	-.016
20	-.053	-.052	-.049	-.050	-.055	-.028	-.027	-.026	-.027	-.027	-.016	-.014	-.014	-.015	-.015
21	-.049	-.052	-.053	-.052	-.045	------	------	------	------	------	-.014	-.016	-.016	-.015	-.015
22	-.046	-.049	-.050	-.049	-.041	------	------	------	------	------	-.014	-.016	-.017	-.016	-.015
23	------	------	------	------	------	------	------	------	------	------	------	------	------	------	------
24	-.052	-.052	-.052	-.050	-.056	-.029	-.026	-.026	-.029	-.032	-.016	-.013	-.014	-.016	-.017

*Maximum or minimum value.

TABLE I. – TEST RESULTS - Continued

(g) Configuration 7 ($\delta_h = 0°$, $\delta_{sb} = 0°$, ventral on).

Orifice number	$M_\infty = 2.30$					$M_\infty = 2.96$					$M_\infty = 3.95$				
	C_p for α =					C_p for α =					C_p for α =				
	-4.93°	-0.40°	4.21°	8.83°	18.21°	-4.86°	-0.50°	3.90°	8.31°	17.26°	-4.43°	-0.19°	4.04°	8.29°	16.94°
1	-0.165	-0.168	-0.162	-0.153	-0.158	-0.115	-0.113	-0.112	-0.113	-0.118	-0.071	-0.068	-0.068	-0.069	-0.072
2	-.161	-.165	-.163	-.153	-.161	-.108	-.114	-.114	-.115	-.122*	-.069	-.068	-.068	-.069	-.073
3	-.159	-.158	-.155	-.147	-.162	-.108	-.105	-.102	-.104	-.110	-.067	-.064	-.063	-.065	-.069
4	-.152	-.148	-.159	-.151	-.169	-.107	-.106	-.108	-.108	-.097	-.071	-.068	-.067	-.067	-.053
5	-.153	-.148	-.154	-.150	-.081	-.107	-.105	-.106	-.101	-.047	-.071	-.069	-.068	-.064	-.033
6	-.158	-.162	-.157	-.153	-.157	-.112	-.113	-.113	-.113	-.117	-.069	-.067	-.067	-.068	-.071
7	.001	-.037	-.102	-.132	-.159	-.016	-.048	-.054	-.086	-.077	-.035	-.056	-.027	-.063	-.073
8	-.159	-.153	-.148	-.144	-.163	-.109	-.103	-.100	-.100	-.116	-.069	-.064	-.065	-.065	-.064
9	-.151	-.151	-.148	-.136	.034	-.106	-.101	-.091	-.037	.111	-.069	-.066	-.037	.041	.213*
10	-.150	-.148	-.141	-.104	.066	-.106	-.104	-.094	-.063	.041	-.071	-.068	-.066	-.051	.014
11	-.132	-.139	-.145	-.150	-.155	-.099	-.102	-.104	-.108	-.113	-.065	-.065	-.065	-.067	-.070
12	.143	.121	.043	-.032	-.116	.129	.073	.048	-.014	-.044	.082	-.003	.002	-.043	-.067
13	-.112	-.094	-.100	-.097	-.148	-.090	-.078	-.066	-.075	-.105	-.066	-.056	-.054	-.058	-.017
14	-.077	-.090	-.045	.023	.263*	-.037	-.002	.039	.100	.231*	-.003	.012	.045	.046	.177
15	-.130	-.123	-.090	-.031	.112	-.087	-.083	-.055	-.004	.123	-.065	-.058	-.049	-.017	.097
16	-.130	-.134	-.147	-.142	-.067	-.094	-.090	-.093	-.089	-.039	-.052	-.049	-.048	-.044	-.016
17	-.161	-.163	-.159	-.151	-.153	-.109	-.110	-.111	-.112	-.113	-.067	-.067	-.066	-.068	-.071
18	-.149	-.153	-.156	-.154	-.102	-.109	-.106	-.108	-.104	-.065	-.070	-.067	-.067	-.065	-.037
19	-.166	-.167	-.160	-.151	-.154	-.114	-.113	-.112	-.113	-.112	-.071	-.068	-.067	-.068	-.070
20	-.166	-.167	-.164	-.153	-.157	-.111	-.109	-.108	-.106	-.113	-.070	-.067	-.066	-.067	-.072
21	-.174	-.181	-.174	-.167	-.185*	-.112	-.119	-.120	-.114	-.114	-.070	-.073	-.076*	-.072	-.069
22	-.161	-.158	-.153	-.156	-.169	-.100	-.104	-.107	-.104	-.100	-.066	-.070	-.069	-.065	-.059
23	------	------	------	------	------	------	------	------	------	------	------	------	------	------	------
24	-.166	-.169	-.166	-.156	-.154	-.112	-.111	-.111	-.106	-.115	-.070	-.067	-.066	-.066	-.072

*Maximum or minimum value.

TABLE I.– TEST RESULTS - Continued

(g) Configuration 7 ($\delta_h = 0°$, $\delta_{sb} = 0°$, ventral on) - Concluded.

Orifice number	$M_\infty = 4.63$					$M_\infty = 6.04$					$M_\infty = 8.01$				
	C_p for α =					C_p for α =					C_p for α =				
	-3.92°	0.22°	4.40°	8.58°	17.06°	-4.04°	-0.04°	4.00°	7.99°	16.18°	-4.00°	0.01°	4.02°	8.05°	16.00°
1	-0.053	-0.050	-0.050	-0.052	-0.052	-0.027	-0.029	-0.029	-0.030	-0.029	-0.012	-0.015	-0.016	-0.016	-0.014
2	-.053	-.052	-.050	-.052	-.053	-.028	-.030	-.029	-.030	-.030	-.014	-.015	-.016	-.016	-.011
3	-.050	-.049	-.048	-.048	-.048	-.029	-.028	-.028	-.030	-.032*	-.015	-.015	-.016	-.016	-.015
4	-.053	-.052	-.050	-.050	-.038	-.029	-.029	-.029	-.028	-.011	-.014	-.016	-.016	-.014	.022
5	-.053	-.053	-.052	-.048	-.023	-.030	-.029	-.027	-.019	.001	-.014	-.016	-.014	-.008	.010
6	-.050	-.049	-.049	-.050	-.052	-.023	-.029	-.029	-.030	-.029	-.010	-.014	-.015	-.015	-.014
7	-.039	-.045	-.045	-.050	-.053	-.024	-.027	-.029	-.029	-.030	-.012	-.011	-.015	-.016	-.012
8	-.052	-.049	-.049	-.050	-.045	-.030	-.027	-.027	-.030	-.022	-.015	-.015	-.015	-.016	.004
9	-.050	-.050	-.033	.053	.221*	-.028	-.021	.009	.081	.174	-.014	-.009	.006	.066	.164
10	-.053	-.052	-.049	-.038	-.003	-.029	-.028	-.024	-.012	.012	-.014	-.015	-.013	-.005	.020
11	-.048	-.048	-.048	-.049	-.049	-.019	-.026	-.028	-.029	-.028	-.009	-.012	-.014	-.015	-.014
12	.018	-.024	-.027	-.041	-.050	.003	-.011	-.021	-.026	-.028	-.004	.001	-.013	-.014	-.015
13	-.049	-.044	-.044	-.050	-.004	-.021	-.022	-.026	-.020	.007	-.013	-.012	-.015	-.012	.008
14	-.011	-.010	.037	.050	.169	-.008	.020	.025	.067	.215*	-.018*	.014	.027	.065	.212*
15	-.049	-.048	-.039	-.016	.055	-.028	-.023	-.016	.005	.072	-.014	-.013	-.010	.003	.062
16	-.027	-.026	-.024	-.022	.007	------	------	------	------	------	------	------	------	------	------
17	-.045	-.048	-.048	-.049	-.052	-.028	-.029	-.029	-.029	-.029	-.014	-.015	-.016	-.015	-.013
18	-.052	-.050	-.049	-.046	-.024	-.029	-.029	-.027	-.021	.003	-.015	-.015	-.014	-.009	.009
19	-.053	-.052	-.050	-.050	-.052	-.028	-.029	-.029	-.028	-.028	-.015	-.015	-.016	-.015	-.014
20	-.053	-.050	-.050	-.052	-.052	-.028	-.028	-.028	-.029	-.029	-.016	-.016	-.016	-.015	-.014
21	-.053	-.053	-.054*	-.054	-.052	-.029	-.030	-.031	-.029	-.028	-.014	-.015	-.016	-.015	-.013
22	-.048	-.049	-.049	-.049	-.038	-.030	-.031	-.032	-.029	-.028	-.015	-.016	-.017	-.015	-.013
23	------	------	------	------	------	------	------	------	------	------	------	------	------	------	------
24	-.052	-.050	-.049	-.052	-.053	-.029	-.029	-.029	-.030	-.030	-.016	-.015	-.015	-.016	-.015

*Maximum or minimum value.

TABLE I. – TEST RESULTS - Continued

(h) Configuration 8 ($\delta_h = -35°$, $\delta_{sb} = 0°$).

Orifice number	$M_\infty = 6.04$				
	C_p for α =				
	-4.00°	-0.02°	3.99°	8.00°	15.97°
1	-0.018	-0.024	-0.024	-0.030	-0.030
2	.043	-.012	-.027	-.030	-.029
3	-.027	-.028	-.027	-.028	-.028
4	-.024	-.024	-.023	-.017	.006
5	-.025	-.028	-.026	-.019	.027
6	-.010	-.016	-.023	-.030	-.030
7	.119	.010	.008	-.026	-.024
8	-.023	-.028	-.026	-.028	-.026
9	-.022	-.028	-.024	-.014	.066
10	-.025	.052	.086	.072	.129
11	.005	-.009	-.022	-.029	-.030
12	.082	.063	.021	-.013	-.019
13	-.004	-.016	-.025	-.026	-.027
14	-.020	-.023	.015	.053	.231
15	-.016	.037	.065	.116	.328*
16	-.025	-.026	-.020	-.009	.046
17	-.017	-.018	-.027	-.029	-.029
18	-.025	-.028	-.027	-.019	.031
19	-.025	-.028	-.028	-.029	-.029
20	-.027	-.027	-.025	-.026	-.027
21	------	------	------	------	------
22	------	------	------	------	------
23	------	------	------	------	------
24	-.027	-.025	-.024	-.028	-.031*

*Maximum or minimum value.

TABLE I. – TEST RESULTS - Continued

(i) Configuration 9 ($\delta_h = 0°$, $\delta_{sb} = 35°$, ramjet on).

Orifice number	$M_\infty = 6.04$					$M_\infty = 8.01$				
	C_p for α =					C_p for α =				
	-4.01°	0.00°	4.00°	8.00°	15.98°	-4.03°	0.00°	3.99°	8.01°	16.00°
1	-0.026	-0.028	-0.028	-0.028	-0.028	-0.013	-0.013	-0.014	-0.015	-0.016
2	-.026	-.028	-.029	-.028	-.029	-.013	-.014	-.015	-.015	-.014
3	-.026	-.025	-.028	-.029	-.032	-.013	-.013	-.015	-.016	-.017
4	-.026	-.025	-.025	-.020	.006	-.013	-.012	-.013	-.010	.014
5	-.027	-.026	-.021	-.012	.023	-.013	-.013	-.009	-.002	.024
6	-.023	-.027	-.028	-.028	-.028	-.013	-.013	-.014	-.014	-.016
7	-.022	-.023	-.029	-.028	-.029	-.009	-.009	-.014	-.015	-.015
8	-.026	-.023	-.026	-.024	-.033*	-.013	-.013	-.015	-.015	-.018*
9	-.025	-.026	-.012	.001	.024	-.014	-.012	.005	.032	.041
10	-.026	-.025	-.014	-.001	.049	-.014	-.013	-.005	.002	.041
11	-.018	-.023	-.028	-.028	-.028	-.010	-.011	-.014	-.015	-.016
12	.041	.023	-.020	-.028	-.028	.030	.016	-.013	-.015	-.015
13	-.017	-.017	-.018	-.026	-.010	-.003	-.007	-.011	-.014	-.009
14	-.019	.007	.033	.066	.180*	-.011	.018	.033	.056	.151*
15	-.026	-.021	.002	.025	.115	-.013	-.012	.000	.009	.085
16	-.026	-.026	-.022	-.012	.029	-.014	-.013	-.009	.000	.032
17	-.023	-.027	-.028	-.028	-.029	-.011	-.013	-.014	-.015	-.015
18	-.027	-.026	-.023	-.015	.014	-.014	-.013	-.011	-.004	.019
19	-.026	-.027	-.028	-.028	-.029	-.014	-.014	-.015	-.015	-.015
20	-.028	-.025	-.028	-.028	-.025	-.014	-.013	-.015	-.015	-.014
21	------	------	------	------	------	-.014	-.014	-.015	-.014	-.014
22	------	------	------	------	------	-.013	-.014	-.016	-.016	-.014
23	------	------	------	------	------	------	------	------	------	------
24	-.028	-.026	-.028	-.030	-.030	-.014	-.013	-.015	-.017	-.016

*Maximum or minimum value.

TABLE I. – TEST RESULTS - Continued

(j) Configuration 10 (δ_h = -35°, δ_h = 35°, ramjet on).

Orifice number	M_∞ = 6.04					M_∞ = 8.01				
	C_p for α =					C_p for α =				
	-3.98°	-0.01°	4.01°	7.99°	15.99°	-4.00°	0.00°	4.00°	8.00°	16.07°
1	-0.020	-0.022	-0.027	-0.029	-0.031	-0.010	-0.009	-0.013	-0.015	-0.016
2	-.016	-.023	-.027	-.026	-.030	-.010	-.012	-.014	-.014	-.015
3	-.026	-.024	-.027	-.027	-.032*	-.012	-.011	-.013	-.015	-.017
4	-.024	-.022	-.022	-.016	.008	-.012	-.011	-.010	-.007	.016
5	-.026	-.024	-.021	-.012	.014	-.013	-.011	-.009	-.002	.021
6	-.019	-.019	-.027	-.027	-.031	-.009	-.008	-.013	-.014	-.017
7	-.004	-.004	-.025	-.011	-.027	-.012	.004	-.013	-.013	-.014
8	-.026	-.026	-.028	-.026	-.031	-.013	-.012	-.013	-.016	-.018*
9	-.026	-.024	-.024	-.019	.000	-.013	-.010	-.006	.010	.041
10	-.027	-.031	-.008	.009	.061	-.013	-.011	-.002	.006	.051
11	-.016	-.015	-.026	-.027	-.030	-.008	-.006	-.013	-.014	-.016
12	.022	.016	-.022	-.011	-.027	.036	.017	-.007	-.009	-.015
13	-.018	------	-.025	-.023	-.031	.001	-.006	-.008	-.013	-.010
14	-.023	-.016	.016	.036	.124	-.012	.011	.029	.047	.112*
15	-.024	-.020	.015	.053	.157*	-.013	-.010	.014	.025	.110
16	-.025	-.024	-.023	-.016	.008	-.013	-.012	-.010	-.004	.020
17	-.022	-.022	-.026	-.027	-.030	-.007	-.010	-.013	-.014	-.015
18	-.026	-.024	-.025	-.020	-.001	-.013	-.011	-.011	-.006	.015
19	-.027	-.026	-.027	-.028	-.031	-.011	-.012	-.013	-.014	-.016
20	-.026	-.025	-.028	-.025	-.028	-.013	-.012	-.014	-.014	-.016
21	------	------	------	------	------	-.013	-.012	-.015	-.016	-.015
22	------	------	------	------	------	-.012	-.012	-.016	-.017	-.017
23	------	------	------	------	------	------	------	------	------	------
24	-.026	-.024	-.027	-.025	-.032	-.012	-.011	-.013	-.015	-.017

*Maximum or minimum value.

TABLE I. – TEST RESULTS - Concluded

(k) Configuration 11 (δ_h = -35°, δ_{sb} = 0°, ramjet on).

Orifice number	M_∞ = 6.04					M_∞ = 8.01				
	C_p for α =					C_p for α =				
	-4.01°	0.00°	4.00°	8.00°	15.96°	-4.00°	0.00°	4.01°	8.01°	15.99°
1	-0.018	-0.024	-0.024	-0.031	-0.032	-0.013	-0.014	-0.015	-0.016	-0.017
2	.042	-.010	-.027	-.030	-.032	-.004	-.011	-.014	-.016	-.016
3	-.028	-.028	-.027	-.029	-.031	-.014	-.013	-.014	-.015	-.018
4	-.024	-.024	-.022	-.017	.008	-.014	-.013	-.011	-.006	.020
5	-.026	-.025	-.021	-.014	.012	-.014	-.013	-.009	-.003	.021
6	-.010	-.016	-.024	-.031	-.032	-.011	-.012	-.014	-.016	-.017
7	.115	.010	.003	-.028	-.027	.047	.014	-.011	-.014	-.013
8	-.027	-.028	-.024	-.029	-.030	-.009	-.014	-.013	-.016	-.019*
9	-.024	-.025	-.024	-.019	-.002	-.015	-.012	-.006	.011	.041
10	-.024	-.024	-.009	.005	.057	-.014	-.012	-.003	.006	.051
11	.005	-.010	-.022	-.030	-.032	-.011	-.011	-.014	-.015	-.017
12	.078	.058	.021	-.012	-.024	.020	.018	.002	-.011	-.015
13	-.004	-.015	-.023	-.028	-.028	.004	-.012	-.012	------	-.012
14	-.018	-.014	.016	.032	.123	-.013	.013	.030	.046	.110*
15	-.025	-.017	.014	.048	.151*	-.014	-.009	.015	.024	.110
16	-.025	-.026	-.024	-.018	.006	-.015	-.013	-.010	-.004	.020
17	-.016	-.018	-.026	-.029	-.032	-.013	-.014	-.014	-.015	-.017
18	-.025	-.026	-.025	-.020	-.002	-.014	-.013	-.011	-.006	.015
19	-.025	-.028	-.028	-.029	-.032	-.015	-.015	-.015	-.015	-.017
20	-.026	-.028	-.026	-.027	-.029	-.015	-.014	-.015	-.014	-.015
21	------	------	------	------	------	-.013	-.015	-.015	-.016	-.015
22	------	------	------	------	------	-.013	-.014	-.015	-.017	-.015
23	------	------	------	------	------	------	------	------	------	------
24	-.025	-.026	-.025	-.027	-.033*	-.013	-.012	-.013	-.014	-.018

*Maximum or minimum value.

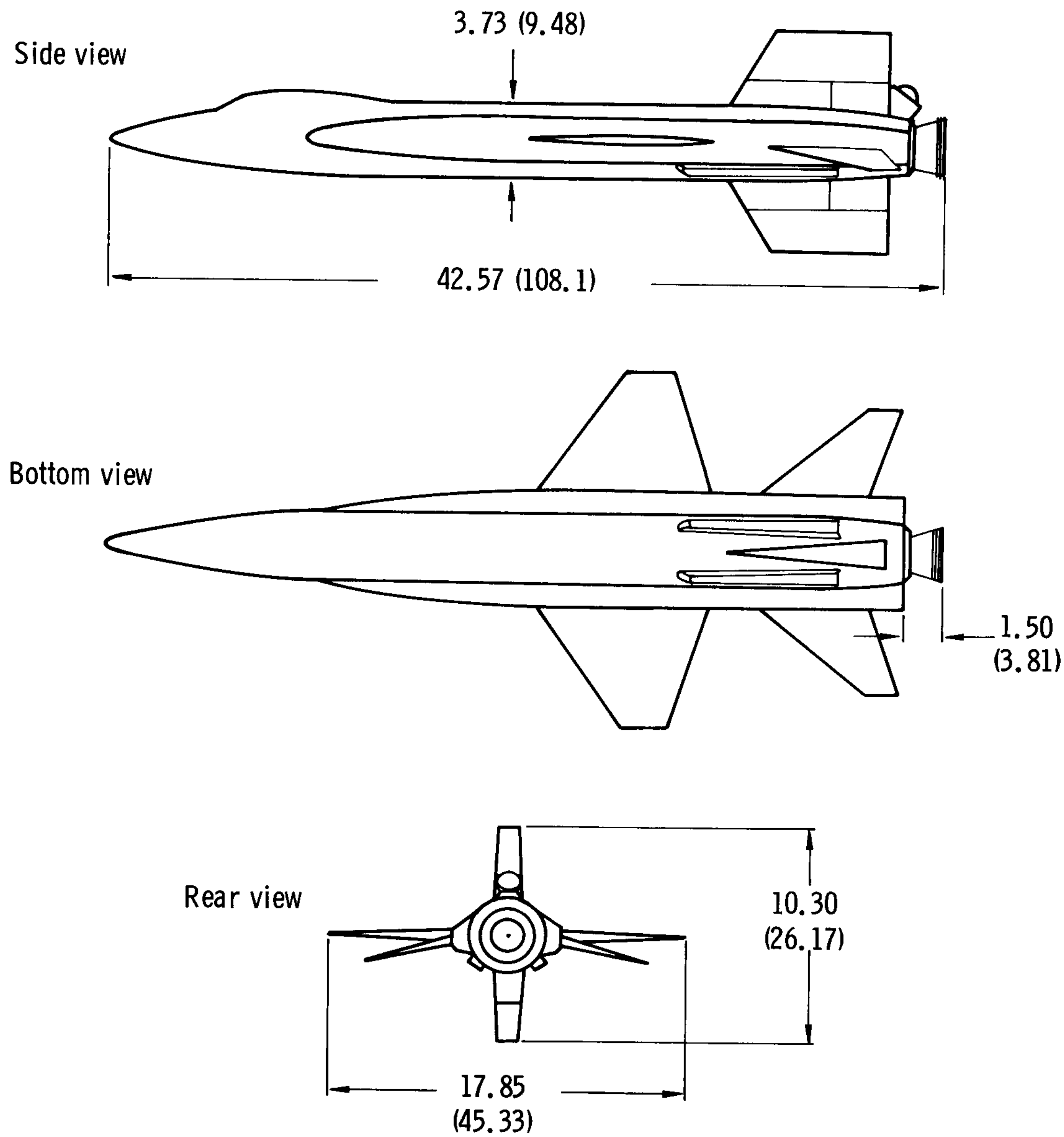

Figure 1. – Three-view drawing of the 1/15-scale X-15-2 model with the extended fuselage and the $\epsilon = 22.1$ nozzle extension. Dimensions in inches (centimeters).

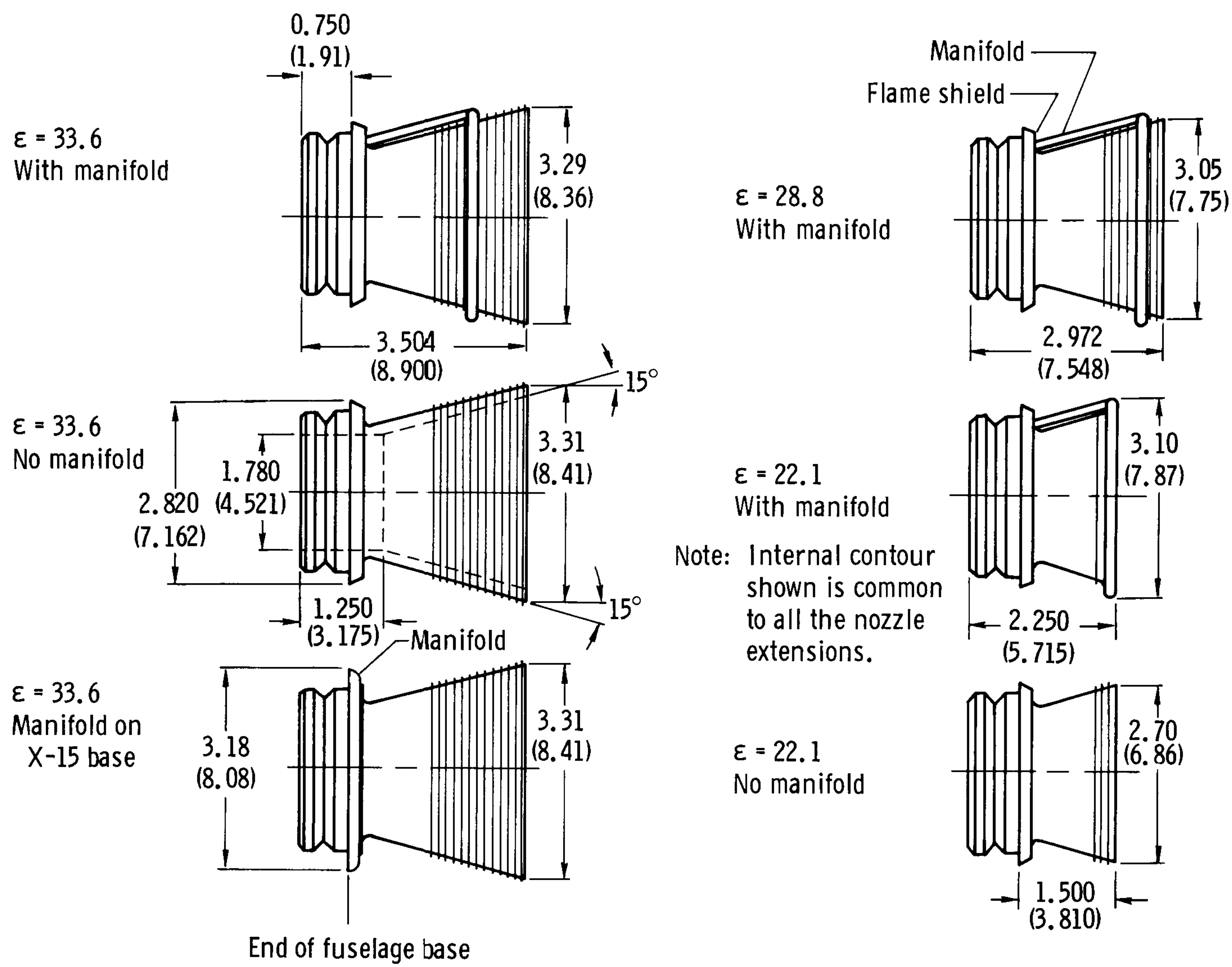

(a) Unshrouded nozzle extensions used for the LaRC drag investigation.

Figure 2.– Nozzle extensions used in force and pressure investigations. Dimensions in inches (centimeters).

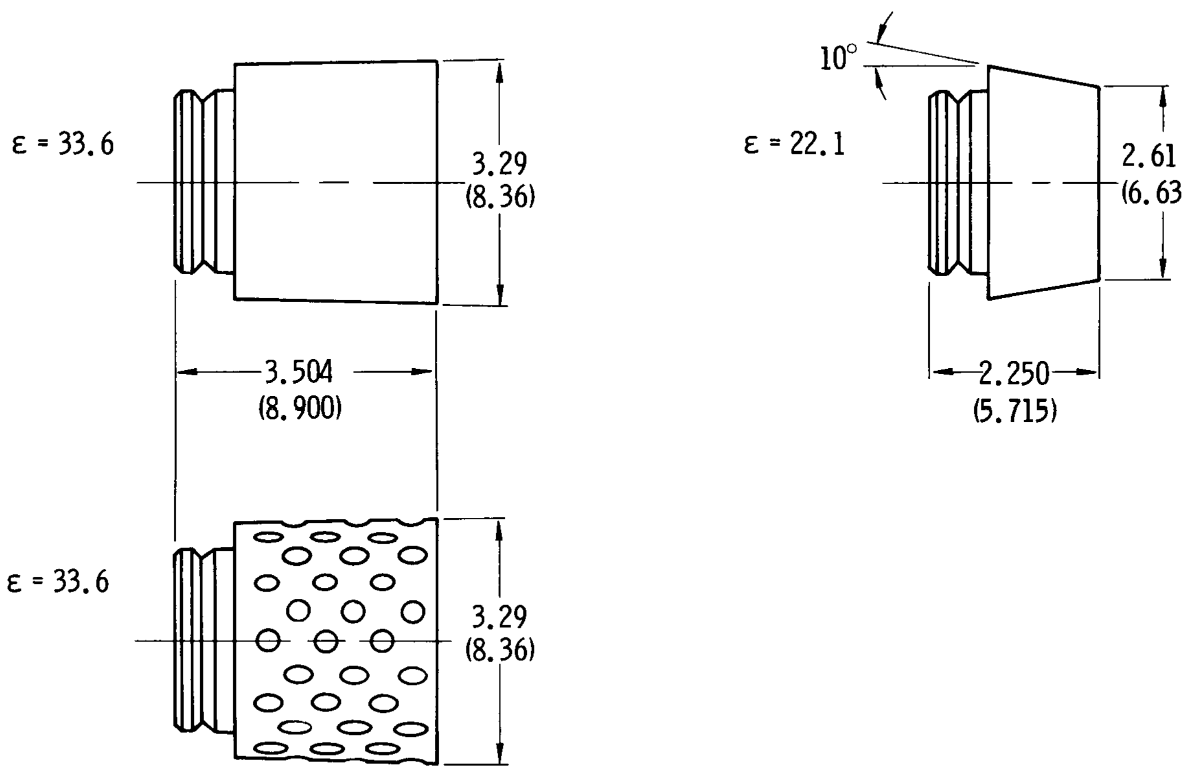

(b) Shrouded nozzle extensions used for the LaRC drag investigation.

Figure 2. – Continued.

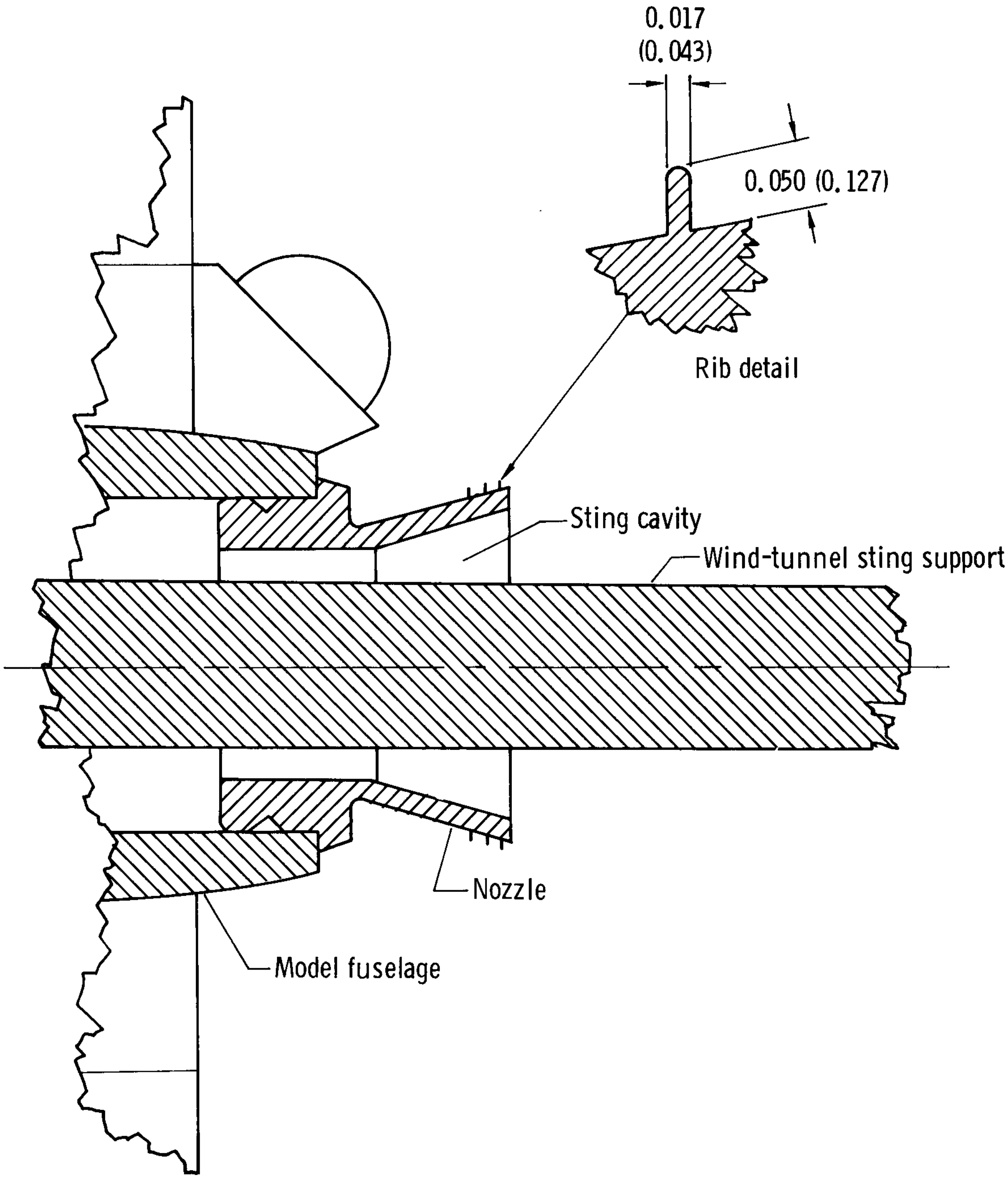

(c) Sketch of a typical nozzle-extension mounting.

Figure 2. – Continued.

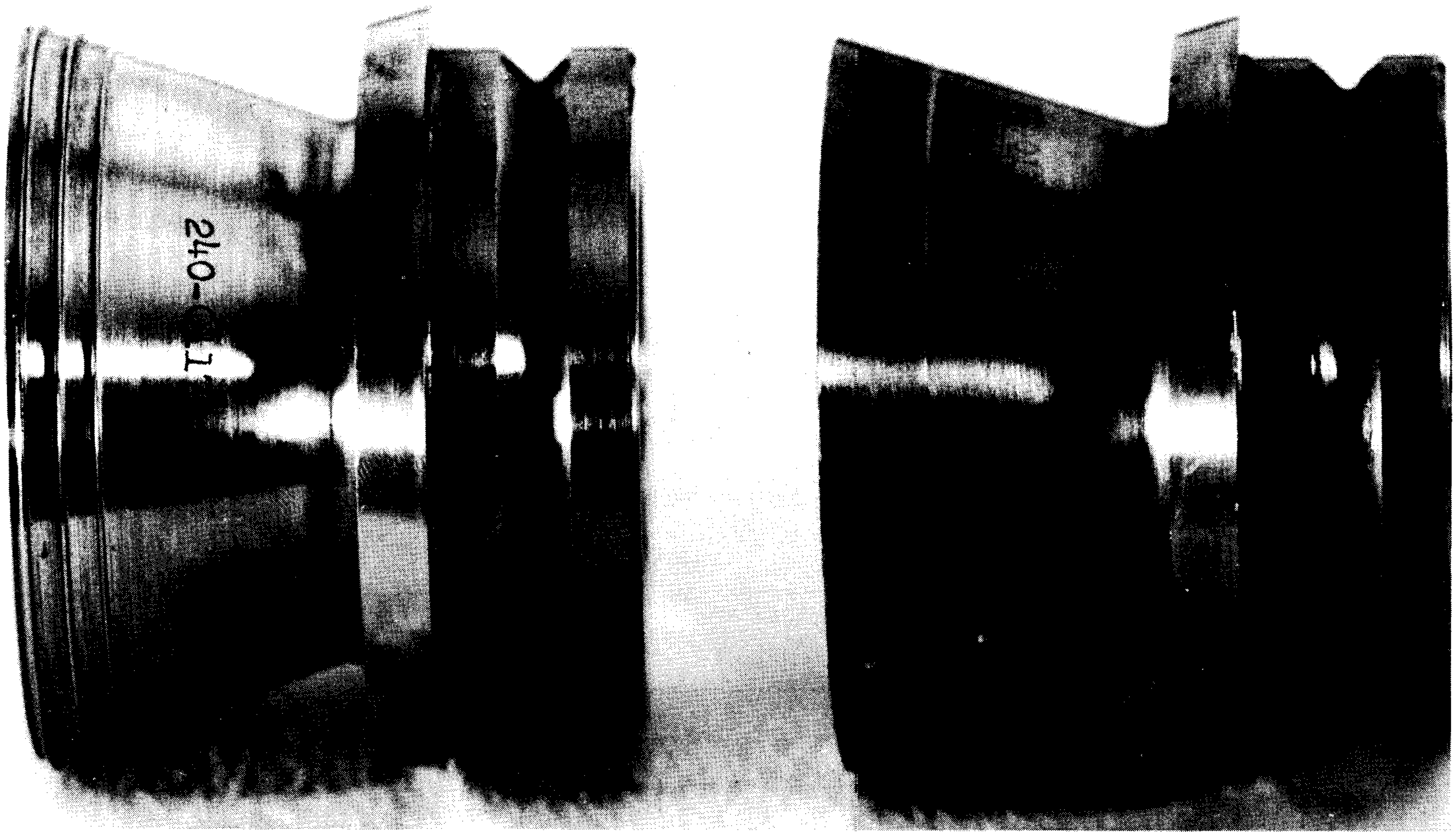

(d) Photo of $\epsilon = 22.1$ nozzle extensions used for the LaRC pressure investigation and AEDC tests.

Figure 2. – Concluded.

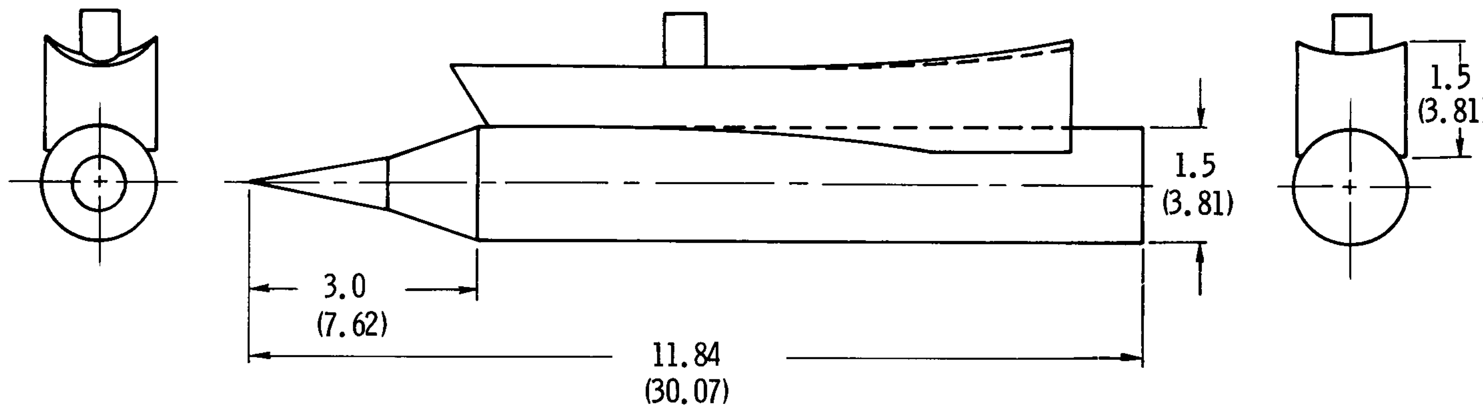

(a) Model ramjet used for the LaRC drag investigation.

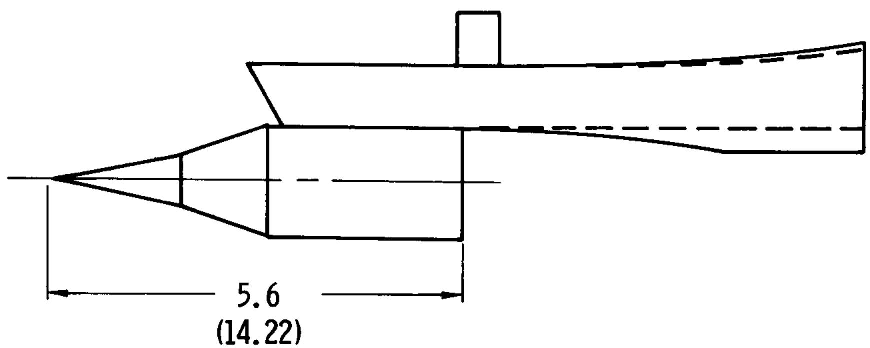

(b) Shortened model ramjet used for the LaRC pressure investigation and all AEDC tests.

Figure 3.– Model ramjets tested. Dimensions in inches (centimeters).

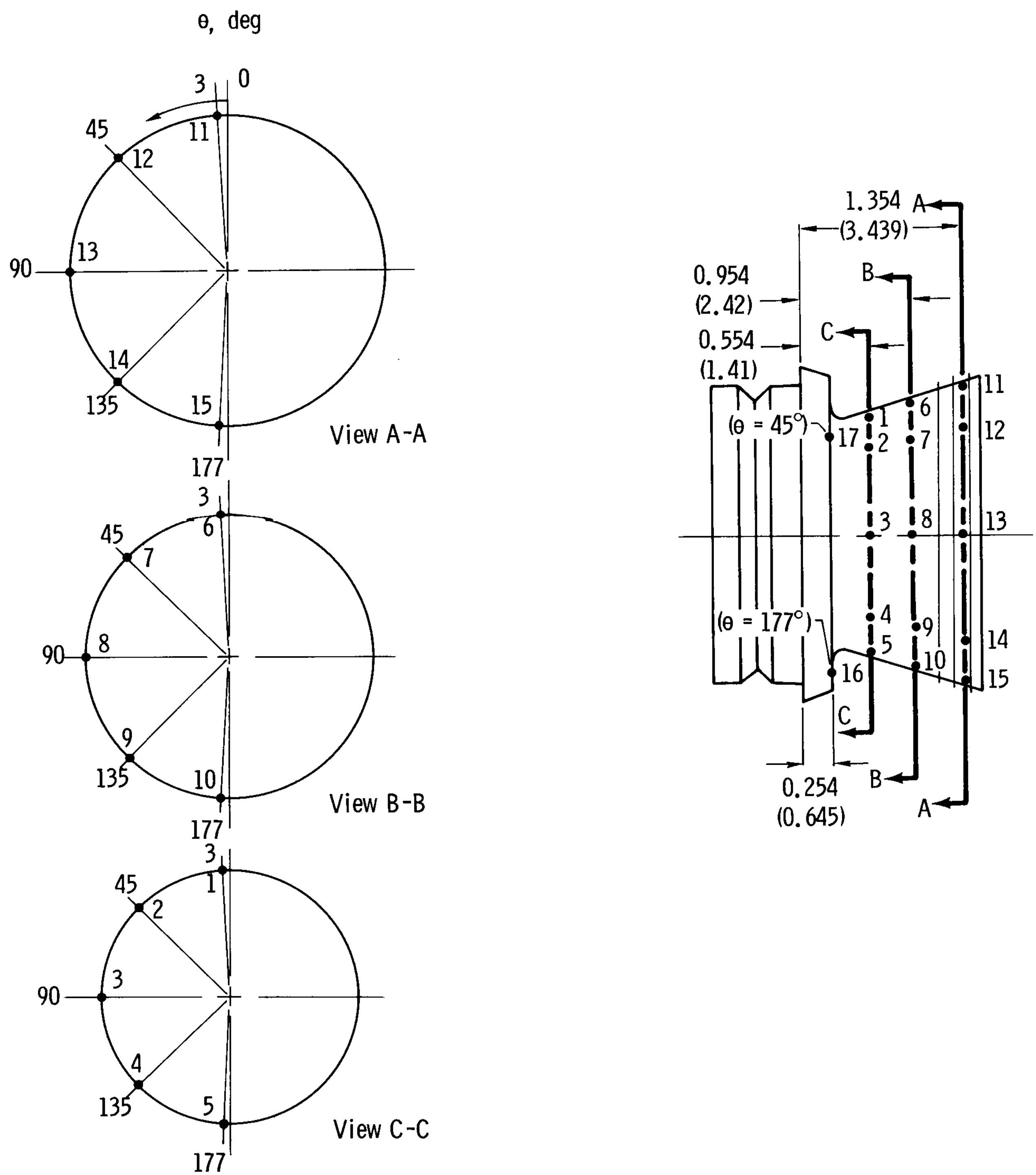

(a) Pressure-orifice locations on nozzle extensions.

Figure 4.— Pressure-orifice locations. Dimensions in inches (centimeters) unless otherwise noted.

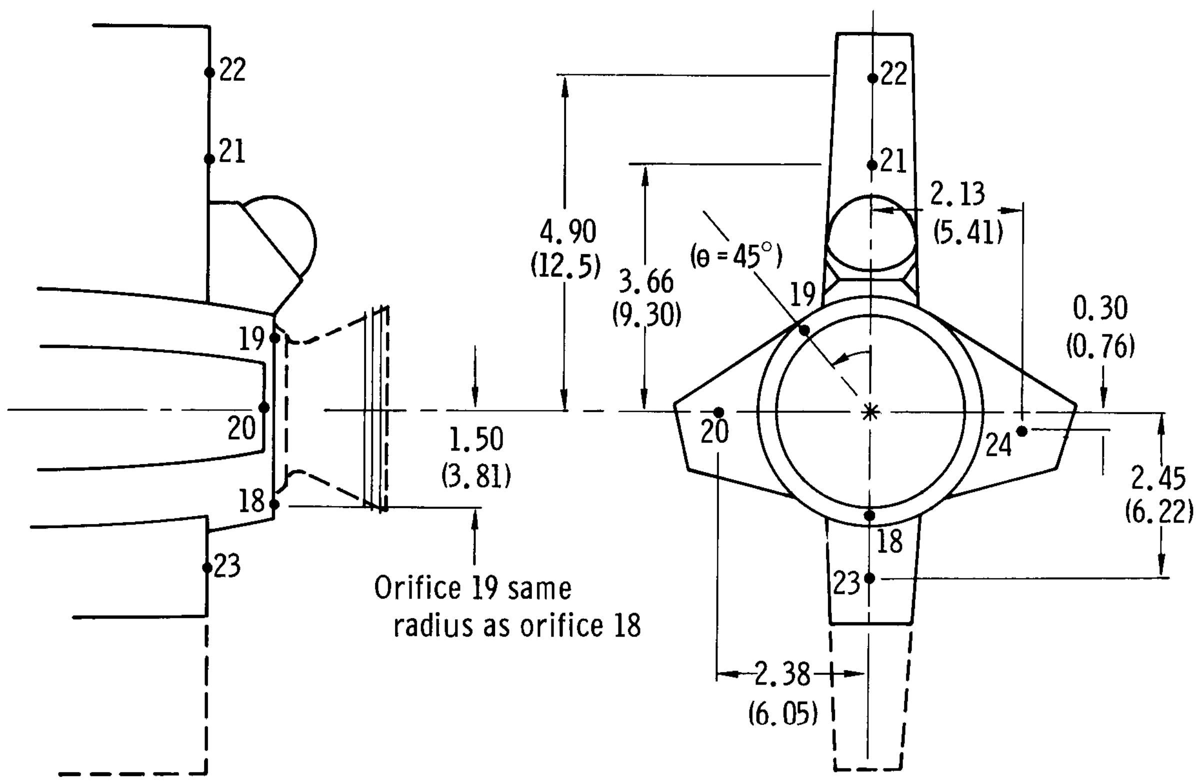

(b) Base pressure orifices on the airplane model.

Figure 4. – Concluded.

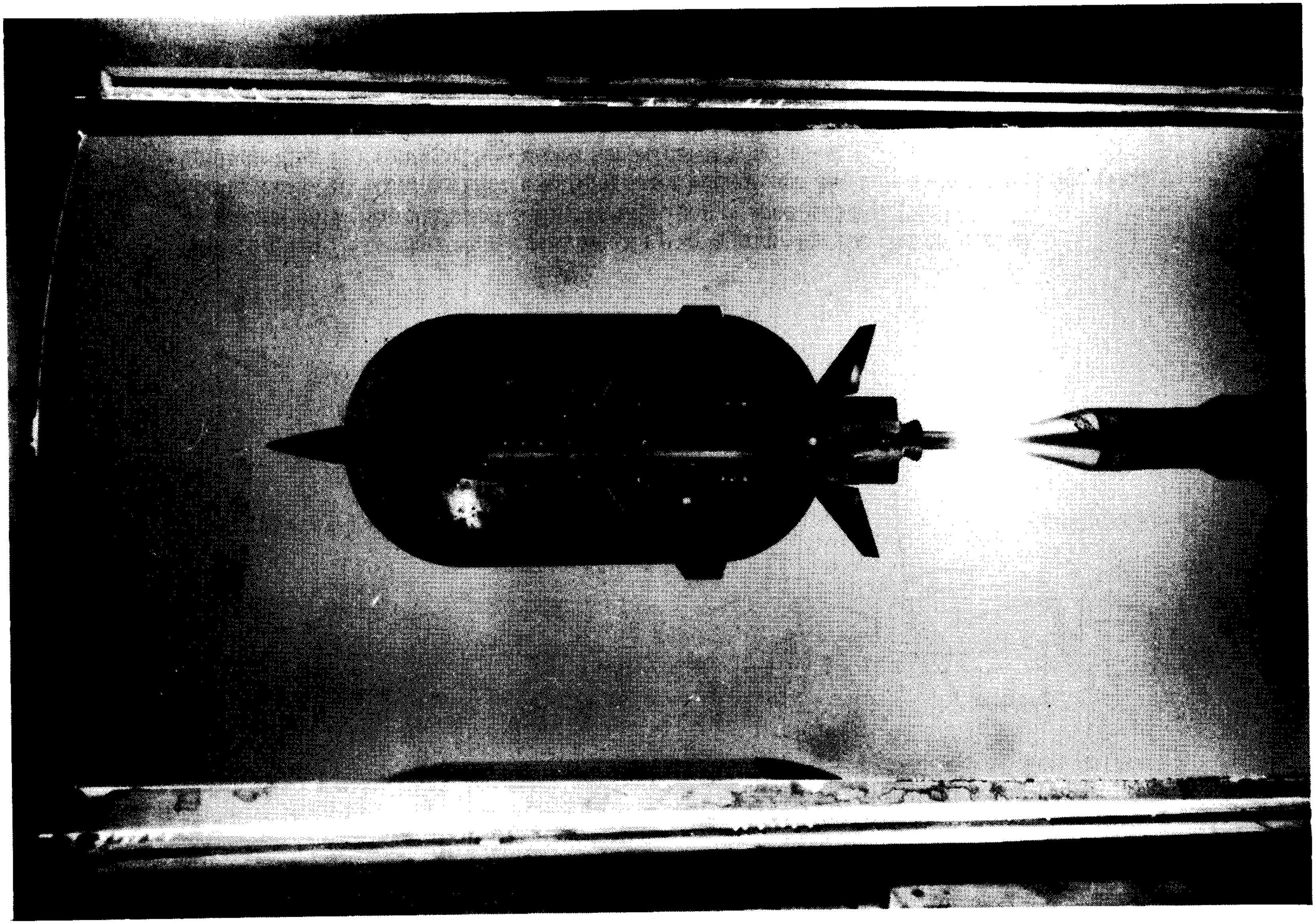

Figure 5.– Bottom view of model in AEDC Tunnel B.

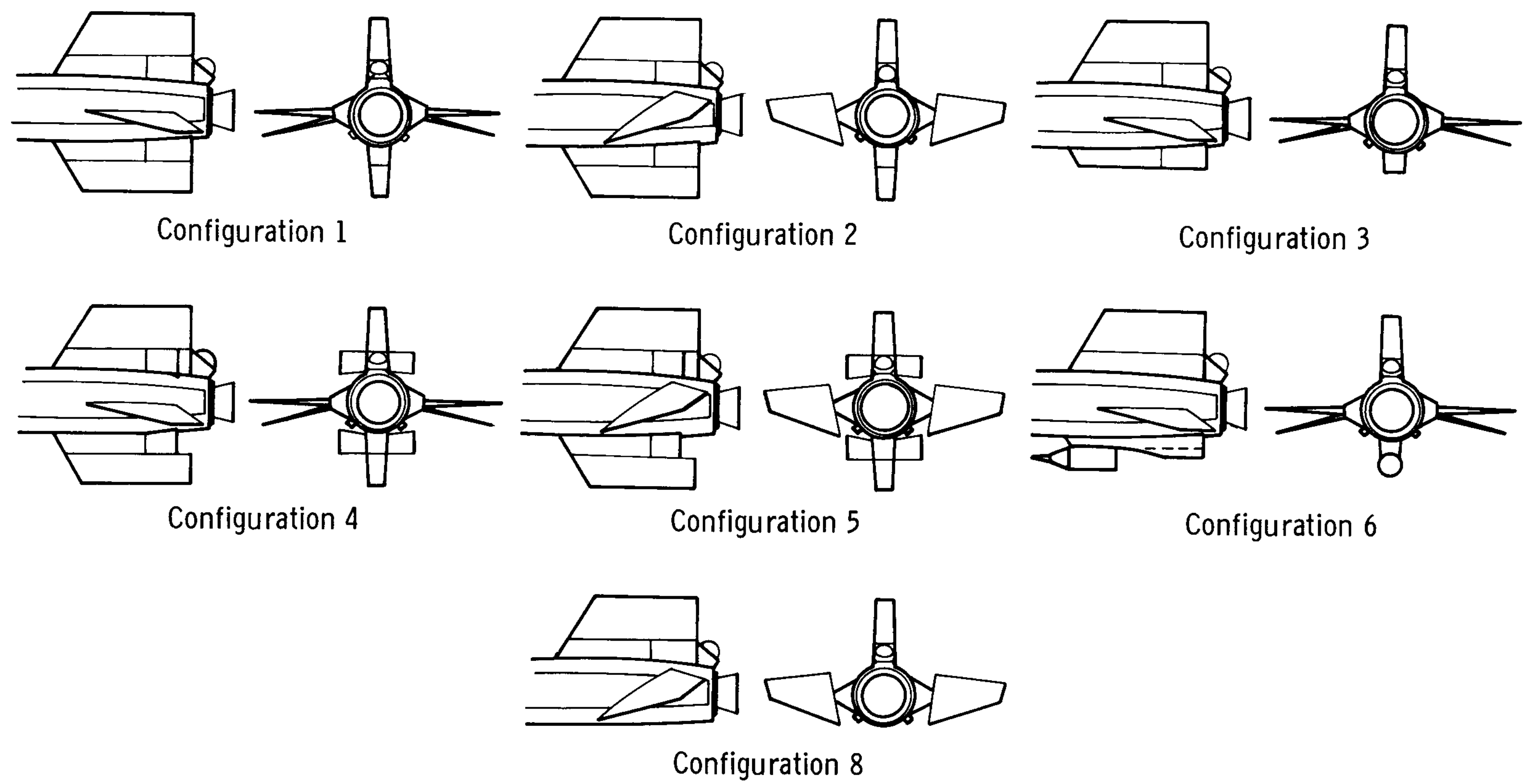

Configuration 7 - configuration 1 plus smooth nozzle extension (no ribs on nozzle).
Configuration 9 - configuration 6 with top speed brakes open (see fig. 15(b)).
Configuration 10 - configuration 6 with top speed brakes open and tails deflected (see fig. 15(c)).
Configuration 11 - configuration 6 with horizontal tails deflected.

Figure 6. – Sketches of configurations tested in the pressure investigation with the $\epsilon = 22.1$ nozzle extension.

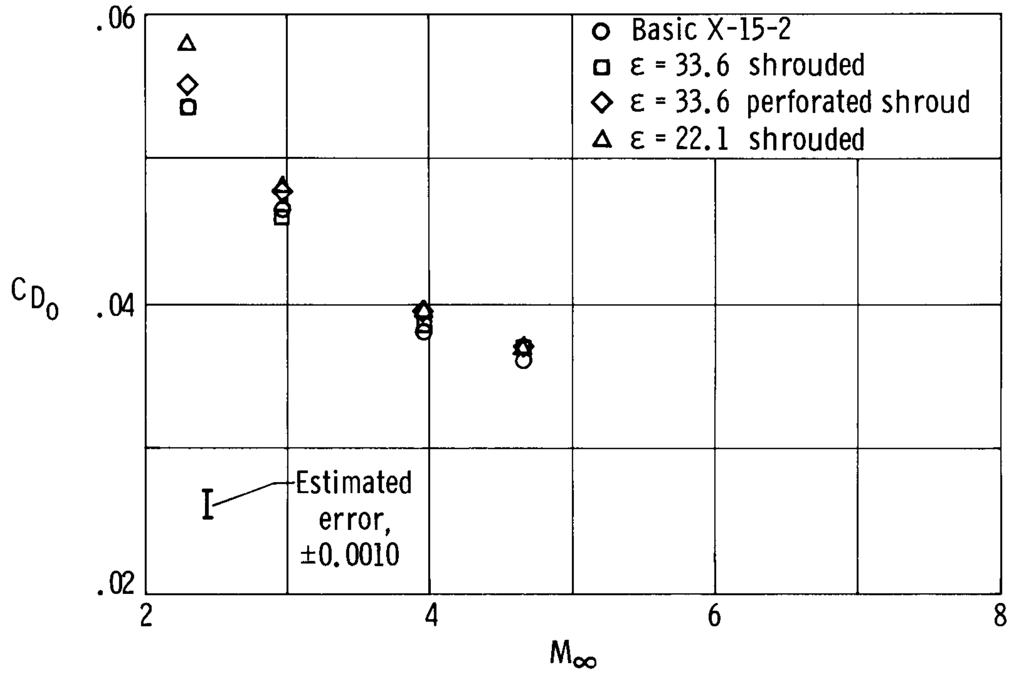

(a) Shrouded nozzle extensions.

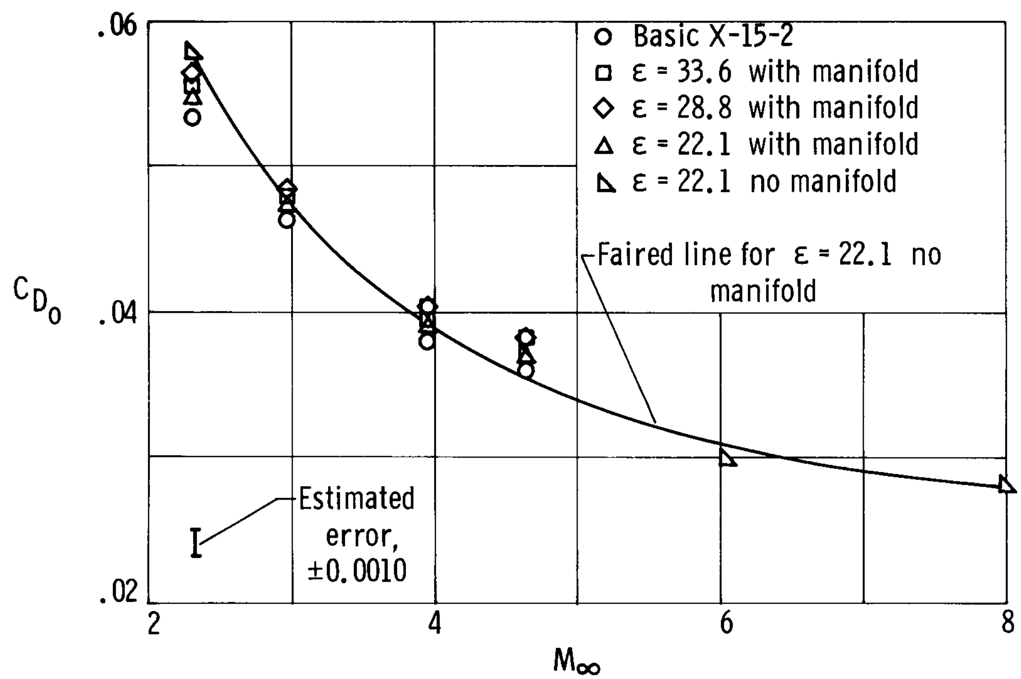

(b) Unshrouded nozzle extensions.

Figure 7.— Variation of zero-lift drag coefficient with Mach number for the X-15-2 with various nozzle extensions.

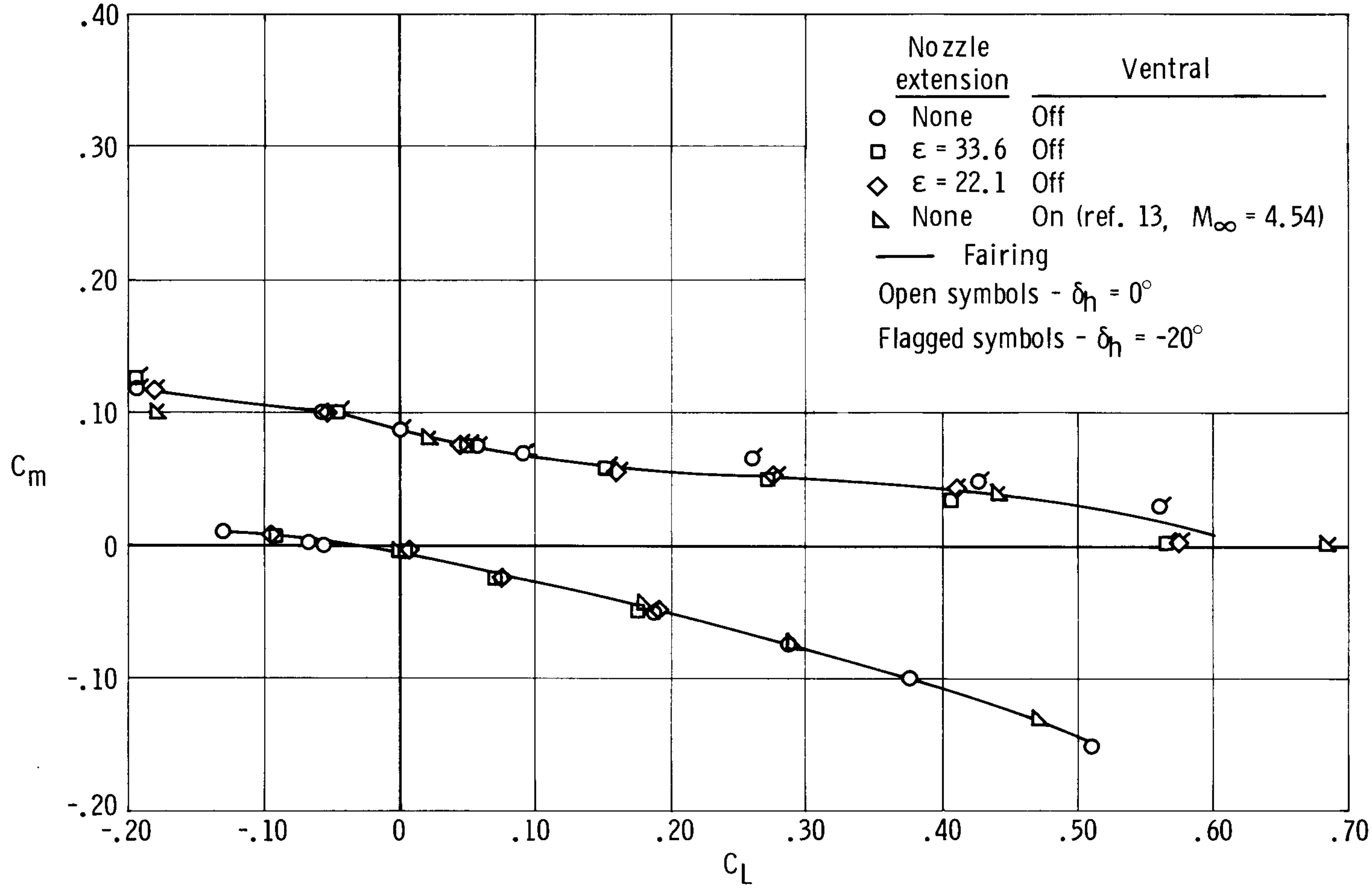

Figure 8.— Variation of pitching-moment coefficient with lift coefficient for several airplane and nozzle configurations ($\delta_{sb} = 0°$) at $M_\infty = 4.63$.

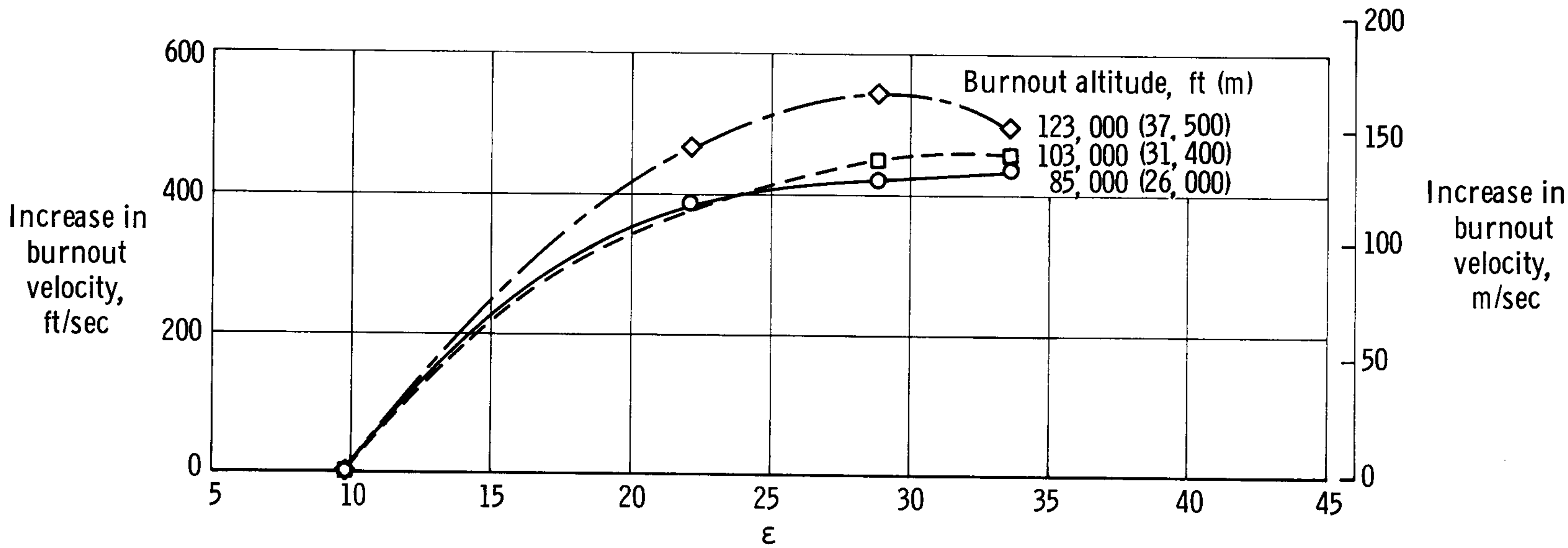

Figure 9.– Effect of varying nozzle internal-expansion ratio on X-15-2 calculated burnout performance.

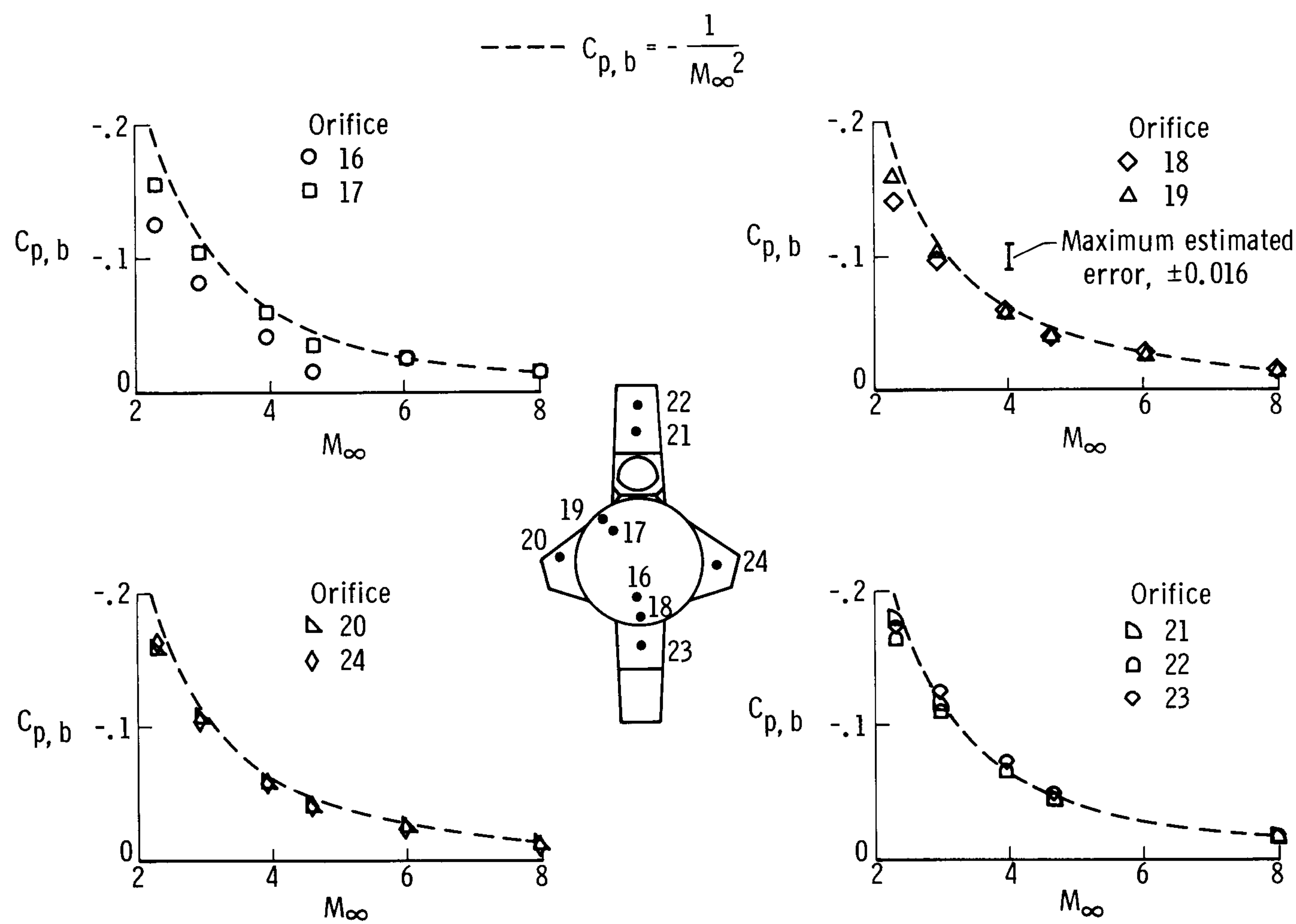

(a) Undeflected control surfaces (configuration 1).

Figure 10.– Effect of configuration on base pressures for $\alpha \approx 0°$.

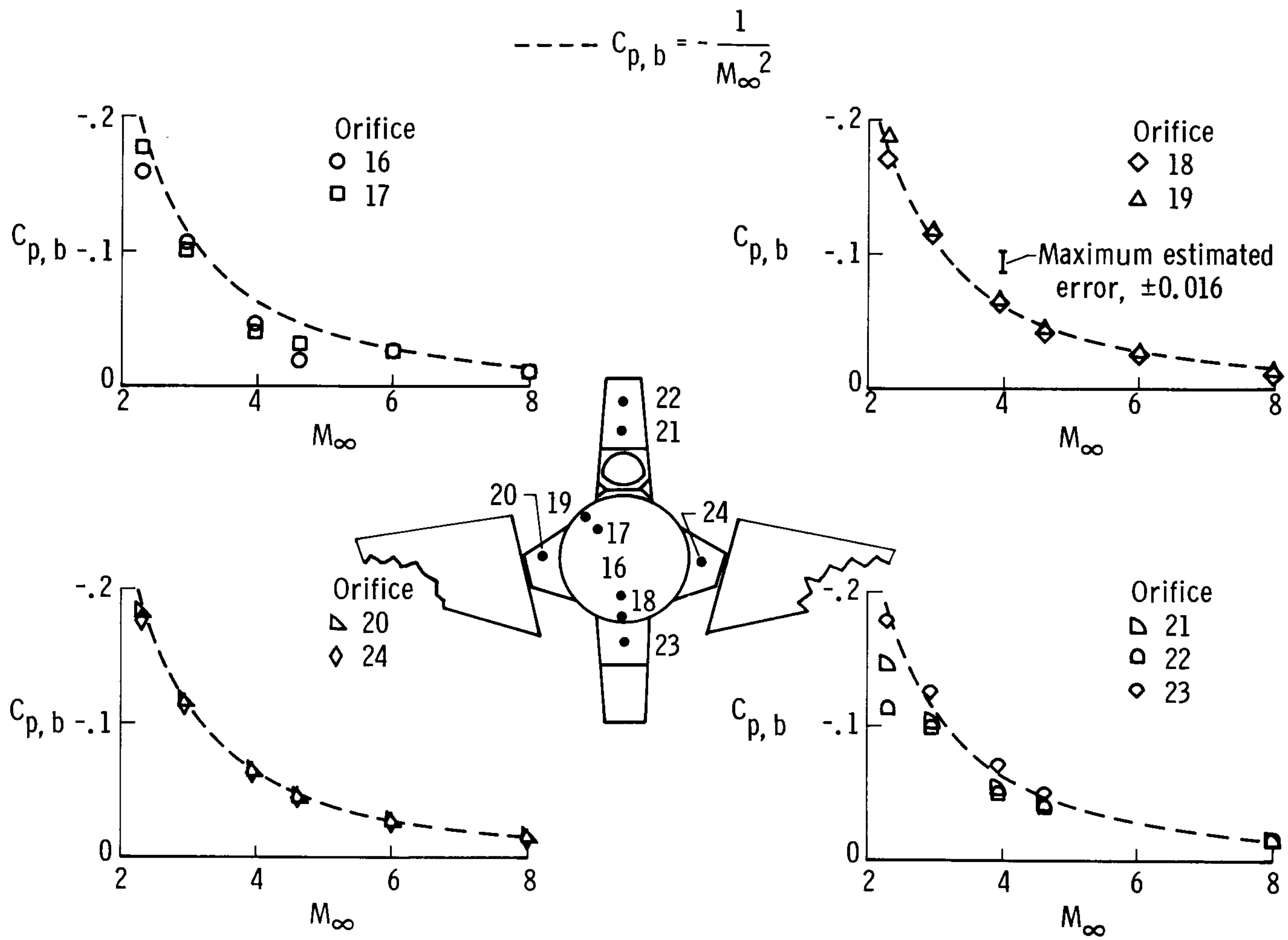

(b) Deflected horizontal tail (configuration 2).

Figure 10.– Concluded.

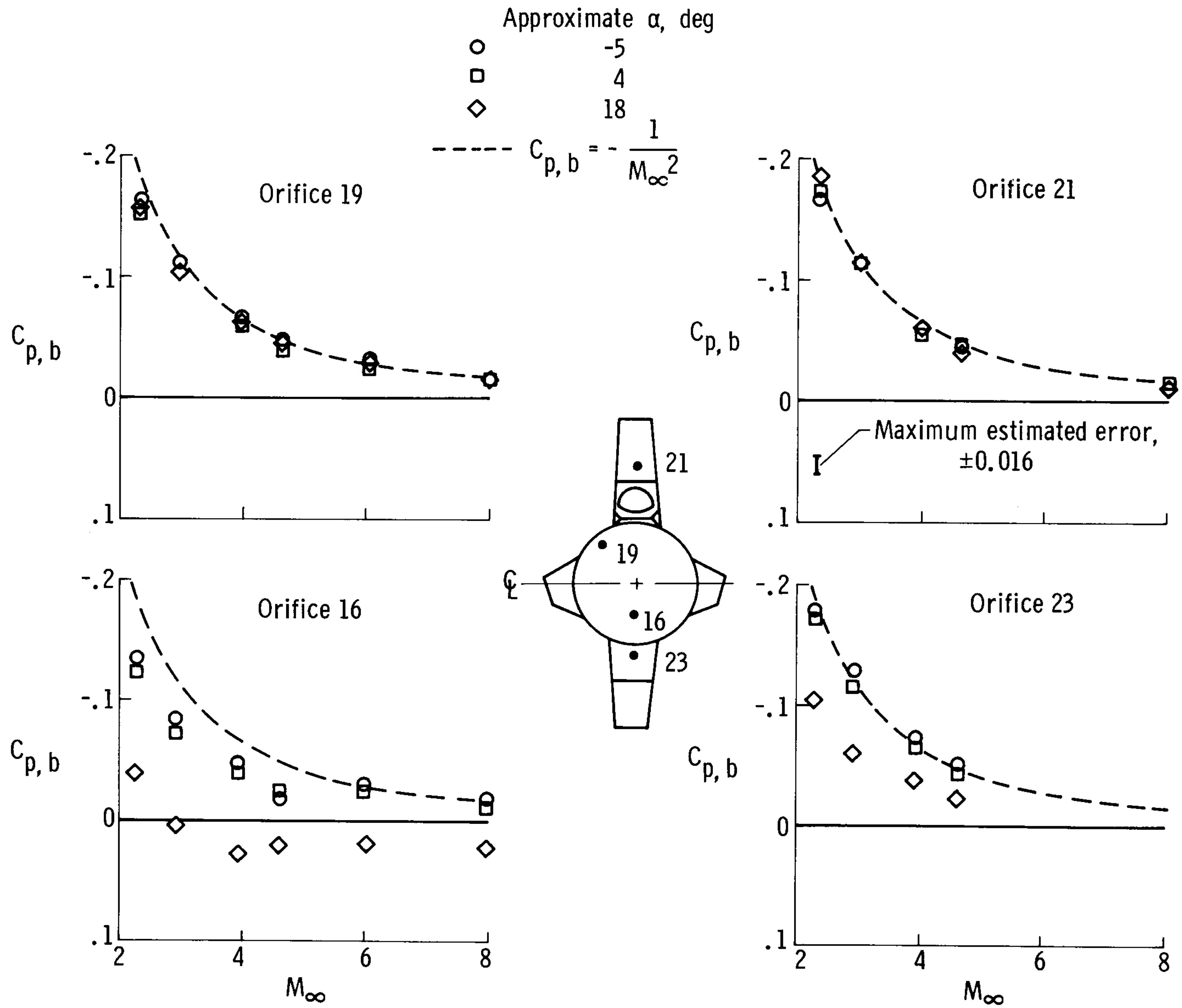

Figure 11.– Angle-of-attack effects on base pressure coefficients (configuration 1).

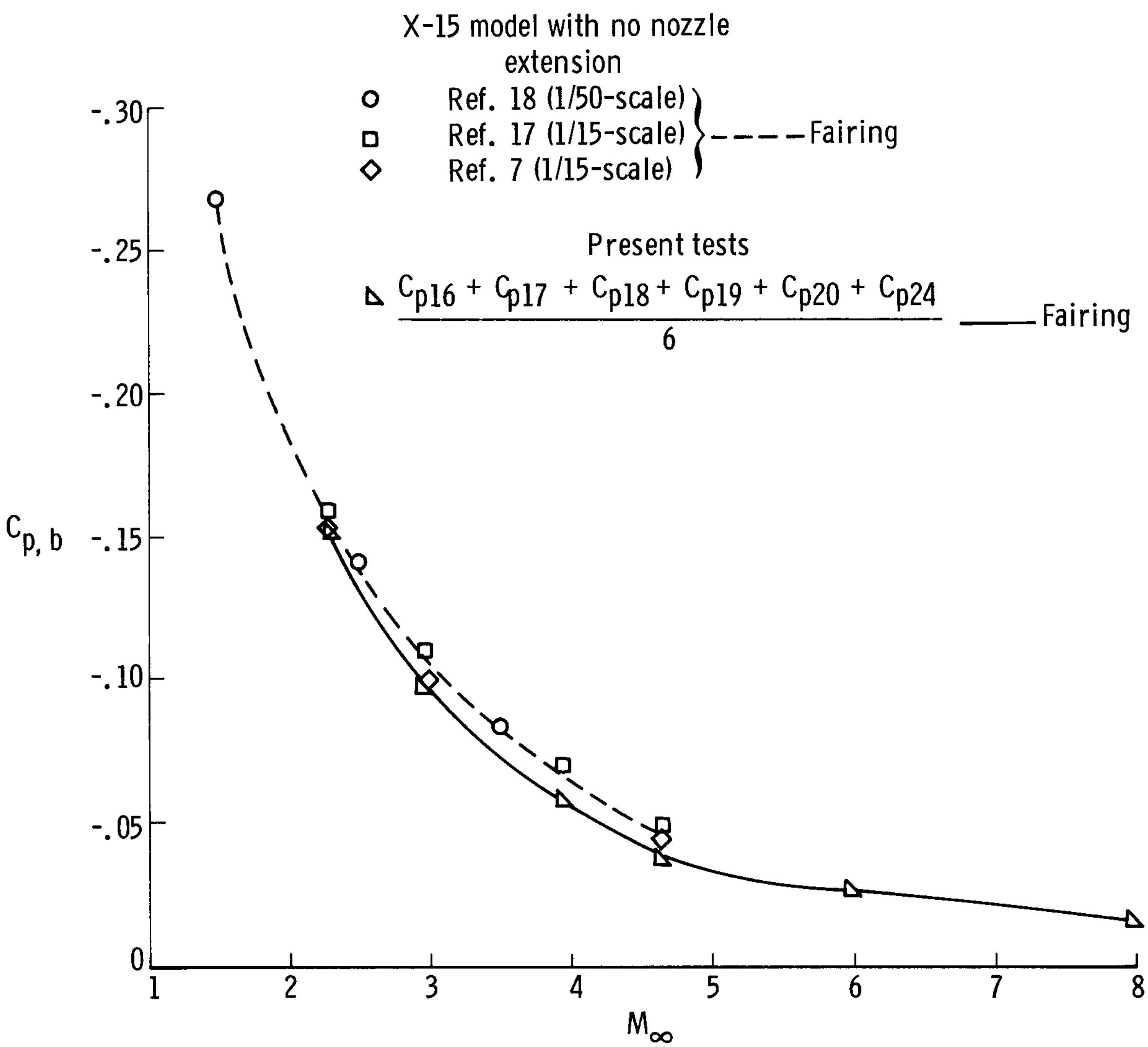

Figure 12.— Effect of nozzle extension (configuration 1) on average base pressure coefficient for $\alpha \approx 0°$.

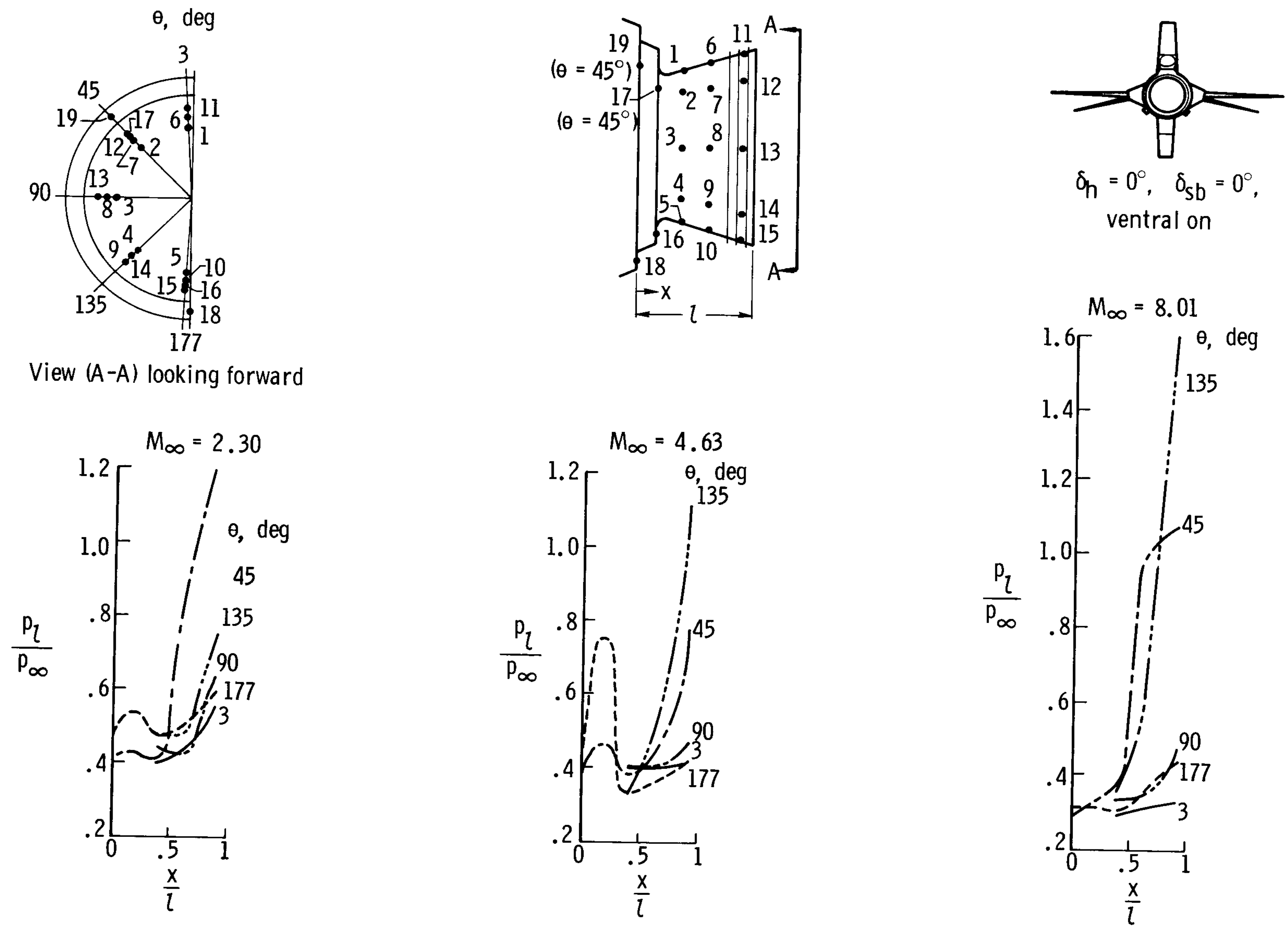

(a) Configuration 1.

Figure 13.— Variation of pressures on nozzle extensions at $\alpha \approx 0°$.

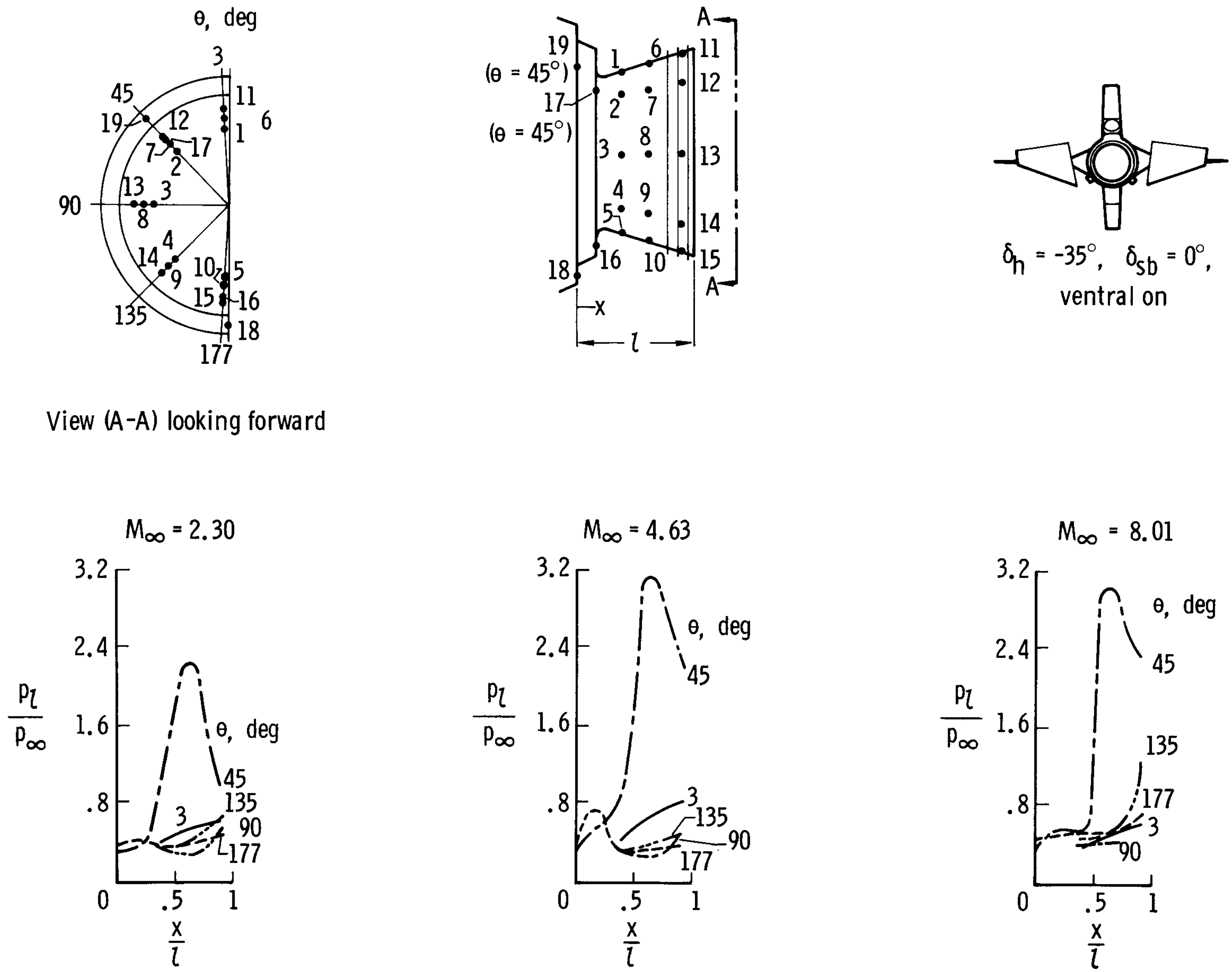

(b) Configuration 2.

Figure 13. – Continued.

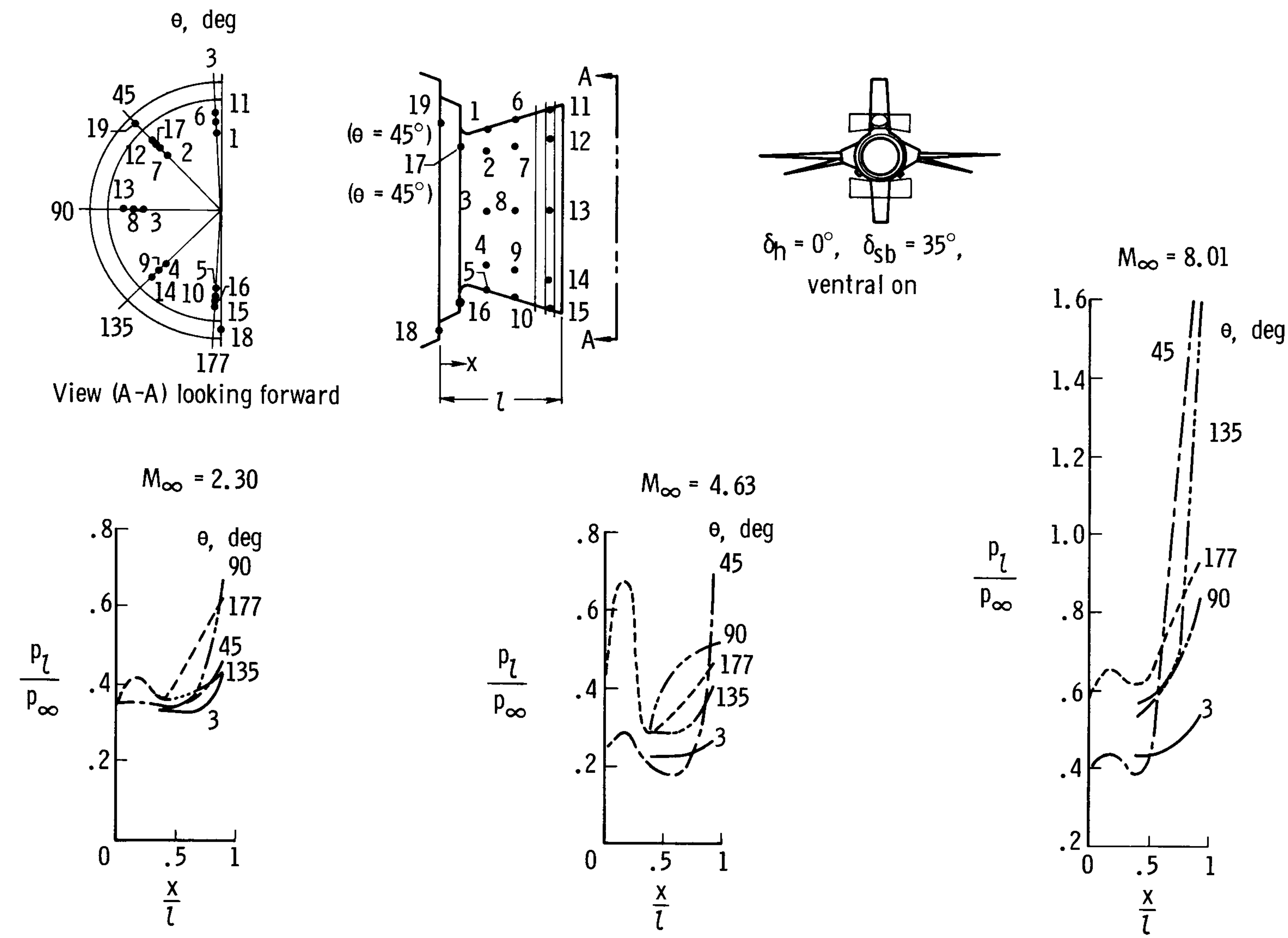

(c) Configuration 4.

Figure 13.– Continued.

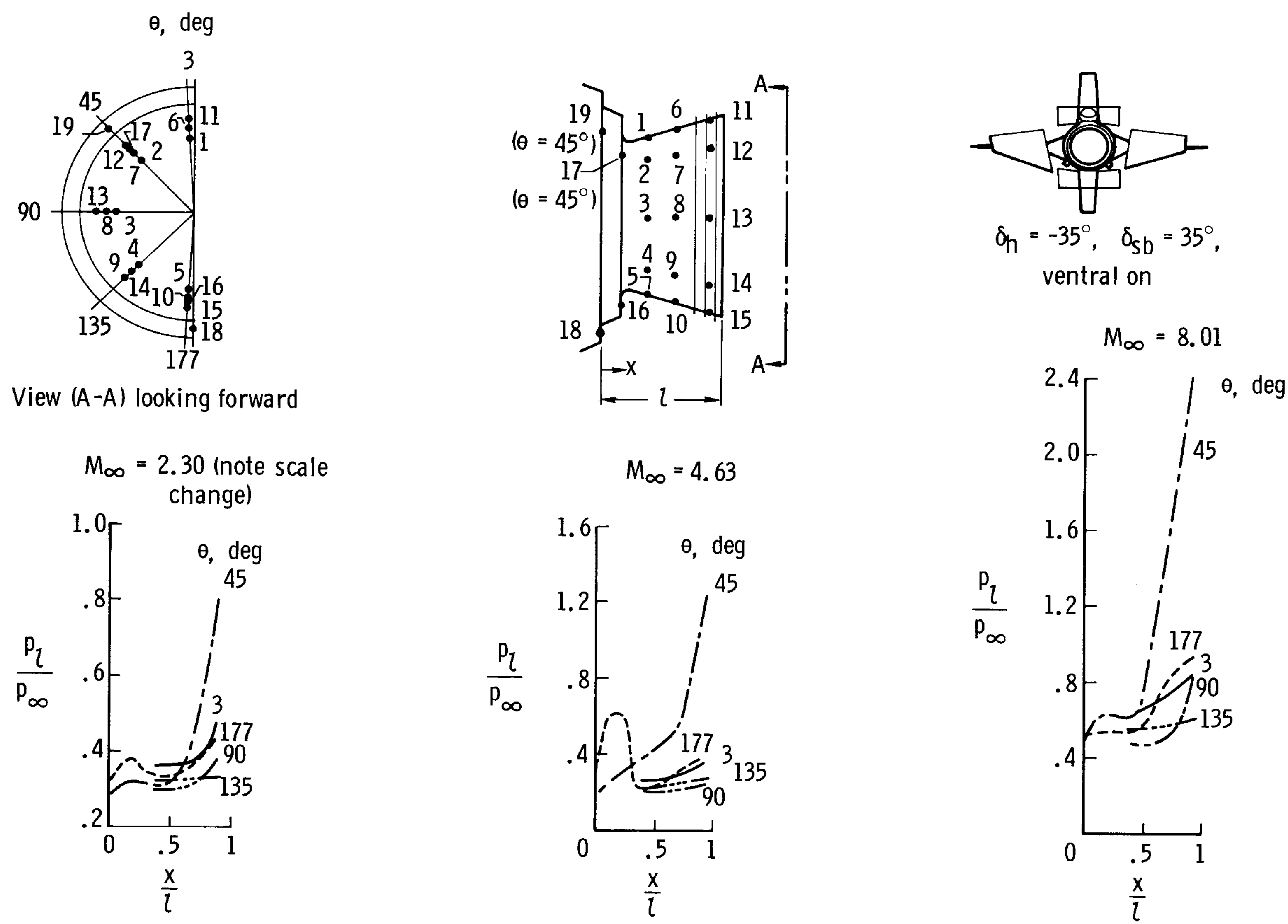

(d) Configuration 5.

Figure 13. – Concluded.

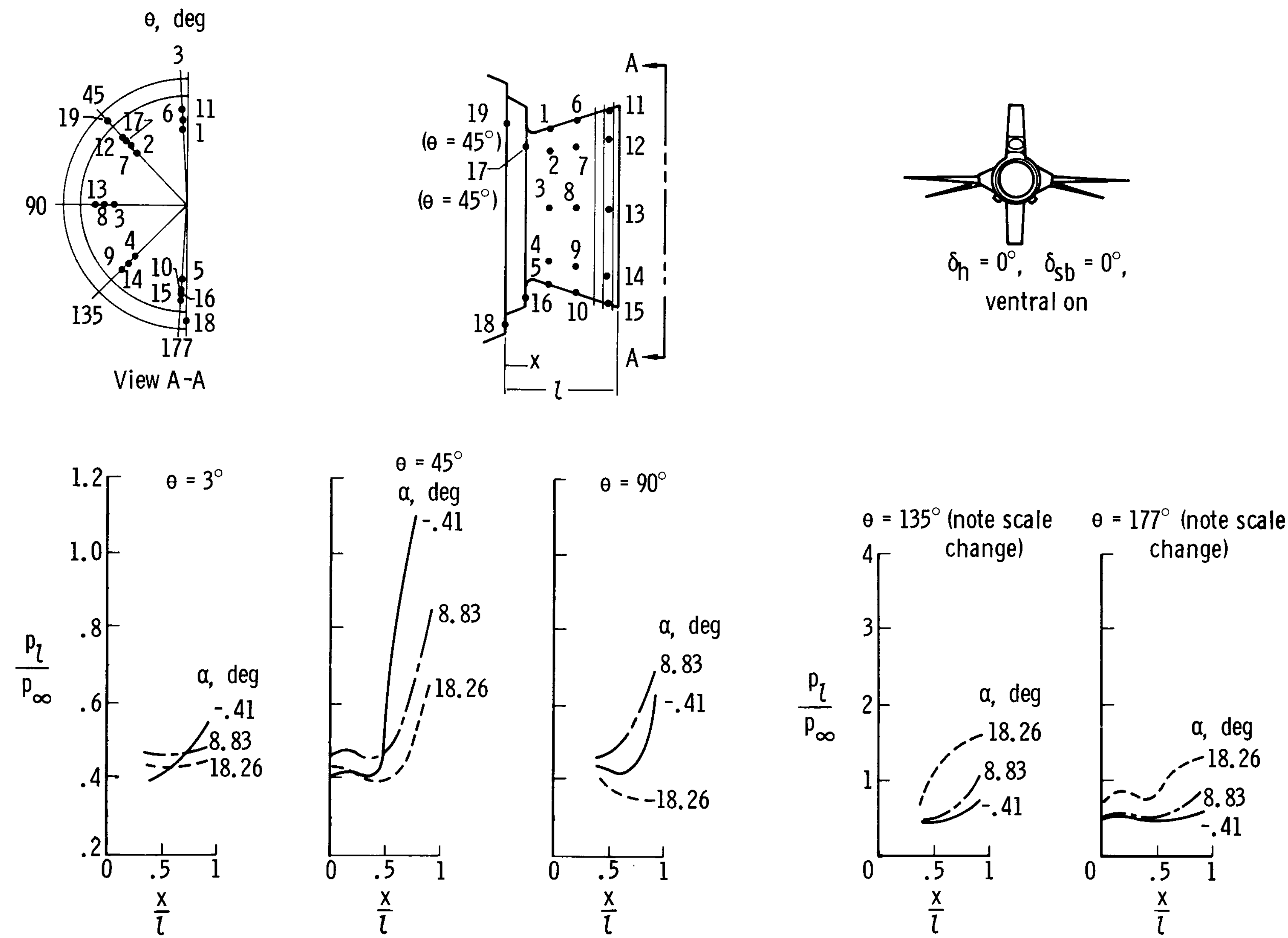

(a) $M_\infty = 2.30$.

Figure 14. – Effect of angle of attack on nozzle-extension pressures. Configuration 1.

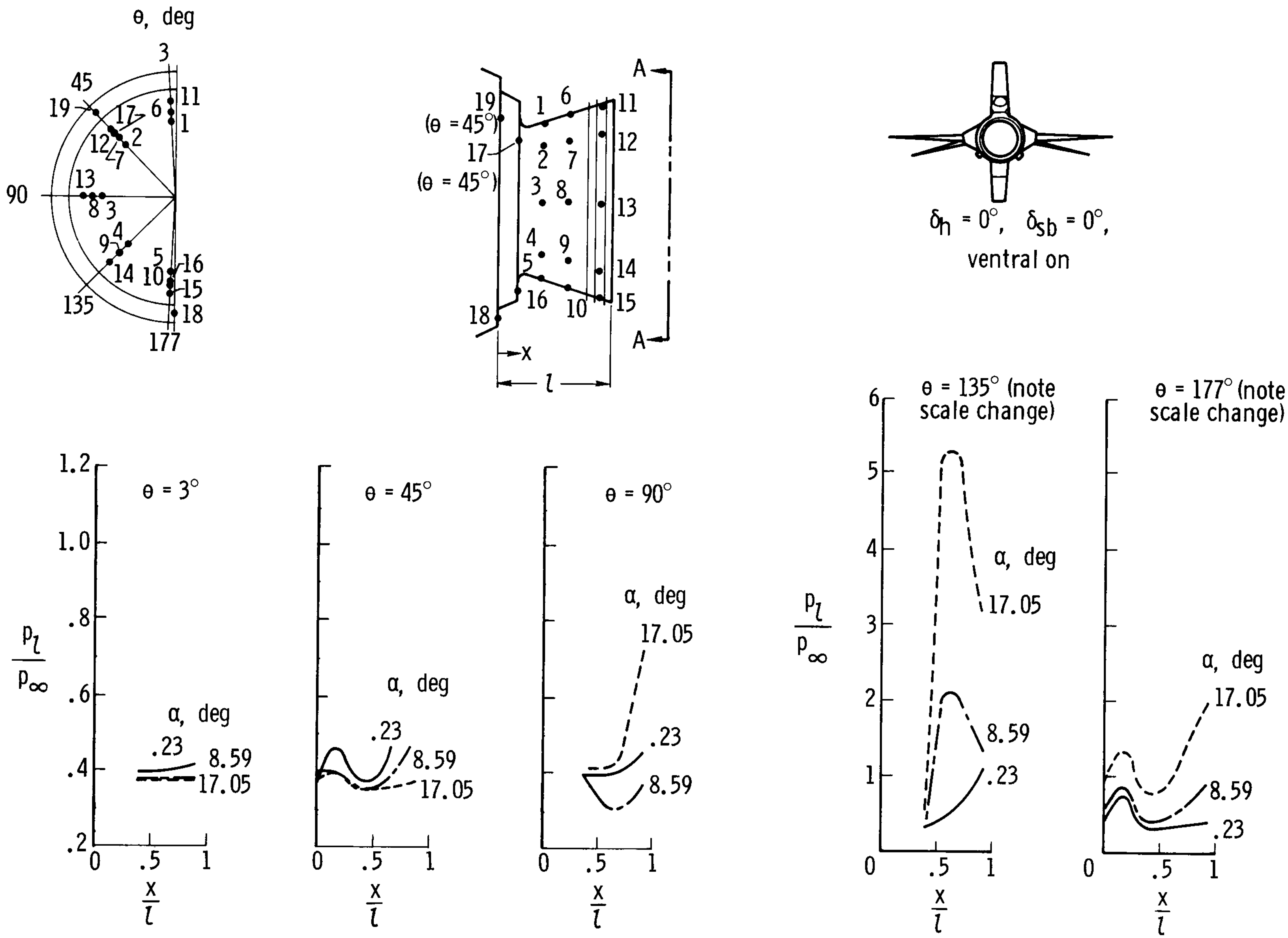

(b) $M_\infty = 4.63$.

Figure 14. – Continued.

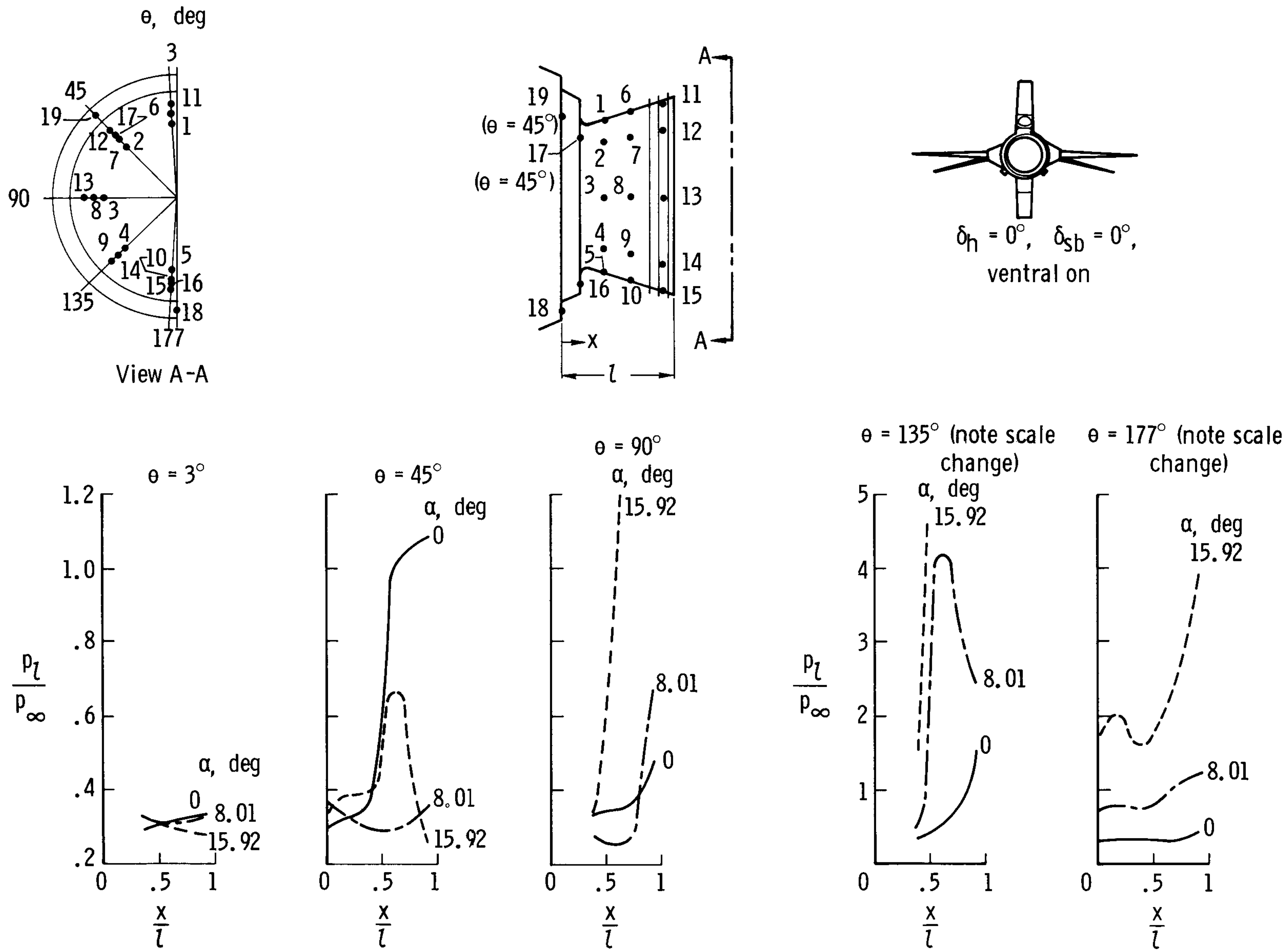

(c) $M_\infty = 8.01$.

Figure 14. – Concluded.

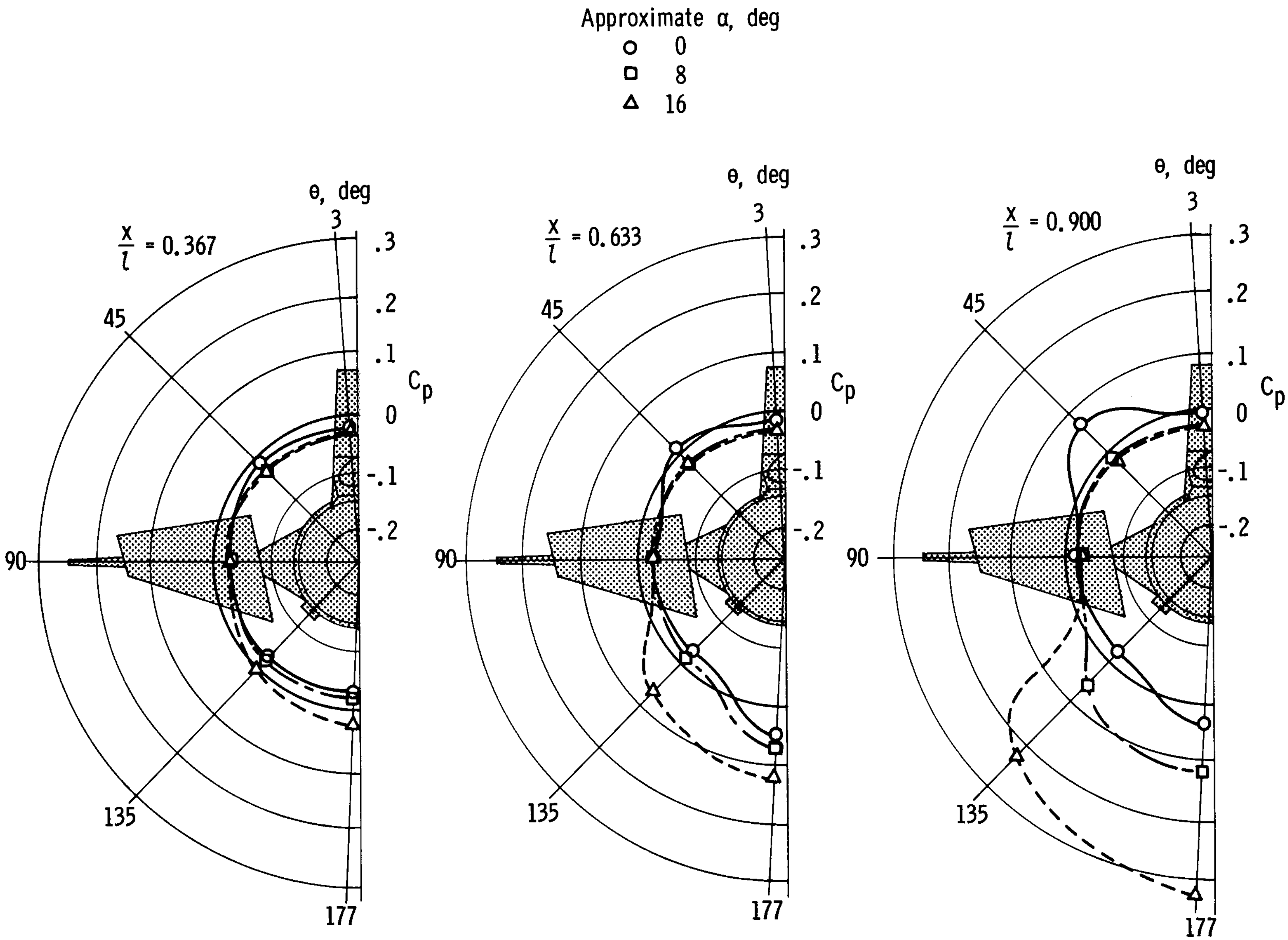

(a) Cross sections for configuration 8.

Figure 15. – Pressure-coefficient distributions on the nozzle extension for $M_\infty = 6.04$.

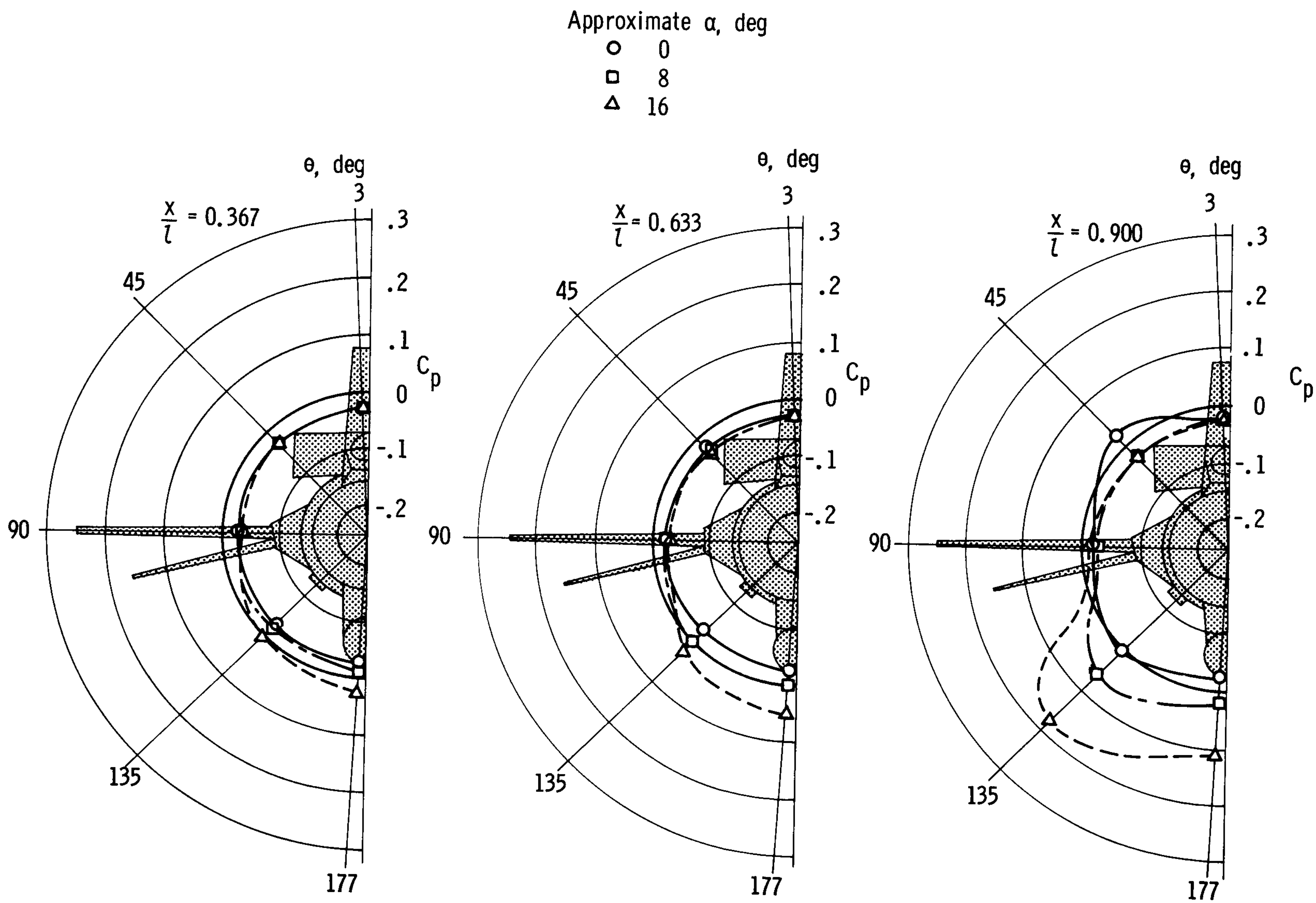

(b) Cross sections for configuration 9.

Figure 15.— Continued.

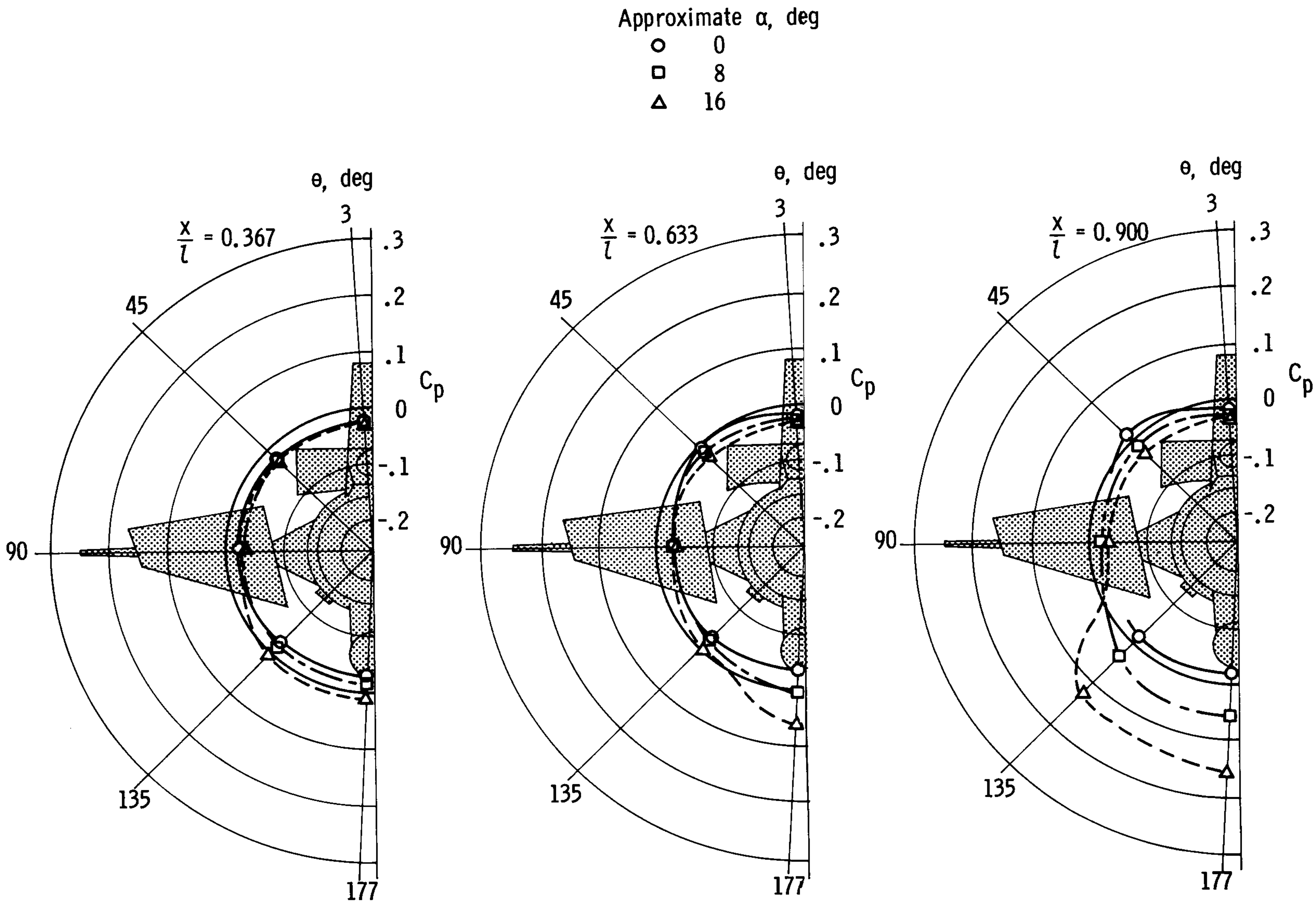

(c) Cross sections for configuration 10.

Figure 15.– Concluded.

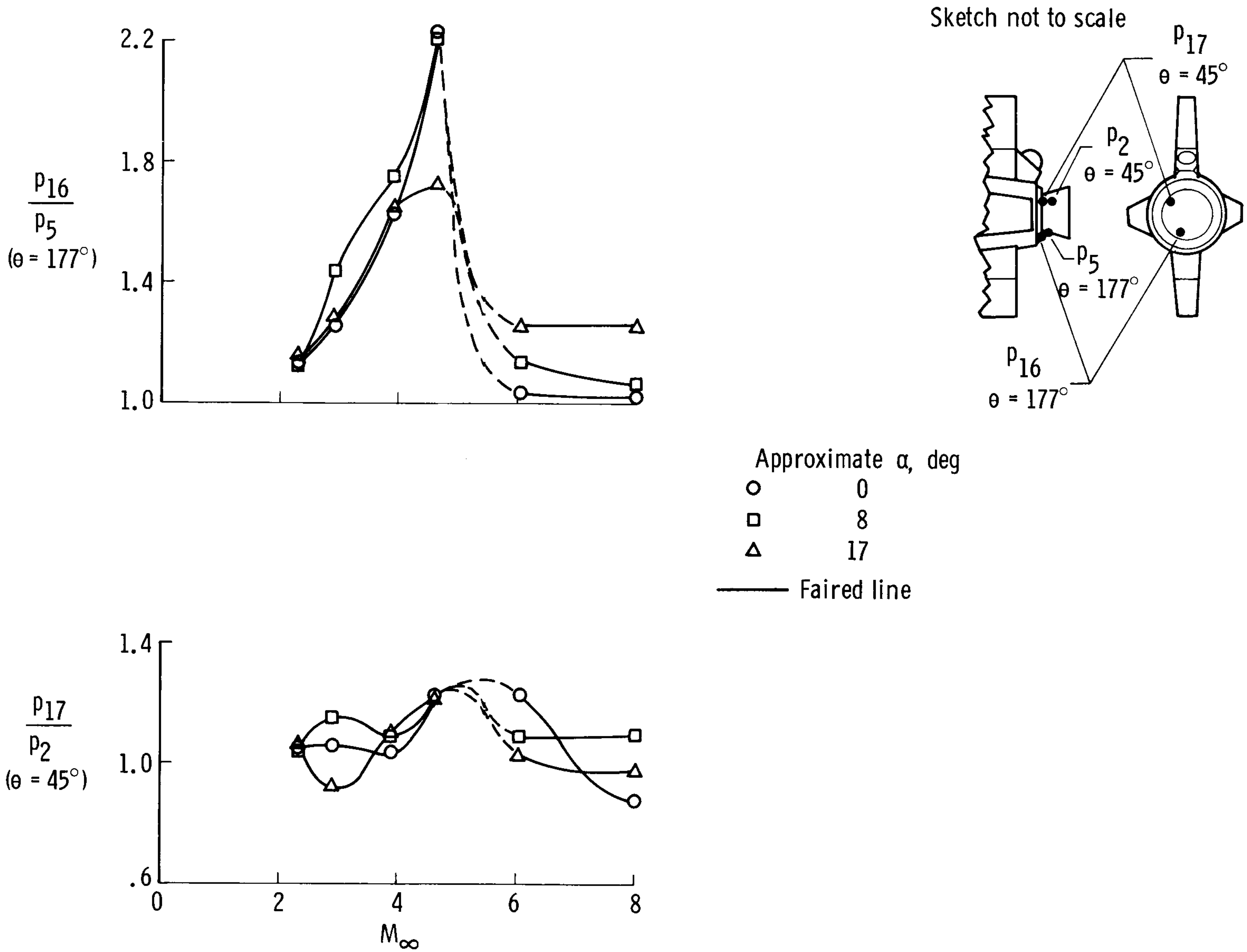

Figure 16. – Flame-shield pressurization by recirculating flow. Configuration 1.

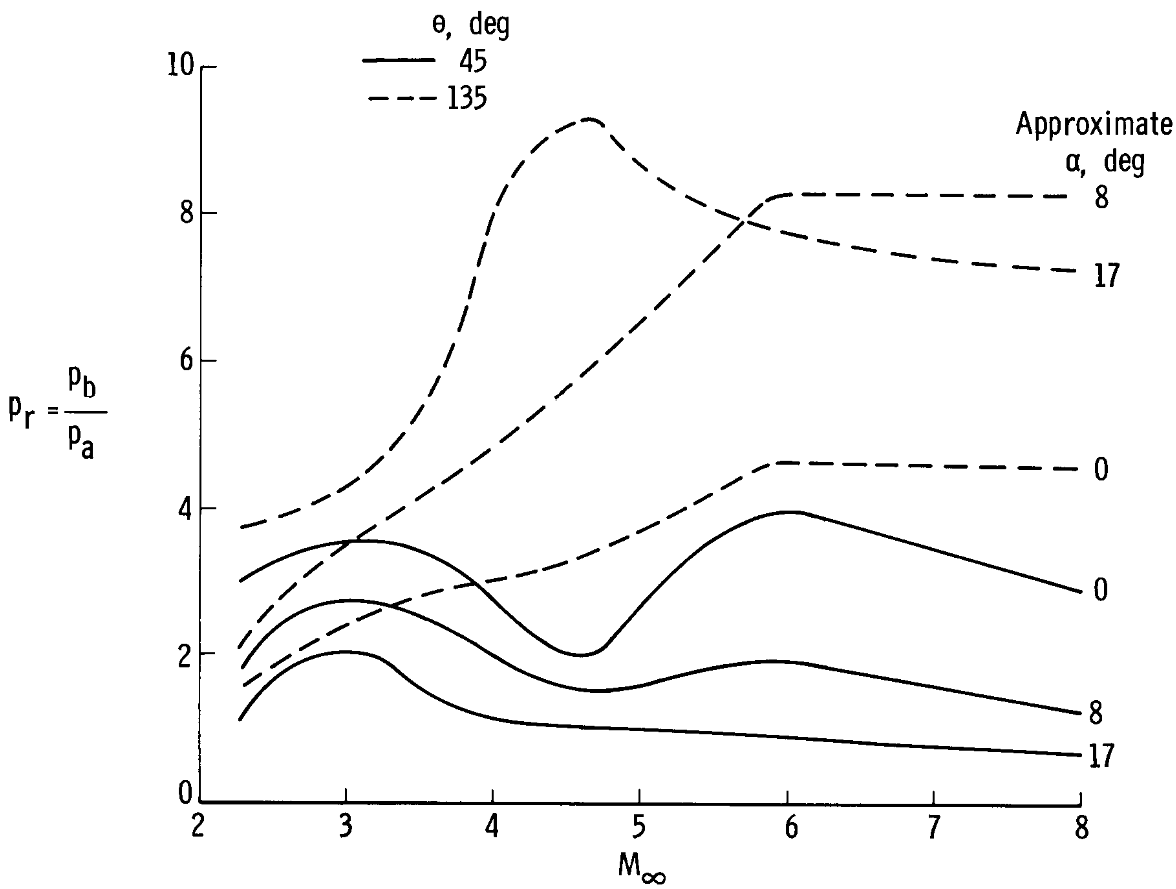

Figure 17.- Trailing-shock-wave pressure ratio. Configuration 1.